REMOVAL OF ANTIMICROBIAL COMPOUNDS FROM WATER BY GAC AND NATURAL MINERALS

by

Derya AYDIN

BS. in Environmental Eng., Istanbul University, 2006

Submitted to the Institute of Environmental Sciences in partial fulfillment of

the requirements for the degree of

Master of Science

in

Environmental Sciences

Boğaziçi University

2010

ACKNOWLEDGEMENT

First and foremost I offer my sincerest gratitude to my supervisor, Prof. Dr. Işıl Balcıoğlu, who has supported me throughout my thesis with her endless patience, encouragement and knowledge. I am also thankful to Assoc. Prof. A. Neren Ökte and Assoc. Prof. Nadim Copty for their critical and supportive suggestions.

I am very grateful to Gülhan Özkösemen, Filiz Ayılmaz, Bige Gedik Uluocak, and Mehmet Ali Küçüker for their kindness and technical assistances during my laboratory study.

I am indebted to my laboratory friends Merih Ötker Uslu, Aslin Erdinç, Asu Ziylan, Sertan Coker, and Nalan Bilgin Öncü for their support and kindness.

I cannot find words to express my thanks to my dear friends Öncü Maracı, Evrim Kalkan, Emrah Çoraman, Tunç Öztunç, Doğa Ertürk, Barış Küçükçıtak, and Emek Çelik for their valuable friendship, support, and positiveness.

I am also very grateful to my classmates Serpil Sarıoğlu, Gül Akınç, and Ayşe Akyapı and housemates Esma Önder, and Gizem Kişioğlu for their good fellowship.

I would like to express my deepest gratitude to my best friend Türev Sarıkurt whose endless support and persistent confidence has taken the load off my shoulder.

Words fail me to express my appreciation to my dear parents Mehmet and Hacer Aydın and my dear sister Tuğba Aydın who always support and trust me through their endless love for being with me whenever I need. Last but not least, thanks to my lovely grandmother Kasime Boztepeli for her earnest prayers and to my grandfather Rüstem Boztepeli for his support from very beginning.

ABSTRACT

The widespread and unrestricted use of antimicrobials resulted in accumulation of them in the environment and due to their adverse effects they can be considered as an emergent pollutant group. Development of antimicrobial resistance in microorganisms is the major adverse effect of antibiotic pollution in the environment. In order to remove sulfonamide and tetracycline group antibiotics namely, sulfamethazine (SMZ), sulfamethoxazole (SMX), and oxytetracycline (OTC) batch experiments have been performed by granular activated carbon (GAC). Adsorption kinetics and equilibrium studies were performed by GAC. Additionally, the adsorption performance of some natural minerals (perlite, pumice, and zeolite) was evaluated for SMZ. The effects of contact time, initial antimicrobial concentration, and pH on the adsorption were investigated. While the highest adsorption capacity of natural minerals for SMZ was obtained with zeolite with a value of 1.42 mg/g, about nine fold higher adsorption was obtained with GAC. Experimental equilibrium data indicates that the isotherms for these antimicrobials on GAC can be satisfactorily described by Temkin isotherm equation. Four different mathematical models proposed in the literature were used to describe kinetics and the adsorption of all antimicrobials could be described more favorably by the pseudo-second order kinetic model. Batch adsorption experiments indicate that the sorption is a pH dependent process.

ÖZET

Antimikrobiyallerin yaygın ve kısıtlanmayan kullanımı çevrede birikimleriyle sonuçlanmaktadır ve zararlı etkileri sebebiyle önemli kirleticiler olarak kabul edilmektedirler. Mikroorganizmalar arasında antimikrobiyallere karşı direnç gelişimi, çevredeki antimikrobiyal kirliliğinin en önemli yan etkisidir. Sulfamethazin (SMZ), sulfametoksazol (SMX) ve oksitetrasiklin (OTC) olarak adlandırılan sulfonamid ve tetrasiklin grubu antibiyotiklerin uzaklaştırılması amacıyla granül aktif karbon ile kesikli adsorpsiyon deneyleri uygulanmıştır. Adsorpsiyon kinetikleri ve kararlılık çalışmaları aktif karbon ile yapılmıştır. Buna ek olarak, bazı doğal minerallerin (perlit, ponza ve zeolit) adsorpsiyon performansları SMZ için değerlendirilmiştir. Temas süresi, başlangıç antibiyotik derişimi ve pH değişiminin adsorpsiyon üzerindeki etkileri incelenmiştir. SMZ için doğal minerallerin en yüksek adsorpsiyon kapasitesi 1.42 mg/g ile zeolit ile elde edilmesine rağmen, GAC ile dokuz kat daha yüksek adsorpsiyon sağlanmıştır. Deneysel kararlılık verilerine uygunluk bu dört antibiyotiğin GAC ile adsorpsiyonunu tatmin edici şekilde Temkin izoterm eşitliği ile açıklanabildiğini göstermiştir. Literatürde önerilen dört değişik matematiksel model kinetikleri tanımlamak için kullanılmış ve tüm antibiyotiklerin adsorpsiyonu sözde-ikinci-derece kinetik model ile daha uygun şekilde tanımlanmıştır. Kesikli adsorpsiyon deneyleri adsorpsiyonun çözelti pH'ına bağlı olduğunu göstermiştir.

TABLE OF CONTENTS

LIST OF FIGURES

LIST OF TABLES

1. INTRODUCTION

Recent investigations revealed that pharmaceuticals and personal-care products as well as algal and cyanobacterial toxins, hormones and other endocrine-disrupting compounds, surfactants, perfluorinated compounds which are not currently covered by existing regulations on water quality are classified as emerging pollutants. Among pharmaceuticals, antimicrobial are of particular concern because they can induce microbial resistance through continuous exposure (Halling-Sørensen et al., 1998) and this represents a health risk to humans and animals (Kümmerer, 2004).

Antimicrobials are extensively administered to organisms for the purpose of preventing (prophylactic) and treating (therapeutic) microbial infections. Besides, antimicrobials have been used for promoting growth in animal feeding operations (Smith et al., 2002; Compant et al., 2005; Kumar et al., 2005a). The most widely used antimicrobials in industrialized countries include tetracyclines, macrolides, penicillins, aminoglycosides, and sulfonamides (Campbell, 1999; Haller et al., 2002). As a consequence of high consumption of them, antimicrobial compounds and/or their metabolites have been found in various environmental compartments such as soil, sediment, and water resources (Sarmah et al., 2006; Kemper, 2008; Karcı and Balcıoğlu, 2009; Cengiz et al., 2010). The application of animal manure and biosolids to agricultural fields as fertilizer that contains excreted antimicrobials can constitute one of the pathway for antimicrobial release in the environment (Boxall et al., 2003; Diaz-Cruz et al., 2003; Kemper, 2008). Thus, antimicrobials and their metabolites can directly enter to the nearby streams, lakes or other aquatic environments or leach downward through the soil and exposed to the groundwater (Kolpin et al., 2002; Garcia-Galan et al., 2010).

Recent studies revealed that existing water and wastewater treatment technologies are ineffective for removing many pharmaceuticals including antimicrobials, since they were not designed to remove these pollutants (Adams et al., 2002; Glassmeyer et al., 2005). However, oxidative processes are able to reduce the concentrations of some antimicrobials (Balcıoğlu and Ötker, 2003; Uslu and Balcioglu, 2008; Uslu and Balcioglu, 2009; Yalap and Balcioglu, 2009; Lin et al., 2009). On the other hand, in the practical

application of oxidation processes, the possible formation for the degradation products should be seriously taken into account because in some cases antimicrobial by-products can be more toxic than the parent compound (Li et al., 2008).

An efficient removal of antimicrobials can be achieved by adsorption processes. Because of the regeneration possibility of activated carbon, it can be used for the removal of antimicrobials (Choi et al., 2008; Putra et al., 2009; Rivera-Utrilla et al., 2009). Clay minerals are other alternative sorbents for adsorption of antimicrobials (Polubesova et al., 2006; Chang et al., 2009; Putra et al., 2009; Erdinç, 2009; Şalcıoğlu, 2007.).

Within the above scope, the objective of this study was to determine the sorption behavior of GAC in the removal of sulfonamide and tetracycline group antimicrobials (SMZ, SMX, OTC) from water at different antimicrobial concentrations and pH values. In addition, the adsorption performance of some natural minerals such as perlite, pumice, and zeolite were evaluated for SMZ and adsorption performances of these minerals were compared to those obtained by GAC. The sorption kinetics and the sorption isotherm studies on GAC were evaluated by using different models.

2. THEORETICAL BACKGROUND

2.1. Antibiotic Usage and Consumption

Antibiotics have been used for several years in both human medicine for therapeutic purposes and animal husbandry as prophylactic feed additive and growth promoter. The world-wide antibiotic consumption is estimated at between 100,000 and 200,000 tons per year (Wise, 2002). It was reported that 65 % of manufactured antibiotics are used in human medicine, 29% in the veterinary field, and 6% as growth promoters in Europe (FEDESA, 2001). According to data from the European Federation of Animal Health (FEDESA), 13,288 tons of antibiotics were used in the EU and Switzerland in 1999 (FEDESA, 2001). About 5,000 ton of antibiotics (70% for non-therapeutic purposes) were used in 1999 for veterinary purposes in EU and the consumption rate of them in US is about 9,000 tons/year (Sarmah et al., 2006). In Europe, median national hospital antibiotic consumption based on defined daily dose (DDD) was 2.1 DDD/ 1000 inhabitants-day according to the European Surveillance of Antimicrobial Consumption (ESAC) (Stichele et al., 2006). In Turkey, it was reported that total utilization of antibiotics based on defined daily dose was increased from 14.62 to 31.36 DDD/1000 inhabitant-days between 2001 and 2006 (Karabay and Hosoglu, 2008). While the maximum produced medicine group was reported as antibiotic agents with a ratio of 21% in Turkey (Pharmaceutical Industry Special Expert Commission Report, 2001) in 1998, the production capacity of antibiotic agents was 100 tons/year in 2006 (Pharmaceutical Industry Special Expert Commission Report, 2006).

One of the results of antibiotic usage is the development of antibiotic resistance which is a major worldwide public health problem. On 15 November 2001, a European Council Recommendation stated that specific strategies should be pursued for monitoring of antibiotic consumption and on 1 January 2006 the European Union banned the use of antibiotics as growth promoters in animal feed (EU Directive 70/524/EEC). Also in Turkey, the consumption of antibiotics as growth promoters in animal feed has been restricted since 1973 and four growth promoter antibiotics were banned in 2006 (Tuncer, 2007).

2.2. Source and Occurrence of Antibiotics in the Environment

Since antibiotics can be more or less extensively metabolized by humans and animals, after administration, antibiotics or their metabolites are excreted into the effluent and reach the sewage treatment plant (STP). Some of the antibacterial compounds are predominantly water soluble and can enter the environment through wastes of animal farms, domestic wastewater, effluents of pharmaceutical industry, and disposal of unused compounds. While the tetracycline group antibiotics are classified as hydrophobic, sulfonamides are considerably hydrophilic and polar (Tolls, 2001). On the other hand, none of antibiotics is readily biodegradable (Alexy et al. 2004) and most of them are resistant to other elimination mechanisms in the environment (Kümmerer, 2009). As a result of this, antibiotics can be detected in the µg/L range in surface water, groundwater, and STP effluents (Kümmerer, 2008). Source and fate of antibiotics in the environment are summarized in Figure 2.1.

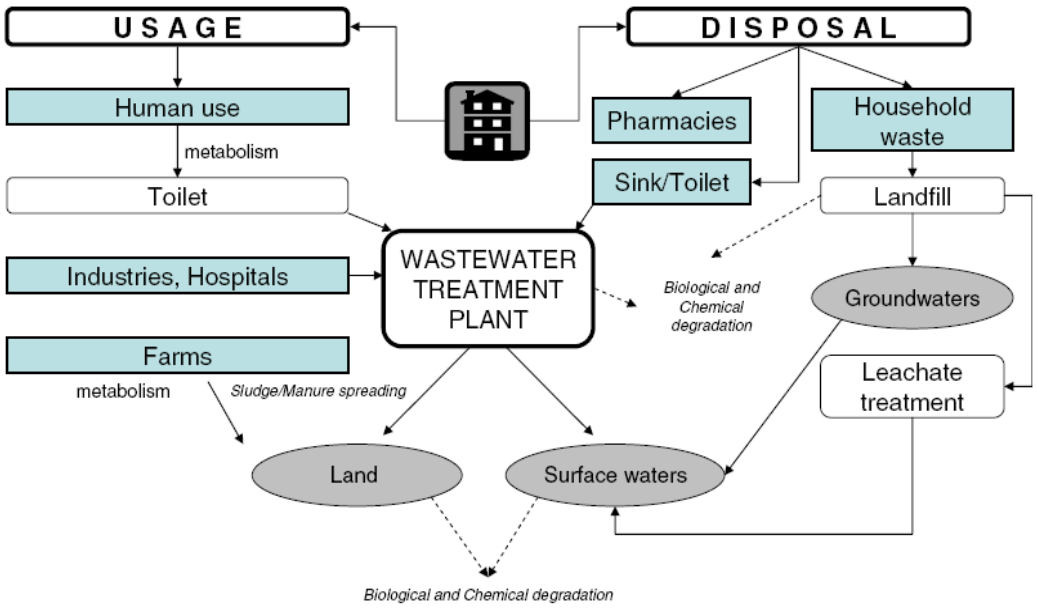

Figure 2.1. Source and fate of pharmaceutical compounds in the environment (Nikolaou et al., 2007).

Since antibiotics are often found in low quantities in the aquatic environment they are classified as micropollutants.

2.2.1. Antibiotics In Soil

Since a significant percentage of the administered antibiotics are excreted in active forms and most of antibiotics are persistent to biotic and abiotic reactions (Alexy et al., 2004), they can be detected in sewage sludge and manure which can further be applied to agricultural field as fertilizer (Boxall et al., 2003; Jorgensen and Halling-Sørensen, 2000). While hydrophobic antibiotics remain in soil others leach through the soil. Consequently, the loads of antibiotics spread by manuring or irrigation with reclaimed wastewater can reach up to hundred grams per hectare on agricultural soils (Chefetz et al., 2008). Some studies show that plants grown in manure amendment soil absorb antibiotic and this plant uptake points out the potential human health risk correlated with consumption of fresh vegetables that grown in these soil systems (Kumar et al., 2005b). Several studies conducted throughout Europe, USA, and Turkey have confirmed the occurrence of antibiotic residues in soil samples and some of them are listed in Table 2.1.

Table 2.1. Concentrations of antibiotics in soil samples.

Antibiotic Group	**Concentration (µg/kg)**	**Reference**
Tetracycline	86.2-171.7	Hamscher et al., 2002
	4-295	Hamscher et al., 2005
	5-18	Andreu et al., 2009
	10-500	Karci, 2008
	25-105	Cengiz et al., 2010
	20.9-2683	Hu et al., 2010
Sulfonamides	40-400	Karci, 2008
	0.03-9.1	Hu et al., 2010
	15	Christian et al., 2003
	4.5	Avisar et al., 2010
Macrolides	1.8 - 57.4	Jacobsen et al., 2004

As it can be seen from the Table 2.1, tetracycline concentrations are remarkably high compared to sulfonamides because the high mobility characteristic of sulfonamides in environmental matrixes obstructs sulfonamides to accumulate in soils. In a recent comparative study for example, investigating the sorption of different antibiotics in arable (Davis et al., 2006) and grassland (Burkhardt and Stamm, 2007) soils revealed that very small apparent K_d values for sulfamethazine, a sulfonamide antibiotics. On the other hand, K_d values of tetracyclines in different soil samples are comparably high (Tolls, 2001).

2.2.2. Antibiotics In Water and Wastewater

It is known that antibiotics mainly release into the environment by human and animal waste. Between 30% and 90% of an administered dose of most antibiotics to humans and animals are excreted in urine and feces as an active substance (Halling-Sørensen et al, 1998; USEPA, 2000) and they have been detected in the influent of sewage treatment plants (STPs) at μg/L level. In addition to STP influents antibiotics can be detected in the effluents of hospitals and antibiotic manufacturing plants. Since conventional treatment processes are generally ineffective for the complete removal of antibiotics these substances have also been detected in STP effluents. Hence, surface, ground, and drinking water can be contaminated with antibiotics due to the improper STP discharge, leaching, and surface runoff. Table 2.2 shows the concentration ranges of four different group antibiotics in surface water, ground, and drinking water as well as in the influent and effluent of wastewater treatment plant and hospital wastewater.

The presence of antibiotics in STPs is important because STPs play an important role in life cycle of antibiotics. There are many studies for the occurrence of antibiotics in the influent and effluent of STP. In Canada, more than 14 antibiotics were detected in STP effluents with the highest concentration belonging to tetracyclines (Miao et al., 2004). The influent and effluent concentration of eight selected antibiotics including chloramphenicol, fluoroquinolone, sulfonamide, and macrolide groups at four STPs in South China ranged from 10 to 1,978 ng/L and from 9 to 2,054 ng/L, respectively (Xu et al., 2007).

As it is represented in Table 2.3, tetracycline group antibiotics have higher concentrations in STP and WWTP effluent although they are more hydrophobic than sulfonamides.

Table 2.2. Antibiotics in different water systems.

Antibiotic Group	Occurrence Matrix	Concentration (µg/L)	Reference
Tetracyclines	WWTP effluent	3.6	Karthikeyan et al., 2006
	WWTP effluent	0.065	Yang et al., 2005
	WWTP effluent	0.061-1.1	Batt et al., 2007
	WWTP effluent	0.02-0.25	Watkinson et al., 2009
	WWTP effluent	95.8-915.3	Pena et al., 2010
	WWTP influent	0.1-0.65	Watkinson et al., 2009
	WWTP influent	0.05-0.27	Yang et al., 2005
	Hospital wastewater	6-531.7	Pena et al., 2010
	Hospital wastewater	0.011-0.455	Lin and Tsai, 2009
	Surface water	0.11-1.34	Lindsey et al., 2001
	Surface water	0.08-0.6	Batt et al., 2007
	Surface water	0.11-0.69	Kolpin et al., 2002
	Surface water	52.7-399.1	Pei et al., 2006
	Groundwater	1	Campagnolo et al., 2002
	Drinking water	0.091-0.106	Ye and Weinberg, 2007
	STP effluents	977	Miao et al., 2004
Sulfonamides	WWTP effluent	0.21-2.8	Batt et al., 2007
	WWTP effluent	0.31	Brown et al., 2006
	WWTP effluent	0.018-0.641	Göbel et al., 2004
	WWTP effluent	0.15-0.6	Watkinson et al., 2009
	WWTP influent	0.07-1.09	Yang et al., 2005
	WWTP influent	0.1-3	Watkinson et al., 2009
	Hospital wastewater	0.4-2.1	Brown et al., 2006
	Hospital wastewater	0.4-12.8	Lindberg et al., 2004
	Surface water	0.015-0.328	Managaki et al., 2007
	Surface water	0.48	Hirsch et al., 1999
	Surface water	3.5-22.4	Pei et al., 2006
	Surface water	0.06-15	Lindsey et al., 2001
	Groundwater	6.98-312.2	Garcia-Galan et al.,
	Groundwater	0.22	Lindsey et al., 2001
	Drinking water	0.09-0.113	Ye and Weinberg, 2007
Quinolones	WWTP effluent	0.20-1.4	Batt et al., 2007
	WWTP effluent	0.2-1	Brown et al., 2006
	WWTP effluent	0.05-0.45	Watkinson et al., 2009
	Hospital wastewater	0.85-35.5	Brown et al., 2006
	Hospital wastewater	0.2-101	Lindberg et al., 2004
	Surface water	4	Campagnolo et al., 2002
	Surface water	0.03-0.12	Kolpin et al., 2002
	Drinking water	0.087-0.103	Ye and Weinberg, 2007
Macrolides	WWTP effluent	0.01-0.374	Göbel et al., 2004
	WWTP effluent	0.15-3.40	Watkinson et al., 2009
	WWTP effluent	0.011-0.199	McArdell et al., 2003
	WWTP influent	0.005-0.5	Watkinson et al., 2009
	Surface water	0.56-1.70	Hirsch et al., 1999
	Surface water	0.009-0.041	Managaki et al., 2007
	Surface water	0.5	Campagnolo et al., 2002
	Groundwater	1.4	Campagnolo et al., 2002

2.3. Possible Adverse Effects of Antibiotics in the Environment

2.3.1. Toxic Effects

The toxic effects of antibiotics on aquatic and terrestrial organisms and on humans have been investigated and reported in literature. A well known side effect of antibiotics on human is allergic reactions (Mellon et al., 2001).

Additionally, antibiotics can exert toxic effects on some plants, soil microorganisms and they can inhibit biological processes (Costanzo et al., 2005; Liu et al., 2009). For instance, the results of Thiele-Bruhn and Beck's investigation (2005) showed that sulfapyridine and oxytetracycline at environmentally relevant concentrations, 0.003–7.35 mg/kg, inhibited microbial activity by 10% in top soils. The inhibition of several antibiotics on sewage sludge bacteria has also been reported (Halling-Sørensen, 2001; Halling-Sørensen et al., 2003).

The use of large amounts of antibiotics that have to be mixed with fish food also creates problems for public health and increases the risk for the presence of residual antibiotics in fish products (Cabello, 2006).

2.3.2. Antibiotic Resistance

Major adverse effect of antibiotic presence in various environmental matrices is the development of antibacterial resistance in microorganisms that represents a health risk to humans and animals (Kümmerer, 2004). The worst consequence is that the dangerous pathogens can immunize to all previously effective antibiotics and so giving rise to bacterial diseases that cannot be easily treated (Hawkey, 2008). Antibiotic resistance genes could be transferred to human body via the consumption of contaminated livestock, fish, crops, and water (Batt et al., 2006). Moreover, antibiotics can act as a kind of hormones in microbial environments (Fajardo and Martinez, 2008).

The contamination of aquatic and terrestrial environment with antibiotic via animal feeding operations, manure applications, hospital effluents, and sewage sludge systems

increases the development of resistance in microorganisms. In a recent study (Heuer and Smalla, 2007), it was reported that the application of manure containing sulfadiazine (10/100 mg/kg soil) to a silt loam and loamy sand soil increased the transferability of sulfadiazine resistance to *E. coli*. In another study, it was found that the growth rate of resistant bacteria increased upon increased tetracycline concentration in wastewater (Kim et al., 2007).

Considering the adverse effects of antibiotics in the environment their removal from water is an important issue

2.4. Treatment Technologies for Antibiotics

The conventional WWTPs including biological treatment processes have been shown to be ineffective for the removal of antibiotics (Kolpin et al., 2002; Xu, et al., 2007). Some studies (Carballo et al., 2007; Batt et al., 2007; Yu et al., 2009) reported that sorption on sludge was the principal removal mechanism for antibiotics during the conventional activated sludge treatment of wastewater and biodegradation had minor importance for removing most of these micropollutants (Gartiser et al., 2007; Mascolo et al., 2009). Although membrane bioreactors enhance the performance of biological processes, antibiotics mostly remain in final effluents and sludge (Watkinson et al., 2007; Göbel et al., 2007; Prado et al., 2009). However, oxidative processes such as chlorination (Qiang et al., 2006), chlorine dioxide (ClO_2) oxidation (Navalon et al., 2008), ozonation (Balcıoğlu and Ötker, 2003; Dodd et al., 2006; Dodd et al., 2009; Yalap and Balcıoğlu, 2009) and Fenton process (Uslu and Balcıoğlu, 2009) are effective for reducing the concentrations of some antibiotics. An integrated process, which combined biological (SBR) and oxidative steps (Fenton's reagent) was found as a feasible method for the treatment of antibiotics (Ben et al., 2009).

In water treatment, membrane filtration processes may provide effective barriers for the rejection of pharmaceuticals. While microfiltration and ultrafiltration membranes are effective only for a few antibiotics with low efficiency, nanofiltration and reverse osmosis are able to eliminate a wide range of antibiotics (Snyder et al., 2007). Besides the membrane processes UV treatment was applied to the removal of antibiotics from water

(Avisar et al, 2010). Similar to chemical oxidation processes, degradation products of target pollutants produced by this treatment process should be monitored.

2.5. Adsorption of Antibiotics

Due to the lack of the complete removal of antibiotics in conventional wastewater treatment plants and the risk of by-product formation during the removal of antibiotics by chemical oxidation processes, the performance of separation processes have to be investigated for the control of antibiotic pollution. Adsorption process by activated carbon and some alternative adsorbents can be a technologically feasible and economically viable method.

2.5.1. Sorption of Antibiotics on Clay Minerals

Figueroa et al. (2004) investigated the sorption interactions of three tetracycline antibiotics with two clays, montmorillonite and kaolinite under different pH values and ionic strength conditions. The results of this study indicate that antibiotic sorption on the clay minerals was controlled by the ionic functional groups of antibiotic.

Gao and Pedersen (2005) studied the adsorption of three sulfonamide to clay minerals, montmorillonite, and kaolinite as a function of pH, ionic strength, and type of exchangeable cation. They concluded that sulfonamide speciation and clay surface charge density were important factors for the sorption mechanism.

Pils and Laird (2007) reported a sorption study for two tetracycline antibiotics on clays, humic substances, and clay-humic complexes derived from two agricultural soils. The sorption performance of each adsorbent was greater than 96% and the highest sorption capacity was achieved with clays. The reason of decreasing sorption of tetracyclines with increasing pH value was explained by cation bridging and cation exchange. The distribution coefficient values of tetracycline antibiotics ranged from 2.2×10^4 to 7.8×10^4 kg/L for clays while these values were much lower for humic substances.

Kahle and Stamm (2007a) compared the sorption of sulfathiazole on clay minerals (montmorillonite, illite) and organic sorbents (compost, manure, humic acid). The sorption of sulfathiazole on the inorganic sorbents exhibited a pronounced pH dependence that was consistent with sorbate speciation and sorbent surface charge properties. They concluded that the sorption on the organic sorbents was 100 fold stronger than the sorption on the clay minerals independently from contact time and pH. While K_d value for the organic sorbents was determined in 100 -1000 kg antibiotic/kg range it was 0.1-1 kg antibiotic/kg for clay minerals.

As a result, clay minerals can be considered as alternative sorbents for the removal of antibiotics with sorption processes.

2.5.2. Sorption of Antibiotics on Soil

Boxall et al. (2002) performed a study to investigate the sorption behavior of a sulfonamide group antibiotic, sulfachloropyridazine in soil and the transport potential of the antibiotic from soil to surface and ground water. The results of this study showed that K_d value was low ranging from 0.9 to 1.8 L/kg that indicated the high mobility of the antibiotic in the soil.

Rabolle and Spliid (2000) investigated the sorption and mobility of four different antibiotic compounds (metronidazole, olaquindox, oxytetracycline and tylosin) in various soil types. Among other antibiotics oxytetracycline showed strong sorption in all investigated soil samples with the K_d values between 417 mL/g in sandy soil and 1026 mL/g in sandy loam. On the other hand, K_d values were ranged from 0.5 to 128 mL/g for other antibiotics studied.

Loke et al. (2002) determined the distribution coefficients of four model antibiotics (oxytetracycline, tylosin A, olaquindox and metronidazole) in manure. The distribution coefficients of oxytetracycline and tylosin were smaller in the manure than those found in the soil. This result was explained by the strong complex forming potential of oxytetracycline with divalent cations which are found in higher concentration in the soil compare to the manure.

In conclusion, the behavior of antibiotics in soil matrices has been recognized as one of the significant issue for the fate of them in the environment.

2.5.3. Sorption of Antibiotics on Activated Carbon

Rivera-Utrilla et al. (2009) presented a study to analyze the performance of activated carbon for nitroimidazole antibiotics sorption. The results showed that the sorption behavior of nitroimidazoles was dependent upon the chemical properties of activated carbon and the pH of solution did not have an important effect on sorption since non-electrostatic interactions were responsible for the sorption.

Putra et al. (2009) studied the adsorption amoxicillin on both bentonite and activated carbon at acidic and neutral pH values. As opposed to the results of Rivera-Utrilla et al. (2009) in this study, pH affected the sorption kinetics of amoxicillin on the activated carbon. It was deduced that chemisorption is the dominant adsorption mechanism in case of bentonite. On the other hand, both physisorption and chemisorption were suggested as responsible adsorption mechanisms for the activated carbon. Activated carbon showed higher removal capacity for amoxicillin compared to bentonite.

Choi et al. (2008) reported the removal of sulfonamide and tetracycline group antibiotics from deionized water and DOC water by powdered activated carbon sorption. The results demonstrated that tetracycline group antibiotics were more easily adsorbed on activated carbon compared to sulfonamide group antibiotics. It was suggested that the presence of phenolic groups in the structure of tetracycline and complex formation potential of tetracycline with metal and metal oxide on the surface of activated carbon can be responsible for the higher sorption of them.

More recently, Kim et al. (2010) studied the adsorption characteristics of trimethoprim onto granular and powdered activated carbon. Kinetic studies revealed that the rate of adsorption on the powdered activated carbon was more rapid than that of GAC. Similar to the results of Putra et al. (2009) the solution pH affected the sorption kinetics trimethoprim on the activated carbon.

2.6. Mechanism of Adsorption

2.6.1. Theoretical Information about Sorption Kinetics

Kinetics of adsorption has an important role on designing and modeling the process since it helps to determine the adsorption rate and rate controls the residence time of adsorbate at solid liquid interfaces. In the kinetic studies as well as contact time properties of adsorbent (e.g. size and amount), physico-chemical conditions (e.g. agitation speed, pH and temperature solution, presence of competitive ions) under which adsorption is carried out affect the rate of adsorption.

In order to evaluate the adsorption mechanism numerous kinetic models based on reaction and diffusion have been developed by evaluating the experimental data obtained at equilibrium period. The pseudo-first-order equation, the pseudo-second-order equation, Elovich equation, and intraparticle diffusion equation are frequently used to evaluate adsorption kinetics.

2.6.1.1. The Pseudo-First-Order Model. Lagergren's first order rate equation which has been called pseudo-first-order model was probably first kinetic model developed and has been widely used to describe the adsorption of metals, organics, and organism from water (Ho and McKay, 1998). The pseudo-first-order kinetic equation is based on adsorbent capacity and it is described by the following equation:

$$\frac{dq}{dt} = k_1(q_e - q_t) \tag{2.1}$$

where, q_e (mg/g) is the sorption concentration at equilibrium which can be determined experimentally or predicted by kinetic models and q_t (mg/g) is the sorption concentration at time t, k_1 is pseudo-first-order sorption rate constant (1/min). By applying the initial condition qt = 0 at t = 0 Equation 2.1 can be integrated:

$$\ln\frac{q_e}{q_e - q_t} = kt \tag{2.2}$$

Equation 2.2 can be rearranged to the linear form:

$$\log(q_e - q_t) = \log(q_e) - \frac{k_1}{2.303}t \quad (2.3)$$

In many studies (e.g Aksu and Tezer, 2000; Chiou and Li, 2002, Cirini et al., 2007) the pseudo-first-order equation of Lagergren did not fit well with the whole range of contact time and is generally applicable over the initial stage of the adsorption processes. The model's assumption is that the adsorption is preceded by diffusion through a boundary and the variation of solute uptake rate with time is directly proportional to difference in saturation concentration and the amount of solid uptake at certain time (Cirini et al., 2007).

2.6.1.2. The Pseudo-Second-Order Model. The pseudo-second-order model can be represented in the following form (Ho and McKay, 1999):

$$\frac{dq}{dt} = k_2(q_e - q_t)^2 \quad (2.4)$$

where q_e and q_t (mol/g) are the sorption concentration at equilibrium and at time *t*, respectively, and k_2 (g/mol min) is the rate constant of pseudo-second-order model. After integrating equation for initial conditions qt=0 at t=0, the following form of equation can be obtained:

$$\frac{t}{q_t} = \frac{1}{k_2 q_e^2} + \frac{t}{q_e} \quad (2.5)$$

Depending on its suitable paraphrasing of the experimental data for most of adsorbent/adsorbate systems, the pseudo-second-order model has been widely used and it is more likely to predict the behavior over the whole range of adsorption (McKay and Ho, 1999a,b). The pseudo-first-order model based on assumption that the rate limiting step can be chemical sorption involving valency forces through sharing or exchange of electrons between sorbent and sorbate (Ho and McKay, 1998; Ho and McKay, 2000). According to this model the sorption equilibrium concentration (q_e) has an influence on the kinetics of sorption reaction (Ho and McKay, 2000).

2.6.1.3. Elovich Model. This model has previously been used to describe the chemisorption mechanism of gas molecules on some sorbents (Low, 1960). However, there are some applications in liquid systems (Demirbas et al., 2004; Wong et al., 2008). The Elovich equation is generally expressed as the following equation (Ho and McKay, 2004):

$$\frac{dq}{dt} = a\, e^{(-bqt)} \tag{2.6}$$

where q_t (mol/g) is the sorption concentration at time t, a (mmol/g min) is the initial adsorption rate and b is related to the extent of surface coverage and the activation energy involved in chemisorption (g/mmol) (Teng and Hsieh, 1999).

For the initial conditions from qt=0 at t = 0, the integrated form of Equation 2.7 becomes,

$$q_t = \frac{1}{b}\ln(t + t_0) - \frac{1}{b}(\ln t_0) \tag{2.7}$$

where t_0 =1/ab. If $t>>t_0$, equation can be simplified as;

$$q_t = \frac{1}{b}\ln(ab) + \frac{1}{b}\ln t \tag{2.8}$$

The assumption of $t>>t_0$ is checked by trial and error method.

Elovich model which describes chemical adsorption mechanism (Cheung et al., 2001) is suitable for systems with heterogenous adsorbing surface. Elovich model assumes that the active sites of adsorbents exhibit different activation energy for the sorption of pollutants (Teng and Hsieh, 1999).

2.6.1.4. Intraparticle Diffusion Model. The intraparticle diffusion approach can be described by the following equation (Weber and Morris, 1963):

$$q_t = k_p\sqrt{t} \tag{2.9}$$

where q_t (mg/g) is the concentration of antibiotics sorbed at time t and k_p (mg/g $min^{0.5}$) is the intraparticle diffusion rate.

In literature the intraparticle model has been applied in three different forms:

1- q_t is plotted versus $t^{1/2}$ to get a straight line that passes through the origin (Serpen et al., 2007; Zhang et al., 2007).

2- The plot of q_t against $t^{1/2}$ can present a multi-linearity, which indicates that two or three steps are involved to follow the whole process (Sun and Yang, 2003; Wang and Li, 2007; Lorenc-Grabowska and Gryglewicz, 2005). In such a case, the first sharper step is the external surface adsorption or instantaneous adsorption. The second portion describes the gradual adsorption step, where intraparticle diffusion is controlled. The third step is the final equilibrium step, where the solute moves slowly from larger pores to micropores causing a slow adsorption rate.

3- q_t is plotted versus $t^{1/2}$ to get a straight line that does not pass through the origin. In such a case there is an intercept (Senthilkumaar et al., 2005; Tseng et al., 2003).

$$q_t = k_p\sqrt{t} + C \tag{2.10}$$

C is the intercept and the values of C give an idea about the thickness of boundary layer. The larger the intercept the greater the boundary layer effect is (McKay et al., 1980).

A summary of kinetic model equations are presented in Table 2.3.

Table 2.3. Kinetic model equations.

Kinetic Model	Equation	Linear Form of Equation	Plot
Pseudo-first-order	$\frac{dq}{dt} = k_1(q_e - q_t)$	$\log(q_e - q_t) = \log(q_e) - \frac{k_1}{2.303}t$	$\log(q_e\text{-}q_t)$ vs. t
Pseudo-second-order	$\frac{dq}{dt} = k_2(q_e - q_t)^2$	$\frac{t}{q_t} = \frac{1}{k_2 q_e^2} + \frac{t}{q_e}$	t/qt vs. t
Elovich	$\frac{dq}{dt} = a\, e^{(-bqt)}$	$q_t = \frac{1}{\beta}(\ln(\alpha\beta) + \ln t)$	q_t vs. ln t
Intraparticle diffusion		$q_t = k_p\sqrt{t}$ $q_t = k_p\sqrt{t} + C$	qt vs. $t^{0.5}$

2.6.2. Theoretical Information about Sorption Isotherms

In the design of sorption systems, sorption isotherms have fundamental importance. Adsorption isotherm describes the equilibrium relationships between sorbent and sorbate at constant temperature and represents the amount of sorbate bound at the surface of a sorbent as a function of the sorbate concentration in solution phase. There are several models to describe the experimental data of adsorption isotherms.

2.6.2.1. Langmuir Isotherm. The Langmuir model is based on reaction hypothesis and often used to describe sorption of a solute from a liquid solution (Langmuir, 1918). This model indicates that uptake of an adsorbate occurs on homogeneous surface of an adsorbent by monolayer sorption without interaction between sorbed molecules. Put another way, the model assumes uniform energies of adsorption onto the surface and no transmigration of adsorbate in the plane of the surface. The Langmuir isotherm equation is represented by the following equation:

$$q_e = \frac{q\, K_L C_e}{1 + K_L C_e} \tag{2.11}$$

where C_e (mg/L) is the equilibrium concentration of the adsorbate in the aqueous solution, q_e (mg/g) is the equilibrium adsorption concentration of adsorbent, q and K_L are characteristic constants of the Langmuir equation related to maximum adsorption capacity and energy of adsorption, respectively.

2.6.2.2. Freundlich Isotherm. The Freundlich isotherm is the earliest known model describing the sorption equation. Model is based on the relation between adsorbed quantity and remained solute concentration. This empirical isotherm indicates non-ideal sorption that involves heterogeneity of the adsorption sites and is expressed by the following equation:

$$q_e = K_F C_e^{\frac{1}{n}} \tag{2.12}$$

where q_e is the solid phase adsorbate concentration (mg/g) in equilibrium, C_e the equilibrium liquid phase concentration (mg/L), K_F (mg/g)(L/mg)^n the Freundlich constant which indicates adsorption capacity and 1/n is the heterogeneity factor.

2.6.2.3. Temkin Isotherm. The Temkin isotherm model considers the effects of the heat of adsorption that decreases linearly with coverage of adsorbent and adsorption is characterized by a uniform distribution of binding energies, up to some maximum binding energy (Temkin and Pyzhev, 1940). Temkin isotherm is represented by the following equation:

$$q_e = \frac{RT}{b} \ln (K_T C_e) \tag{2.13}$$

where RT/b =B_1 and B_1 is related to the heat of adsorption, T (K°) is the absolute temperature, R is the universal gas constant, 8.314 J/mol K^o, K_T (L/mg) the equilibrium binding constant.

2.6.2.4. Redlich-Peterson Isotherm. The Redlich-Peterson isotherm model is represented by incorporating the features of the Langmuir and Freundlich isotherms into a single equation (Redlich and Peterson, 1959).

$$q_e = \frac{K_{RP} C_e}{1 + a C_e^{\beta}} \tag{2.14}$$

where K_{RP} (L/g) and a (L/mg) are the Redlich–Peterson model isotherm constants and β is the Redlich–Peterson model exponent. The exponent β varies between 1 and 0. At low concentrations the Redlich–Peterson isotherm approximates to Henry's law and at high concentrations its behavior approaches that of the Freundlich isotherm. This model is applied to adsorbents that are heterogeneous and can function by more than one mechanism.

The equation of Langmuir, Freundlich, Temkin, and Redlich-Peterson isotherm models and their linear forms are listed in the Table 2.4.

Table 2.4. The equations of adsorption isotherm.

Isotherm	**Equation**	**Linear form of equation**	**Plot**
Freundlich	$q_e = K_F \times C_e^n$	$\log q_e = n \log C_e + \log K_F$	$\log q_e$ vs. $\log C_e$
Langmuir	$q_e = \frac{q K_L C_e}{1 + K_L C_e}$	$\frac{C_e}{q_e} = \frac{C_e}{q} + \frac{1}{K_L q}$	C_e/q_e vs. C_e
Temkin	$q_e = B_1 \ln(K_T C_e)$	$q_e = B_1 \ln K_T + B_1 \ln C_e$	q_e vs. $\ln C_e$
Redlich-Peterson	$q_e = \frac{K_{RP} C_e}{1 + a C_e^{\beta}}$	$\ln\left(K_{RP} \frac{C_e}{q_e} - 1\right) = \ln a + \beta \ln C_e$	$\ln[(K_{RP}C_e/q_e)-1]$ vs. $\ln C_e$

3. MATERIALS AND METHODS

3.1. Materials

3.1.1. Antibiotics

Sulfamethazine, sulfamethoxazole and hydrochloride salt of oxytetracycline were used as model antimicrobial compounds in the adsorption experiments. All antibiotics were analytical grade and purchased from Sigma Aldrich. Stock solution of SMZ and SMX were prepared freshly in acetone while stock solution of OTC was prepared freshly with deionized water. Deionized water was used to dilute the stock solutions while preparing the desired concentrations of antibiotics. The properties and chemical structure of antibiotics are represented in Table 3.1 and 3.2, respectively.

Table 3.1. Properties of SMZ, SMX and OTC.

Antibiotic	**Molecular Weight (g/mol)**	**Water solubility (mg/L)**	**pKa**	**Log K_{ow}**
Sulfamethazine (SMZ)	278.33	1500	$pKa_1 = 2.3$[a] $pKa_2 = 7.4$[a]	0.80[a]
Sulfamethoxazole (SMX)	253.28	610	$pKa_1 = 1.8$[a] $pKa_2 = 5.6$[a]	0.89[a]
Oxytetracycline (OTC)	460.44	1000	$pKa_1 = 3.6$[b] $pKa_2 = 7.52$[b] $pKa_3 = 9.88$[b]	-1.19[c]

[a]Goa et al., 2005

[b]Lindsey et al., 2001

[c]Tolls, 2001

Table 3.2. Chemical structure of SMZ, SMX and OTC.

Antibiotic	Molecular structure
Sulfamethazine $C_{12}H_{14}N_4O_2S$	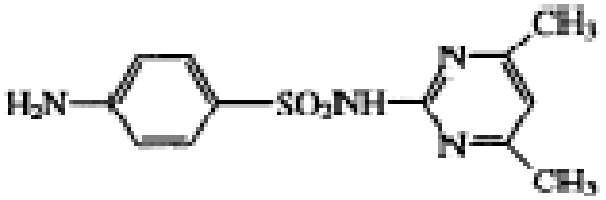
Sulfamethoxazole $C_{10}H_{11}N_3O_3S$	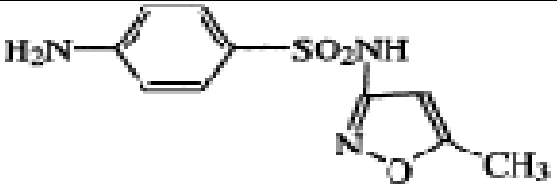
Oxytetracycline $C_{22}H_{24}N_2O_9.2H_2O$	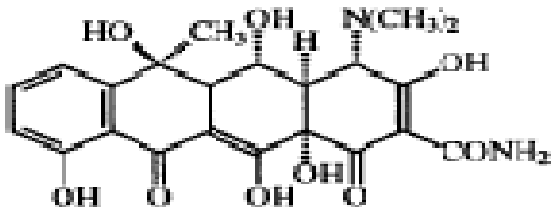

3.1.2. Adsorbents

Granular activated carbon (500μm – 1 mm) was used as adsorbent and provided from Riedel-de Haen. Unexpanded perlite (0 – 45 μm) and pumice (< 1 mm) were obtained from the region of Nevşehir. Natural zeolite (> 0.75μm) was provided by Ultra A.Ş., İzmir.

3.1.3. Other Chemicals

All other chemicals used in this study were of analytical grade and they are listed in Table 3.2.

Table 3.3. Chemicals used in the experiments.

Chemical Name	Formula	Experiment	Supplier
Sodium Hydroxide	NaOH	pH adjustment	Riedel de Haen
Hydrochloric Acid	HCl	pH adjustment	Riedel de Haen
Acetone	C_3-H_6-O	Solvation	Riedel de Haen
Sodium Acetate Trihydrate	$CH_3COONa{\cdot}3H_2O$	CEC determination	Riedel de Haen
Glacial Acetic Acid	CH_3COOH	CEC determination	Merck
Ammonium Hydroxide	NH_4OH	CEC determination	Riedel de Haen
2-Propanol (isopropyl alcohol)	$CH_3CH(OH)CH_3$	CEC determination	Merck

3.2. Methods

3.2.1. Characterization of Adsorbents

3.2.1.1. Determination of Cation Exchange Capacity (CEC). The sodium acetate method was applied to determine the CEC of adsorbents used in the study (http://www.epa.gov/wastes/hazard/testmethods/sw846/pdfs/9081.pdf). Adsorbents were shaked with excess sodium acetate solution (0.1 N). As a result, sodium cations were exchanged with cations on the sorbent surface. Afterwards, the sorbents were washed with isopropyl alcohol and ammonium acetate solution (1 N) was used to replace the sorbed sodium ions with ammonium ions. Lastly, atomic absorption spectroscopy (Perkin Elmer AAS 300) was used to determine the sodium concentration.

CEC of adsorbents is calculated by the following equation:

$$\text{CEC (meq/100 g)} = \frac{[\text{Na}] \text{ x V x DF x } 100}{\text{m x MV}} \quad (3.1)$$

where,

[Na]	= Na^+ concentration (mg/L)
V	= Volume of extract (L)
DF	= Dilution factor
m	= Weighed mass of adsorbent (g)
MV	= Molecular weight of sodium (23 g /mole = 23 mg/meq)

3.2.1.2. Surface Area Analysis. Quantachrome Nova 2200e Surface Areas and Pore Size Analyzer was used to conduct surface area, pore volume and pore size measurements. The multipoint BET technique was applied at 350˚C bath temperature and 200˚C outgas temperature. The analysis gas was nitrogen.

3.2.1.3. Fourier Transform Infrared (FTIR) Analysis. The FTIR analyses were conducted by Thermo Nicolet, FTIR 380 spectrometer, using a diamond ATR accessory. The FTIR spectrophotometer was set to scan in the region of 4000-500 (1/cm) with the resolution of 4 (1/cm).

3.2.1.4. X-ray Diffraction Analysis (XRD). XRD analysis was used to determine the crystalline phases and the basal spacing (d_{001} reflection) of adsorbents. The used equipment was a Rigaku D/MAX-2200 Ultima+/PC X-ray diffraction with CuKα radiation generated at 40 kV, 40 mA, a scanning speed of 2 deg. min^{-1} and 1.5-70 deg. scanning range. XRD analysis was also performed for the adsorbents that sorbed SMZ and OTC at pH 6.5.

3.2.1.5. Scanning Electron Microscopy (SEM) Analysis. The surface morphology of the adsorbents before and after sorption was investigated by SEM analysis (Philips XL-30 ESEM-FEG/EDX microscope). The samples were put on a holder and analysis was performed at 10-25 kV electron beam accelerating voltage. The energy dispersive X-ray

spectroscopy (EDX) was used to determine the semiquantitative surface elemental compositions of adsorbents. SEM and EDX analysis were also conducted after the adsorption of antibiotics on adsorbents within 4 hr period.

3.2.1.6. Elemental Analysis. The elemental analyses of adsorbents were accomplished by an elemental combustion system (Costech ECS 4010). The searched elements were carbon, nitrogen and hydrogen. After drying the samples, they were burned in an excess of oxygen at a temperature between 900°C and 1500°C (European Committee for Standardization, 2001). According to procedure the combustion temperature has to be high enough to convert the organic carbon completely to carbon dioxide. It was seen that during combustion temperature was 980ºC and appropriate to this range. The combustion products, N_2, CO_2 and H_2O, passed through a gas chromatographic (GC) separation column and they were detected with a high sensitivity thermal conductivity detector (TCD). The carrier gas was the Helium in this system.

3.2.1.7. Point of Zero Charge. The determination of point of zero charge (pH_{pzc}) of adsorbents was carried out by pH titration method (Rivera-Utrilla et al., 2001; Putra et al., 2009). According to the method, 50 ml of 0.01 M NaCl solution was placed into several erlenmeyer flasks. The pH of the solution was adjusted to a initial value of 2 to 6 for clay minerals and 2 to 9 for GAC by addition of 0.1 M HCl and 0.1 M NaOH. The adsorbent samples weighted as 0.15 g were added to the flasks and the final pH values were measured after 48 h. Final pH values were plotted against initial pH values and the pH at which pH_{final} equals to $pH_{initial}$ was defined as the pH_{pzc}.

3.2.2. Batch Adsorption Tests

Batch adsorption tests were performed by using, unexpanded perlite, pumice, zeolite, and GAC. A volume of 7.5 mL antibiotic solution at desired concentration and pH was placed in a polyethylene tube. pH of the solutions was adjusted with 0.1 M NaOH and 0.1 M HCl solutions. Accurately weighed natural minerals (10 g/L) and GAC (5 g/L) were then added to the solution. The tubes were sealed with screwed caps and wrapped with aluminum foil to eliminate the photodecomposition of antibiotics. Samples were agitated on a shaker (Julabo Shake Temperature SW 22) at 150 rpm for predetermined contact time

at 25 ^{0}C. The control experiments in the absence of sorbent were assembled in the same manner to account for possible antibiotic losses. Each run was done at least with duplicate samples. The calculations were done by taking the average values of duplicates. After equilibration, adsorbents were separated from the suspension by centrifugation (Eppendorf Centrifuge 5804) at 10,000 x g for 10 minutes and subsequently the natural minerals were filtered through a 0.45 μm membrane filter (Sartorius Minisart). Filtration was not needed for GAC samples due to the easy separation from supernatant. The supernatant was analyzed for the antibiotic concentration. The amount of the antibiotics adsorbed on adsorbents was calculated by a mass balance relationship. The effects of pH, GAC dosage, antibiotic concentration, and contact time on the adsorption efficiency were investigated in batch adsorption experiments.

The equilibrium time is the time required to attain the state of equilibrium and the amount of adsorption at equilibrium, q_e (mg/g), was calculated by the mass balance relationship as follows,

$$q_e = \frac{(C_0 - C_e)V}{W} \tag{3.2}$$

where C_0 and C_e are initial and equilibrium liquid phase concentrations of antibiotics (mg/L) respectively, V is the volume of solution (L) and W is the weight of adsorbent used (g).

3.2.3. Determination of Antibiotics by Spectrophotometric Analysis

The concentration of antibiotics in solution was evaluated by UV/Vis spectrophotometer (SHIMADZU UV-1208) at a wavelength corresponding to the maximum absorbance which varies depending upon the pH of solution. The spectra of SMZ, SMX, and OTC at different pH values studied were recorded between 243.5 – 262.5 nm, 257 – 265.5 nm, and 354.5 – 372 nm wavelengths, respectively. The calibration curves for each pH value were prepared separately (Table A.1-Figure A.1). The initial and final antibiotic concentrations were determined using these calibration curves. In agreement with the Lambert-Beer Law, a linear relationship was found between the concentration of

antibiotics and absorbance. When the absorbance value of solution exceeded 0.9, it was diluted.

3.2.4. Error Analysis Method

Besides the value of correlation coefficient (R^2), the applicability of both kinetic and isotherm models is verified through the sum of error squares (SSE). This analysis was used to determine goodness-of-fit between the experimental data points and the models predictions.

$$\mathrm{SSE} = \sum (q_{exp} - q_{cal})^2 \tag{3.3}$$

where q_{exp} is the experimental sorption concentration data and q_{cal} is the theoretical sorption kinetic model or isotherm model. The most appropriate model should have the least SSE value; therefore, this model can be obtained by comparing the SSE of each model.

4. RESULTS AND DISCUSSION

4.1. Characterization of Adsorbents

To determine the characteristic properties of adsorbents XRD, cation exchange capacity, surface area, FTIR, SEM, and elemental analyses were conducted.

4.1.1. X-Ray Diffraction Analysis (XRD) of Adsorbents

The mineralogical compositions of perlite, pumice, and zeolite were investigated by XRD analyses. The XRD patterns and the interlayer spacings d(Å) of adsorbents are presented in Figures 4.1, 4.2 and 4.3.

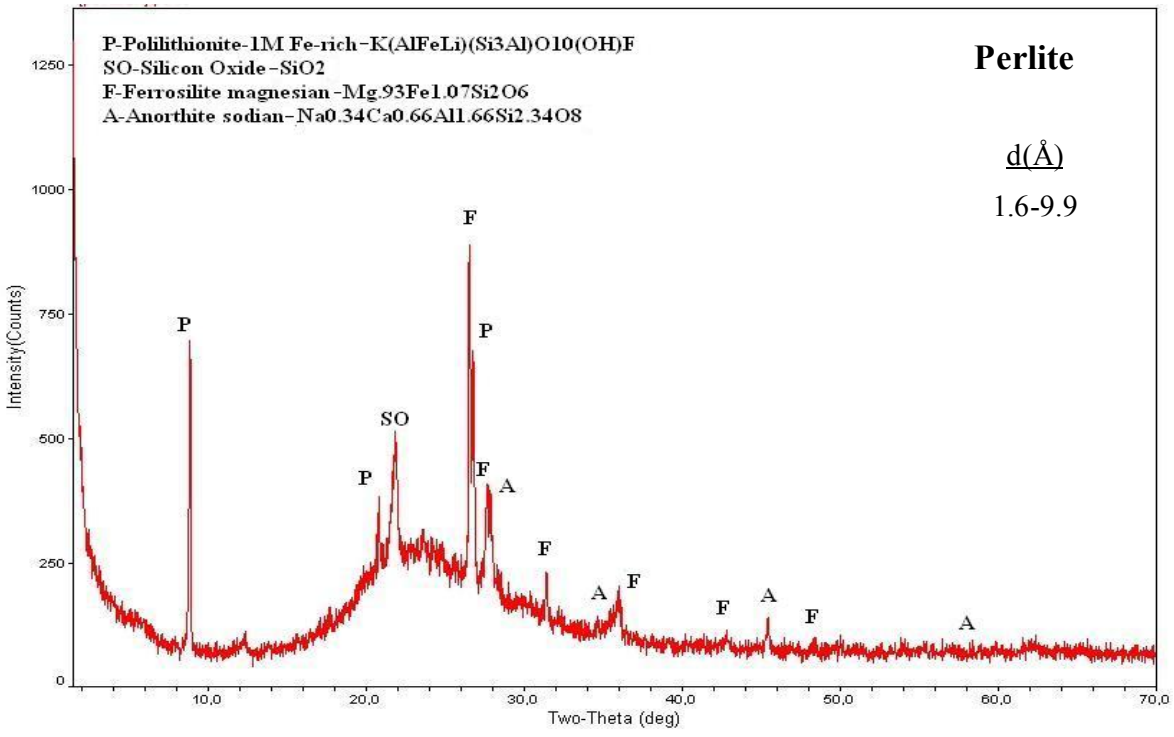

Figure. 4.1. XRD pattern of perlite.

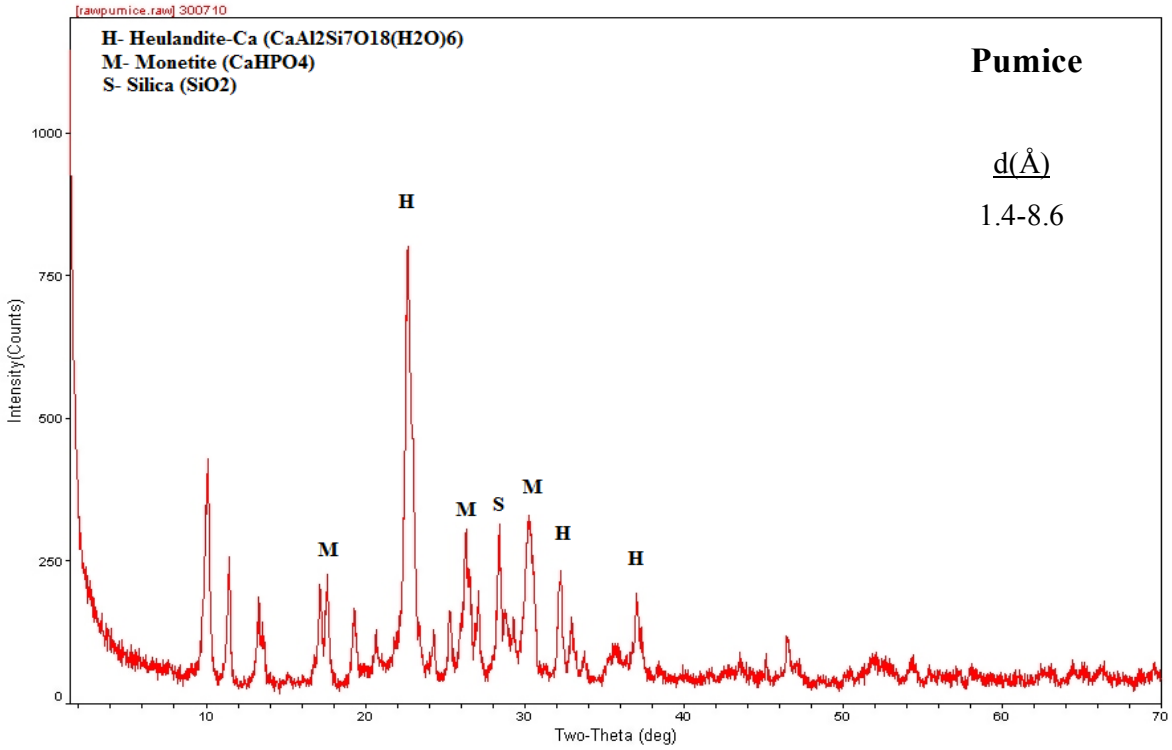

Figure. 4.2. XRD pattern of pumice.

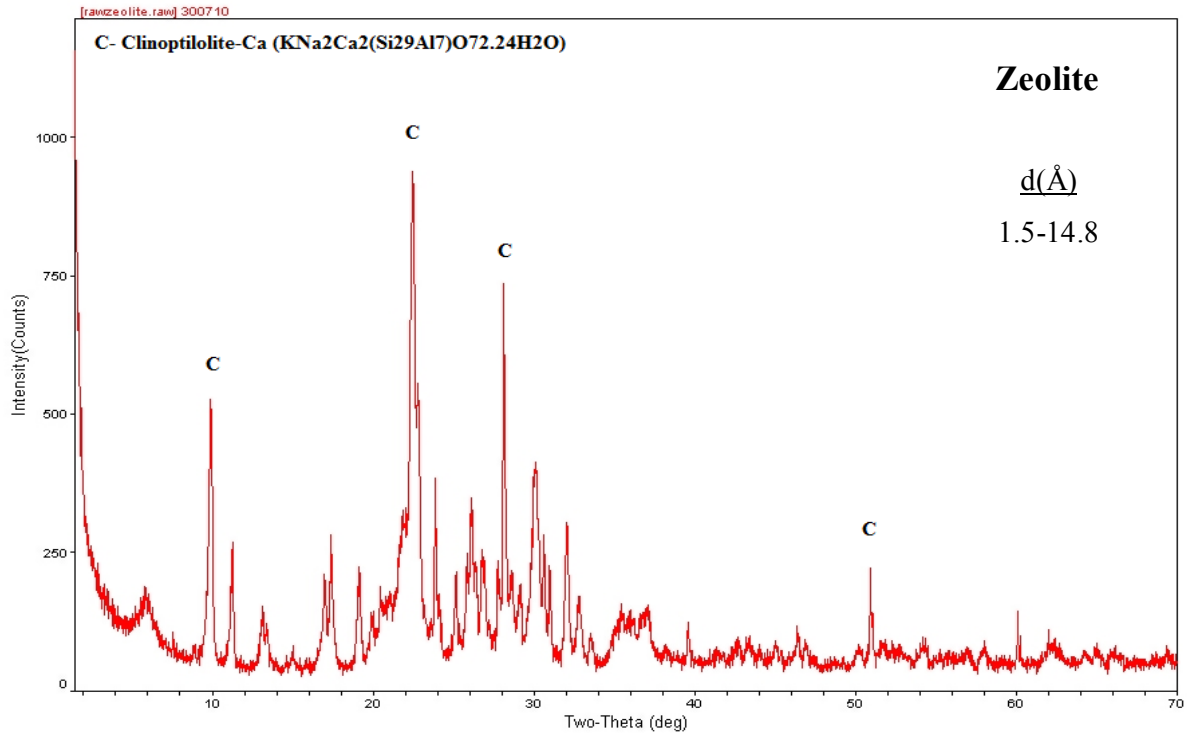

Figure 4.3. XRD pattern of zeolite.

According to the results shown in Figure 4.1 the most intense peaks of perlite were defined as Ferrosilite magnesian ($Mg.93Fe1.07Si_2O_6$) at 2θ= 26.600° (100 %) and Polilithionite-1M Fe-rich ($K(AlFeLi)(Si_3Al)O_{10}(OH)F$) at 2θ= 8.918° (94.6 %).

In the pumice XRD pattern of pumice (Figure 4.2), it can be seen that the most intense peak belongs to Heulandite-Ca ($CaAl_2Si_7O_{18}(H_2O)_6$) at 2θ= 23.038 (57.8 %) which is silicate mineral of zeolite group. Other peaks belong to Monetite ($CaHPO_4$) at 2θ= 30.340 (43.2 %) and Silica (SiO_2) at 2θ= 26.599 (29 %).

The zeolite has one intense peak that was identified as Clinoptilolite-Ca ($KNa_2Ca_2(Si_{29}A_{l7})O_{72}.24H_2O$) at 2θ=22.5 (100 %) (Figure 4.3).

4.1.2. Cation Exchange Capacity (CEC) Determination of Adsorbents

Recent studies indicated that cation exchange capacity of soil and some clays is a key factor influencing the sorption of some antibiotics (Vasudevan et al., 2009; Wang et al., 2010). Considering these results in this study the CECs of adsorbents were determined and the results are presented in Table 4.1.

Table 4.1. Cation exchange capacities of adsorbents.

Adsorbent	CEC (meq/100 g)
Perlite	21.9
Pumice	26.8
Zeolite	62.3

According to the data on Table 4.1, the highest CEC value is for zeolite as 62.3 meq/100 g. These values are comparable with those obtained by previous studies. For instance, the CEC value was determined for unexpanded perlite as 25.97 meq/100g (Doğan and Alkan, 2003); for pumice as 30 meq/100g (Panuccio et al., 2009); for zeolite as 57.2 and 60.5 meq/100g (Yukselen and Kaya, 2008).

4.1.3. Surface Area Analysis of Adsorbents

Surface area and porosity of adsorbent have a great importance for pollutant removal from water. Accordingly, specific surface area (SSA), total pore volume (V_t), and pore size (D_p) of adsorbents were investigated and the results are presented in Table 4.2, Appendix C1, C2, and C3.

Table 4.2. Surface and pore characteristics of adsorbents.

Adsorbents	SSA[a] (m^2/g)	V_t[b] (cm^3/g)	D_p[b] (Å)
Perlite	11.78	0.005	20.48
Pumice	32.73	0.015	13.65
Zeolite	20.25	0.009	16.80
GAC	930.3	0.45	11.96

[a]BET method

[b]Dubinin-Radushkevich method

The textural parameters of adsorbents presented in Table 4.2 shows a wide variation. GAC has the largest surface area and pore volume that provide an advantage for higher adsorption efficiency. On the other hand, pumice has larger surface area among natural minerals used in this study. The pore size value of perlite is higher than all other adsorbents.

4.1.4. Fourier Transformed Infrared (FTIR) Surface Analysis of Adsorbents

Before adsorption of antibiotics, FTIR spectra of natural minerals and GAC were recorded in the wavenumber region between 4000-400 cm^{-1} (Figure 4.4, 4.5).

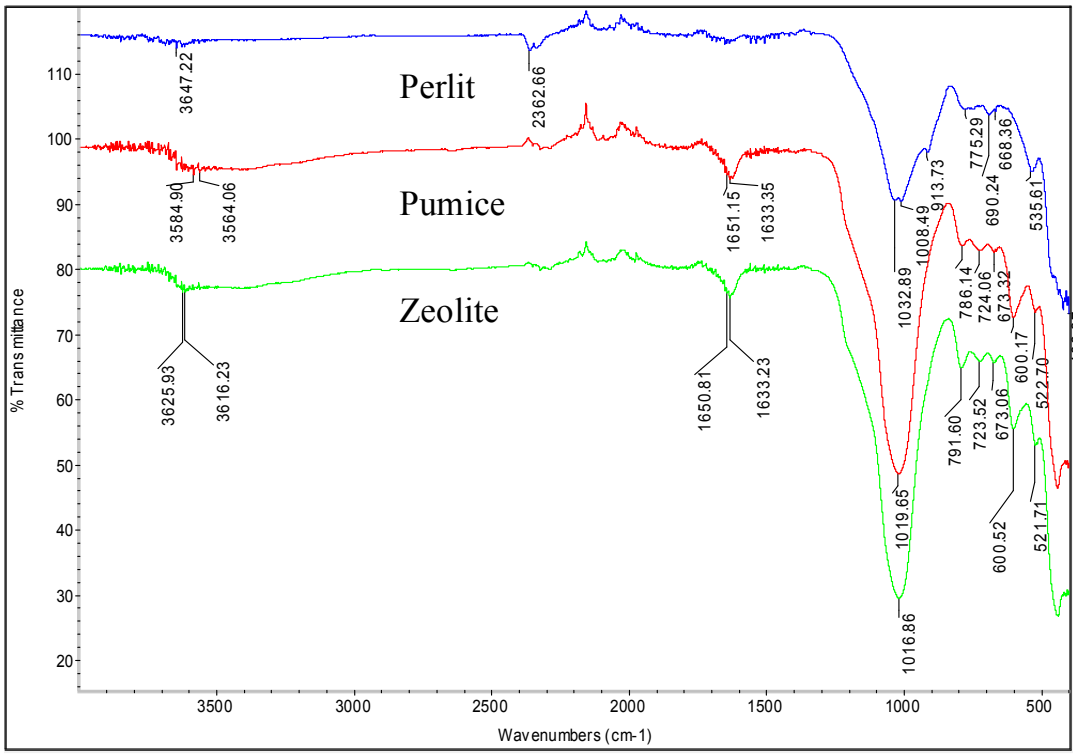

Figure 4.4. FTIR spectra of natural minerals.

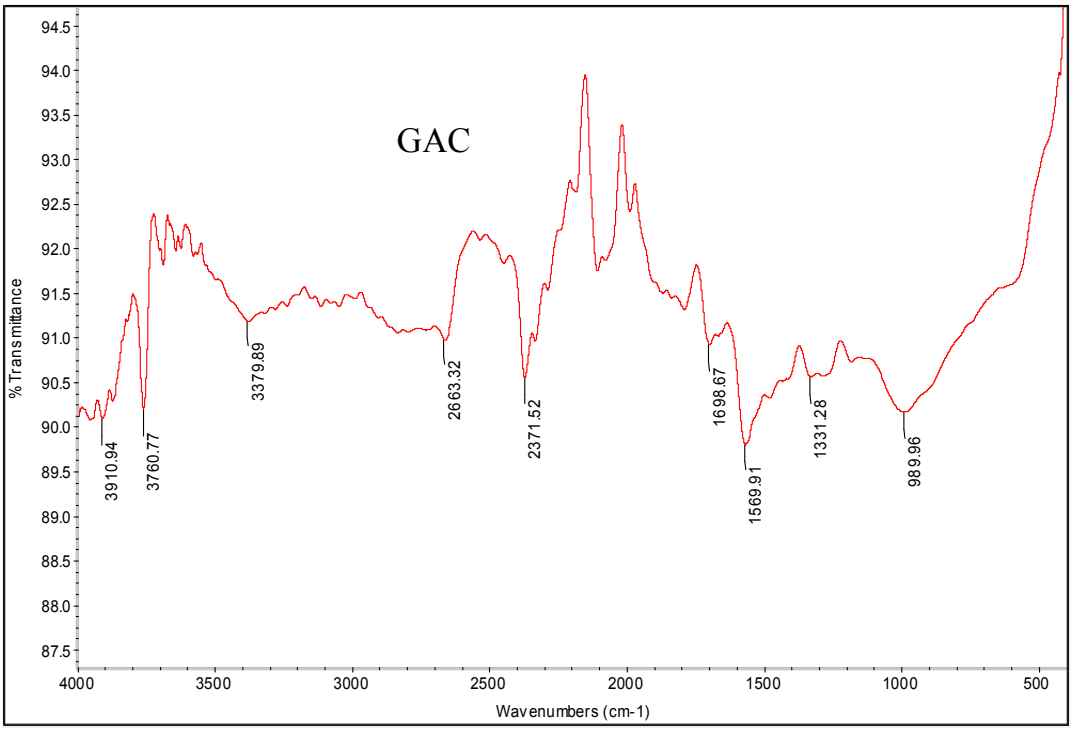

Figure 4.5. FTIR spectra of GAC.

According to the spectra (Figure 4.4), natural minerals show weak bands around 3500-3700 cm^{-1} which can be assigned to OH stretching of the water although samples were lyophilized. The bands near 3620 cm^{-1} may indicate the presence of inner hydroxyl groups, lying between the tetrahedral and octahedral sheets (Madejova, 2003). There are bands around 1630 cm^{-1} for pumice and zeolite that show the water deformation of clays (Chen et al., 2001). In addition, the strong peak around 1100 cm^{-1} can be attributed to Si–O stretching vibrations.

FTIR spectra of GAC were also determined as shown in Figure 4.5. The very broad peak near 3380 cm^{-1} was recognized to be O–H functional groups fr carboxyl and phenol (Goel et al., 2005). The band around 1690 cm^{-1} may indicate the presence of C=O group. There is also a peak at 1569 cm^{-1} corresponding to the aromatic ring stretching of both C=C and C=N groups (Mangun et al., 2001).

4.1.5. Scanning Electron Microscopy (SEM) of Adsorbents

The morphological properties of adsorbents were investigated by SEM and Energy Dispersive X-ray (EDX) analyses. The SEM images of perlite, pumice, zeolite, and GAC are shown in Figure 4.6, 4.7, 4.8, and 4.9 respectively.

Visual examination of unexpanded perlite by SEM (Figure 4.6) reveals the presence of amorphous material with inclusions of crystallites and small holes. Unexpanded perlite is a glassy volcanic rock that these holes might be formed by the slow freezing of lava.

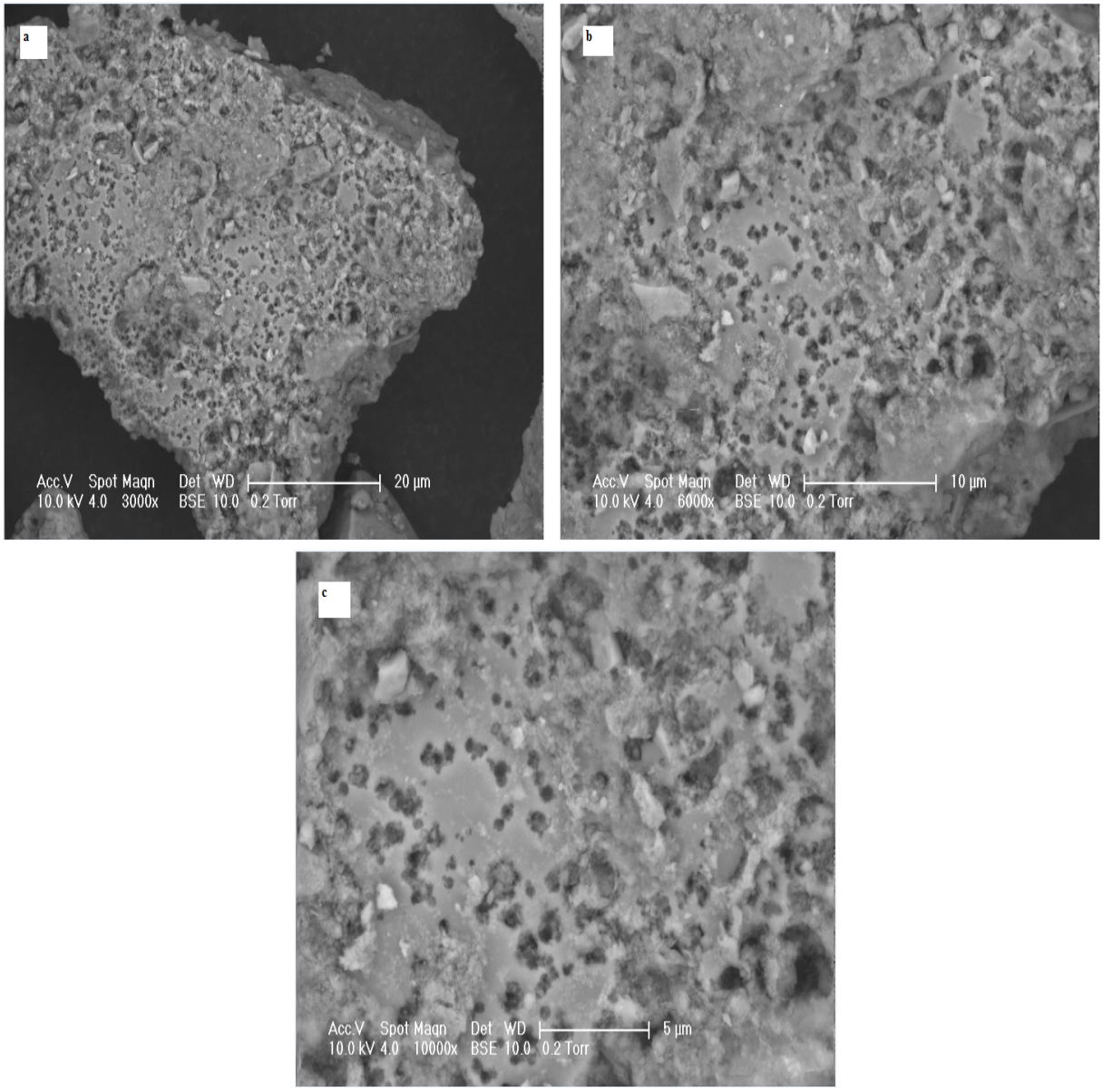

Figure 4.6. SEM images of perlite (a) 3000x, (b) 6000x, (c) 10000x.

As can be seen in the SEM photograph of pumice (Figure 4.7), there are irregular particles in a wide range of size, both inter- and intra-particle voids and fibrous cavities. The heterogeneous structure was deduced from the EDX analysis taken on different sites of pumice sample.

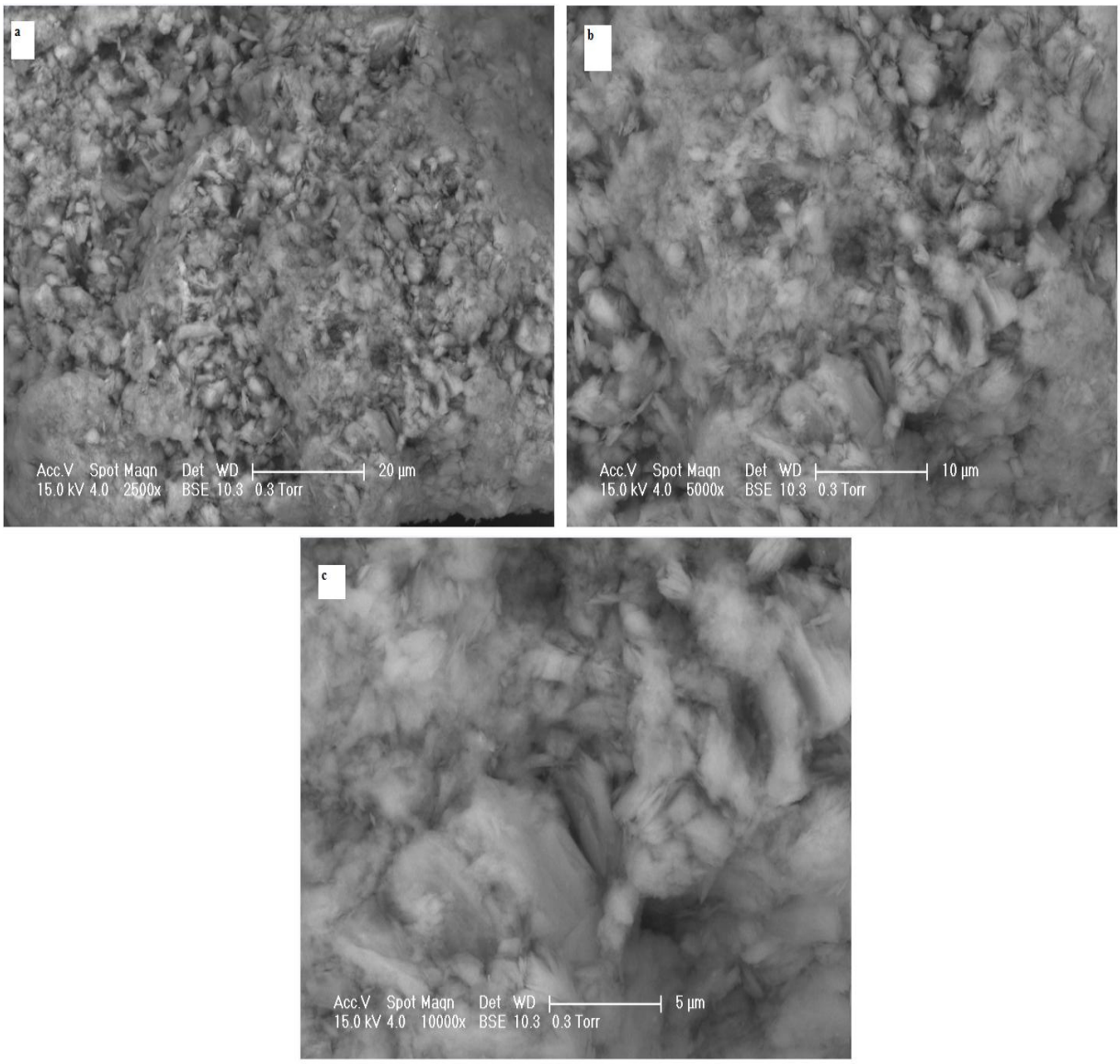

Figure 4.7. SEM images of pumice (a) 2500x, (b) 5000x, (c) 10000x.

SEM images (Figure 4.8) shows that zeolite has a heterogeneous surface morphology. The coffin- and cubic-like flat and well defined shaped crystals can be easily seen.

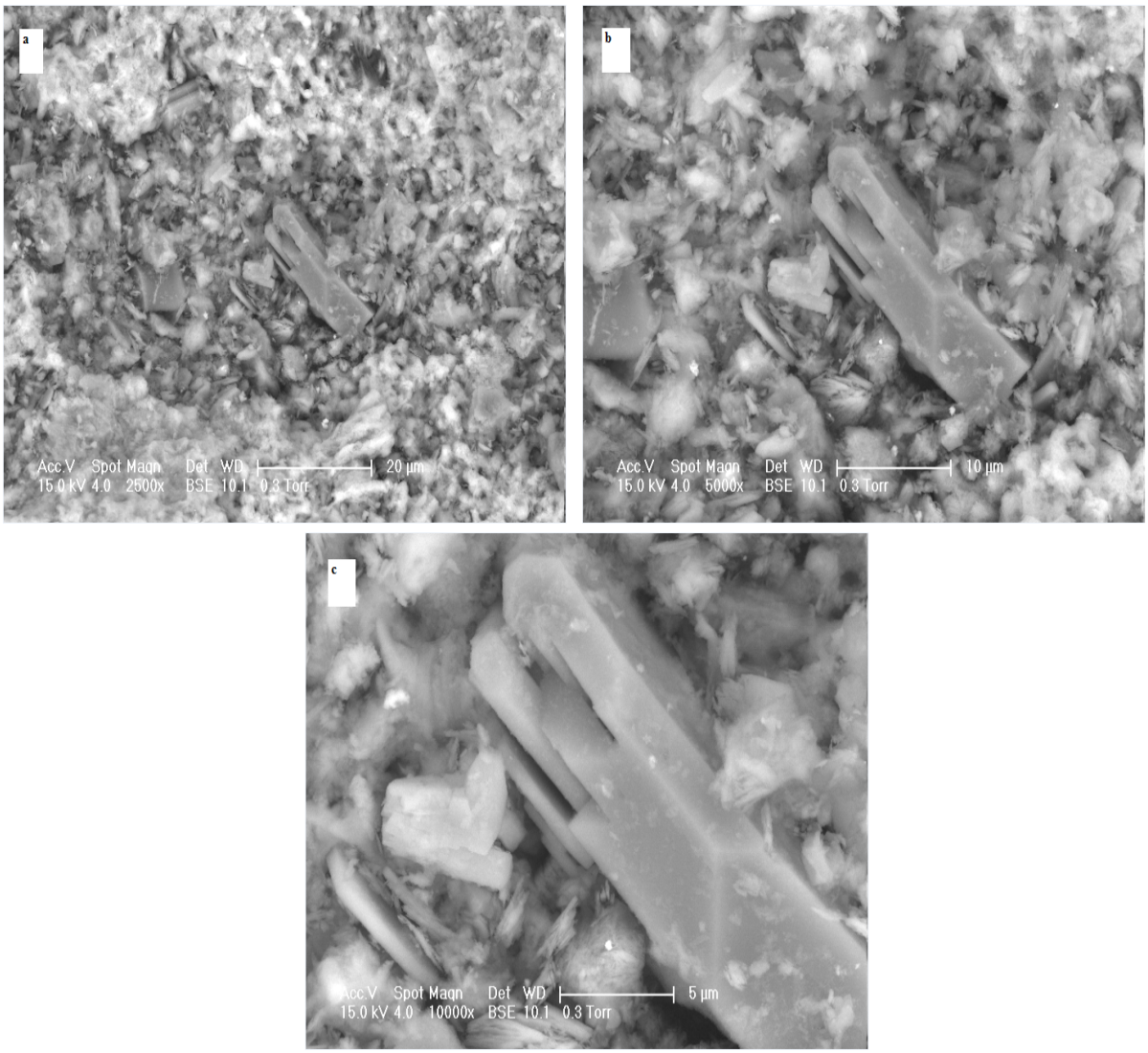

Figure 4.8 SEM images of zeolite (a) 2500x, (b) 5000x, (c) 10000x.

Figure 4.9 demonstrates that there are considerable small cavities and cracks on the surface of GAC. Also the surface looks spongy.

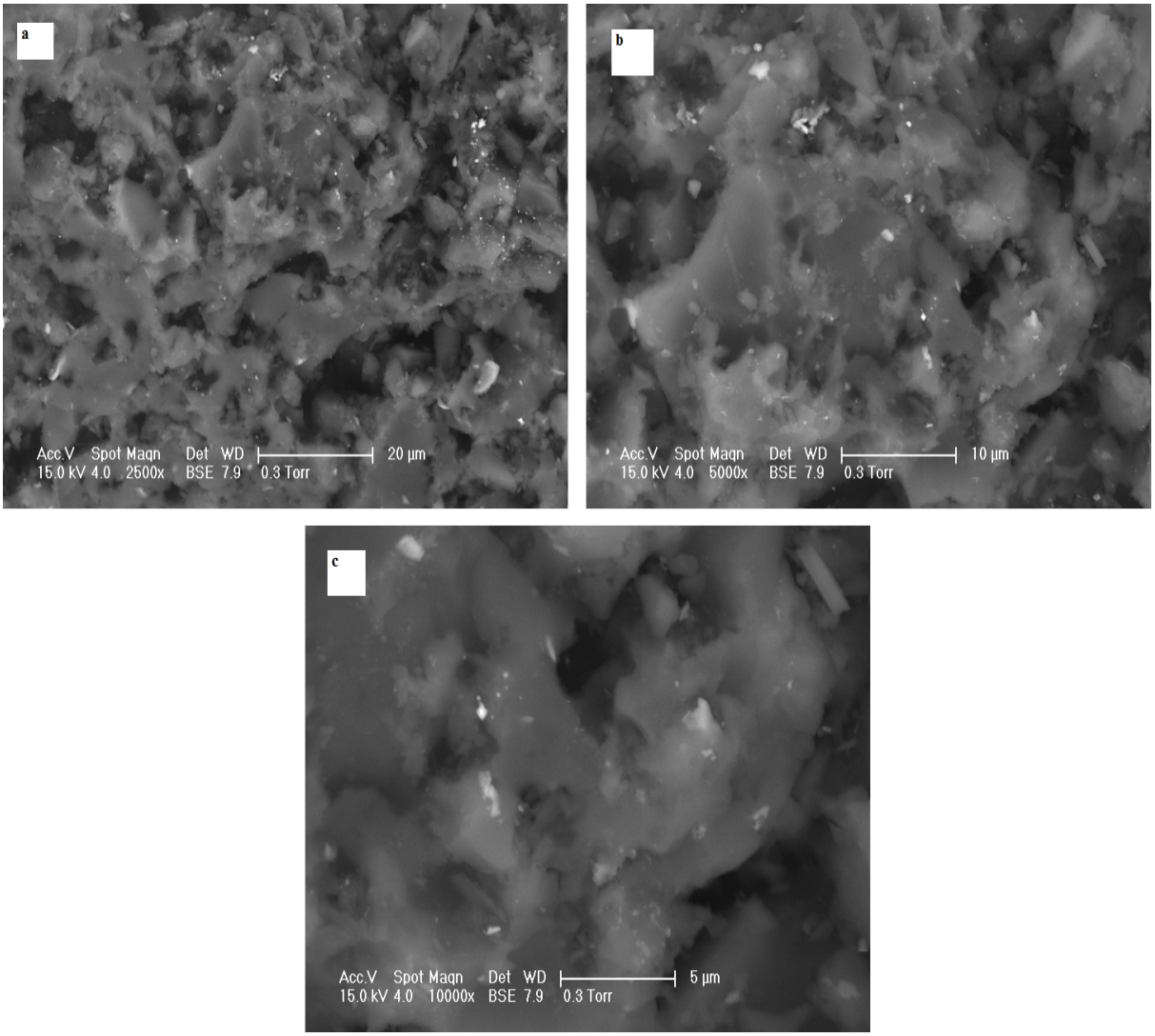

Figure 4.9. SEM images of GAC (a) 2500x, (b) 5000x, (c) 10000x.

Figure 4.9 demonstrates that there are considerable small cavities and cracks on the surface of GAC. Also the surface looks spongy.

The elements found in the structure of natural minerals and GAC were determined by EDX analysis to discuss their function in the adsorption (Table 4.3).

Table 4.3. EDX analysis of adsorbents.

Element	Perlite	Pumice	Zeolite	GAC
		(wt %)		
C K	16.84	21.03	25.85	87.88
O K	29.83	40.82	33.53	5.81
Na K	1.36	1.00	1.67	0.40
Mg K	1.13	1.27	1.77	0.40
Al K	12.50	5.87	9.97	0.91
Si K	21.45	25.26	19.05	0.58
K K	6.34	1.49	0.30	0
Ca K	1.35	1.87	2.04	0.18
Ti K	0.47	0.15	0.35	0.23
Fe K	3.78	0.43	2.56	1.26
Cu K	4.96	0.81	1.36	0.77
Total	**100**	**100**	**100**	**100**

As seen from Table 4.3, natural minerals have high silica contents and the highest amount belongs to pumice. The silanol groups at the external surface of silicate act as neutral adsorption sites and usually they are accessible to organic species (Liu and Zhang, 2007). While natural minerals exhibits higher sorption capacities for OTC (Erdinç, 2009; Avisar, 2010), it is evident that organic materials seem to be much stronger sorbents for sulfonamides than mineral phases (Gao and Pedersen, 2005).

In order to investigate the changes of surface morphology of adsorbents, SEM analyses were conducted after the sorption of antibiotics onto adsorbents (Figure 4.10).

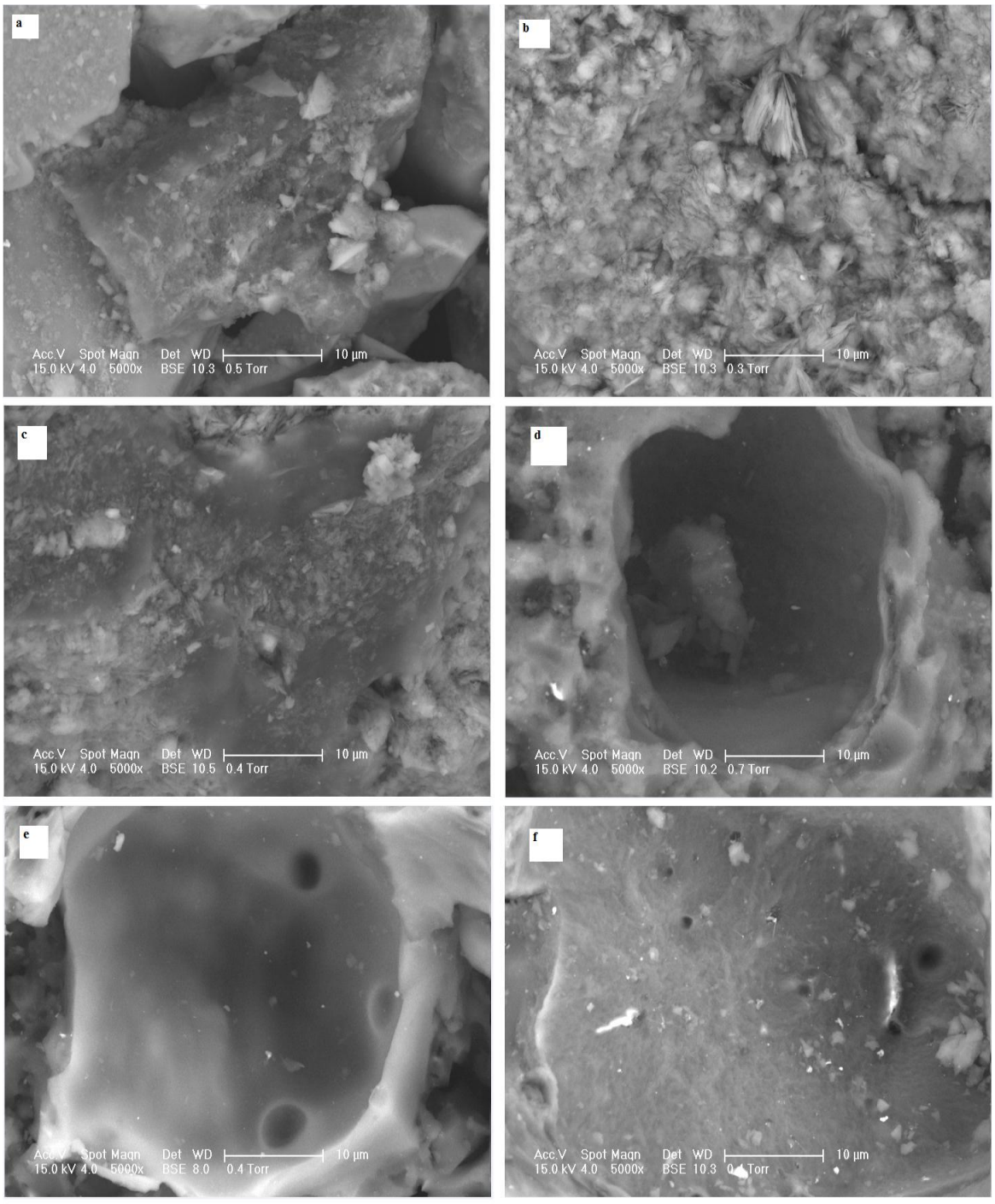

Figure 4.10. SEM images of adsorbents after sorption (a) perlite+SMZ, (b) pumice+SMZ, (c) zeolite+SMZ, (d) GAC+SMZ, (e) GAC+SMX, (f) GAC+OTC.

As shown in Figure 4.10, all sorbents surface images were changed after sorption with antibiotics. The surface is seen like coated with antibiotic solutions. The EDX results are presented in Table 4.4.

Table 4.4. EDX analysis of adsorbents after sorption of antibiotics.

Element	**Perlite**	**Pumice**	**Zeolite**	**GAC[a]**	**GAC[b]**	**GAC[c]**
			(wt %)			
C K	26.01	15.42	51.36	81.20	75.18	83.99
O K	38.47	37.79	32.25	7.45	5.58	8.30
Na K	0.74	0.94	1.06	0.53	0.37	0.47
Mg K	1.05	1.15	1.39	0.48	0.51	0.43
Al K	8.74	6.73	14.18	5.21	14.53	1.94
Si K	19.66	30.33	17.00	0.55	0.55	0.62
P K	0	0.42	0.27	0.35	0.14	0.40
S K	0.20	0.35	0.43	1.24	0.85	1.18
K K	1.90	2.03	1.35	0.28	0.15	0.57
Ca K	0.65	2.37	0.98	0.42	0.15	0.59
Ti K	0.45	0.23	0.41	0.44	0.09	0.60
Fe K	1.75	0.85	1.40	0.40	0.51	0.56
Cu K	0.39	1.40	1.50	1.45	1.40	0.35
Total	**100**	**100**	**100**	**100**	**100**	**100**

a- after sorption of SMZ

b- after sorption of SMZ

c- after sorption of OTC

As seen from Table 4.4, for perlite and zeolite the carbon content was increased after sorption of SMZ. Surface complexation and cation exchange can be responsible for the adsorption of antibiotics on natural mineral and soil (Pils and Laird, 2007; Wang et al., 2010). Multivalent cations can form bridges with tetracycline and sulfonamide group antibiotics on the surface of some minerals (Gao and Pedersen, 2005; Kahle and Stamm, 2007a; Kahle and Stamm, 2007b). However, for other adsorbents there was not a pronounced change in the carbon content after the sorption of antibiotics.

4.1.6. Elemental Analysis of Adsorbents

The elemental analyses of adsorbents were performed to determine the carbon and nitrogen content of adsorbents. The results are presented in Table 4.5.

Table 4.5. Elemental content of adsorbents.

Adsorbent	Carbon	Nitrogen
	Weight (%)	
Perlite	0.075	0.08
Pumice	0.055	0.09
Zeolite	0.125	0.125
GAC	76.75	0.89

Carbon content of adsorbents determined by elemental and EDX analysis exhibited significant variation probably due to the adhesive used in SEM analysis.

4.1.7. Point of Zero Charge of Adsorbents

The pH_{pzc} can be defined as a point where the adsorbent have zero potential charge on its surface. The potential surface charges of adsorbents may be change by the solution pH. If the pH of the solution is below its pH_{pzc} the solution donates more protons than hydroxide groups, and so the adsorbent surface is positively charged. Conversely, if the pH of the solution is above its pH_{pzc} the surface is negatively charged. Figure 4.11 shows the pH drift results of all adsorbents.

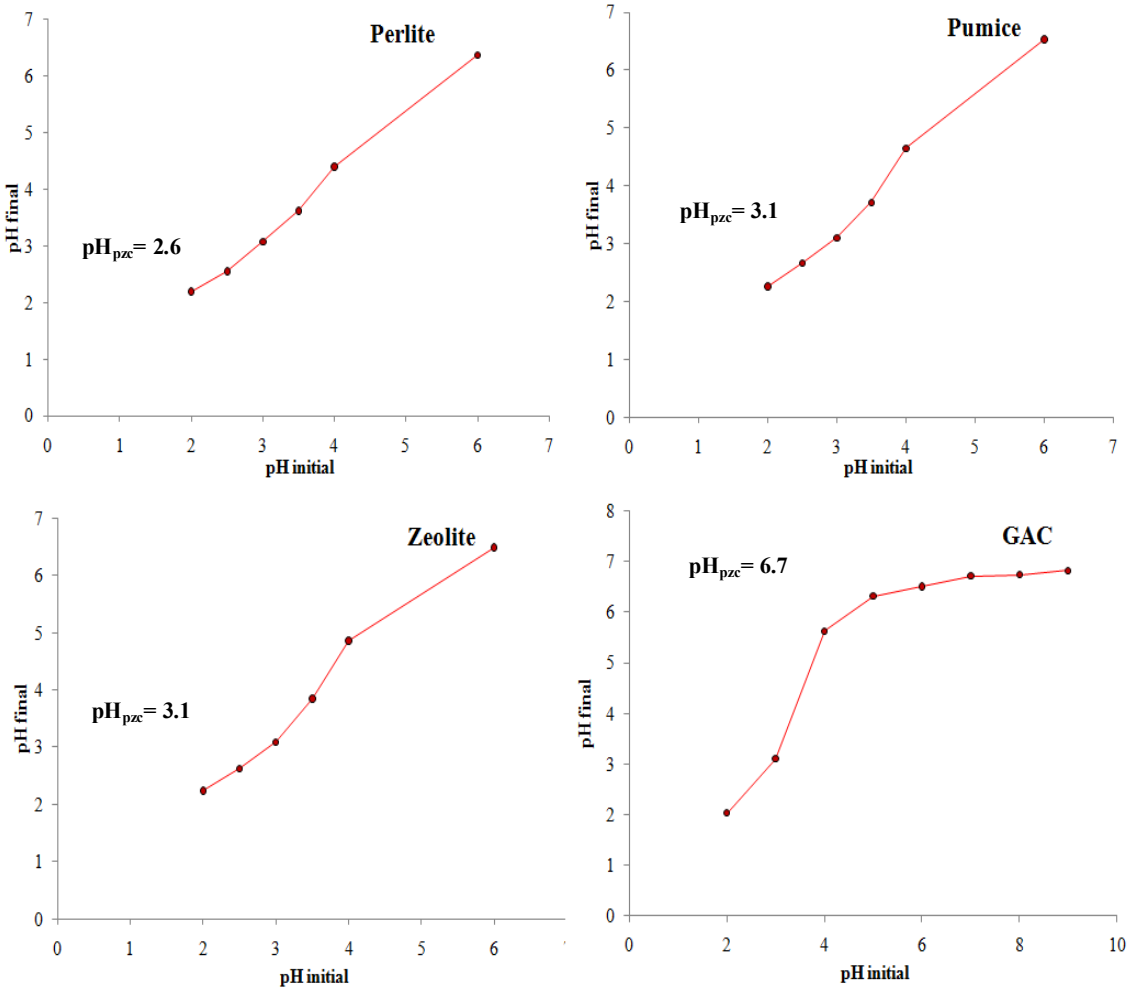

Figure 4.11. Determination of point of zero charge for adsorbents.

According to the results, the pH_{pzc} values of perlite, pumice, zeolite, and GAC are 2.6, 3.1, 3.1 and 6.7, respectively.

4.2. Sorption Kinetics of Antibiotics

In order to investigate the adsorption kinetics of sulfonamide antibiotics on clay minerals SMZ was selected as model compound. For the removal of a sulfonamide antibiotic from water, the adsorption efficiency of GAC was compared with those obtained by natural minerals, namely perlite, pumice, and zeolite. For this purpose a series batch adsorption kinetic experiments were performed with 0.25 mM SMZ at an initial pH of 6.5

for 32 h contact time period. Due to the difficulty in separation of antibiotic from the adsorbents the adsorbed amount of SMZ was calculated by mass balance (Eq. 3.2).

For natural minerals the variation of adsorbed amount of SMZ, q_t is shown as a function of contact time in Figure 4.12.

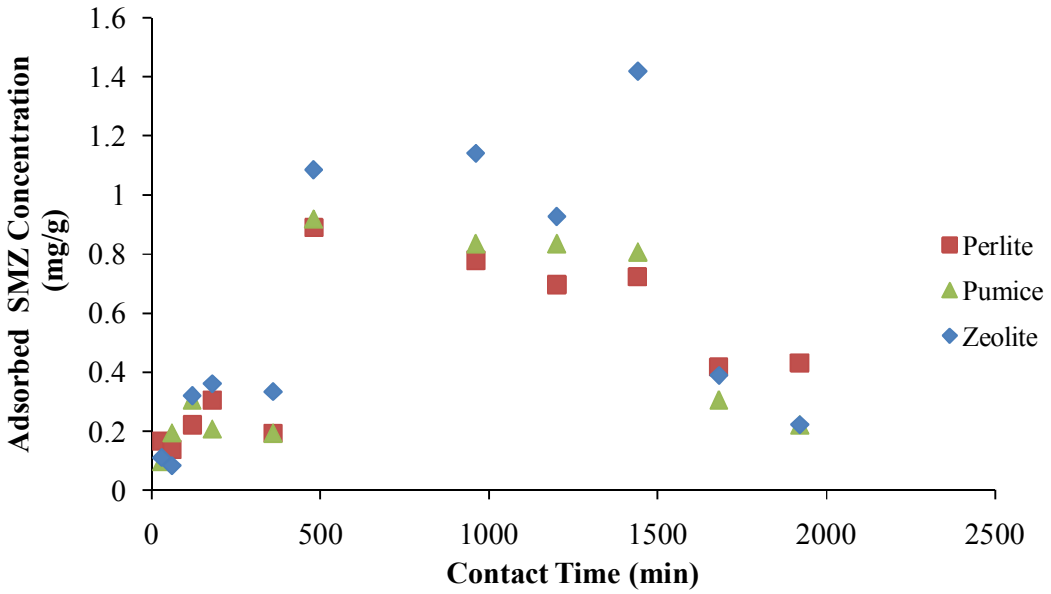

Figure 4.12. Kinetics of SMZ sorption on perlite, pumice, and zeolite ($[SMZ]_i$= 69.58 mg/L; [adsorbent]=10 g/L; pH_i=6.5).

As shown in Figure 4.12, the sorption equilibrium of antibiotic on each adsorbent was not achieved within 32 h contact time. Moreover, the desorption of SMZ from both perlite and pumice was observed after 960 min. About 10% SMZ removal was achieved at 24 h contact time period with perlite and pumice while 19% SMZ removal was obtained with zeolite. The adsorbed amounts of SMZ on perlite and pumice within this period were 0.723 and 0.807 mg/g, respectively. On the other hand, zeolite exhibited slightly higher adsorption concentration which was 1.419 mg/g. The previous studies demonstrated that exchangeable cations had an effect on the sorption of SMZ onto clays (Gao and Pedersen, 2005; Kahle and Stamm, 2007b). Moreover, higher Ca content of zeolite (Table 4.3) can provide an opportunity to form SMX-Ca complex on the surface of adsorbent as suggested by Gao and Pedersen (2005). The higher adsorption capacity of SMZ onto zeolite

compared to perlite and pumice can be attributed to the highest CEC value of zeolite. However, even with zeolite noticeably low sorption was achieved for SMZ. On the other hand, in a previous study the adsorption equilibration of tetracycline group antibiotic, OTC on the perlite used in this study was achieved within 24 hours period and q_e value was 5.87 mg/g (Erdinç, 2009). Therefore, it can be concluded that natural minerals used in this study can be used for the adsorption of OTC whereas they are not appropriate adsorbents for the sulfonamide antibiotic, SMZ.

Due to the low sorption capacity of natural minerals for sulfonamide antibiotic, GAC was used as adsorbent for SMX and OTC as well as SMZ. All kinetic experiments were conducted at the conditions used for natural minerals except adsorbent concentration. The initial concentration of each antibiotic was 0.25 mM and the amount of adsorbent was also kept constant at 5 g/L by which the highest SMZ removal efficiency was obtained as shown in Table 4.6. The results of kinetic experiments obtained by GAC are presented in Figure 4.13.

Table 4.6. Effect of GAC dose on the removal of SMZ and SMX.

	Antibiotic Removal Efficiency (%)	
GAC dosage (g/L)	**SMZ**	**SMX**
0.5	63.3	54.7
1	84.9	72.3
5	89.7	85.4

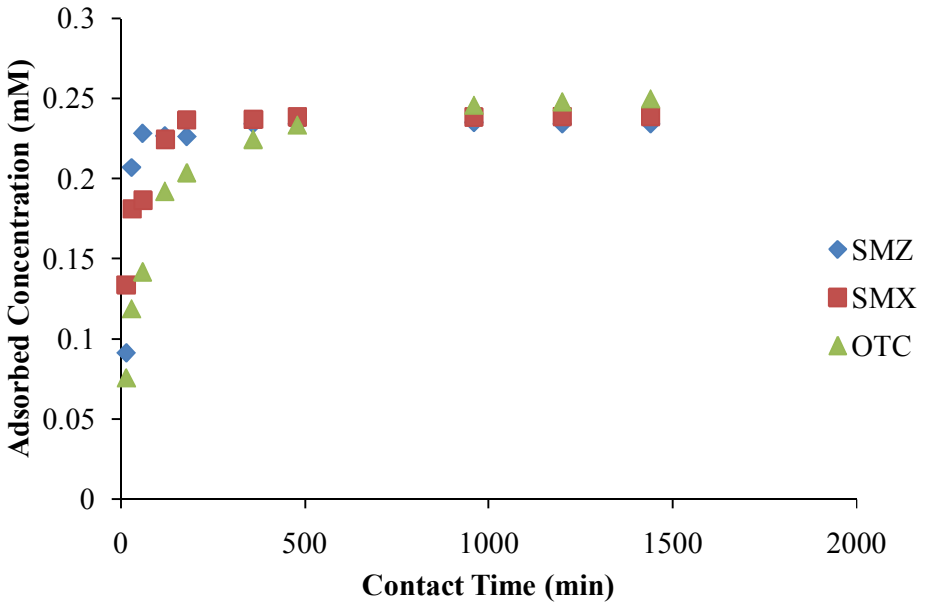

Figure 4.13. Kinetics of antibiotics sorption on GAC ([antibiotics]$_i$= 0.25 mM; [GAC]=5 g/L; pH$_i$=6.5).

As opposed to the results obtained by natural minerals a rapid sorption of antibiotics was obtained with GAC and equilibration was achieved within 6 h contact time for SMZ, SMX, and OTC. In agreement with observed results, the specific experiments with clay minerals and organic sorbents revealed that mineral phases seem to be much weaker sorbents for sulfonamides than organic materials (Gao and Pedersen, 2005; Kahle and Stamm, 2007a). The amounts of antibiotics adsorbed exhibited no significant difference when the contact time was longer than 10 h. The q_e values of SMZ, SMX, and OTC are 6.24 mM/g, 6.32 mM/g, and 5.97 mM/g, respectively.

To describe the sorption kinetics of antibiotics pseudo-first-order, pseudo-second-order, Elovich, and intraparticle diffusion kinetic models were applied to the experimental data. Since equilibration of antibiotics was not achieved with natural minerals in reasonable time period, kinetic models were only used for the data obtained by GAC.

First, the data obtained at the initial stage of adsorption (120-300 min) were fitted to pseudo-first-order kinetic model by the plotting the log ($q_e - q_t$) vs. t (Figure 4.14) for each antibiotic.

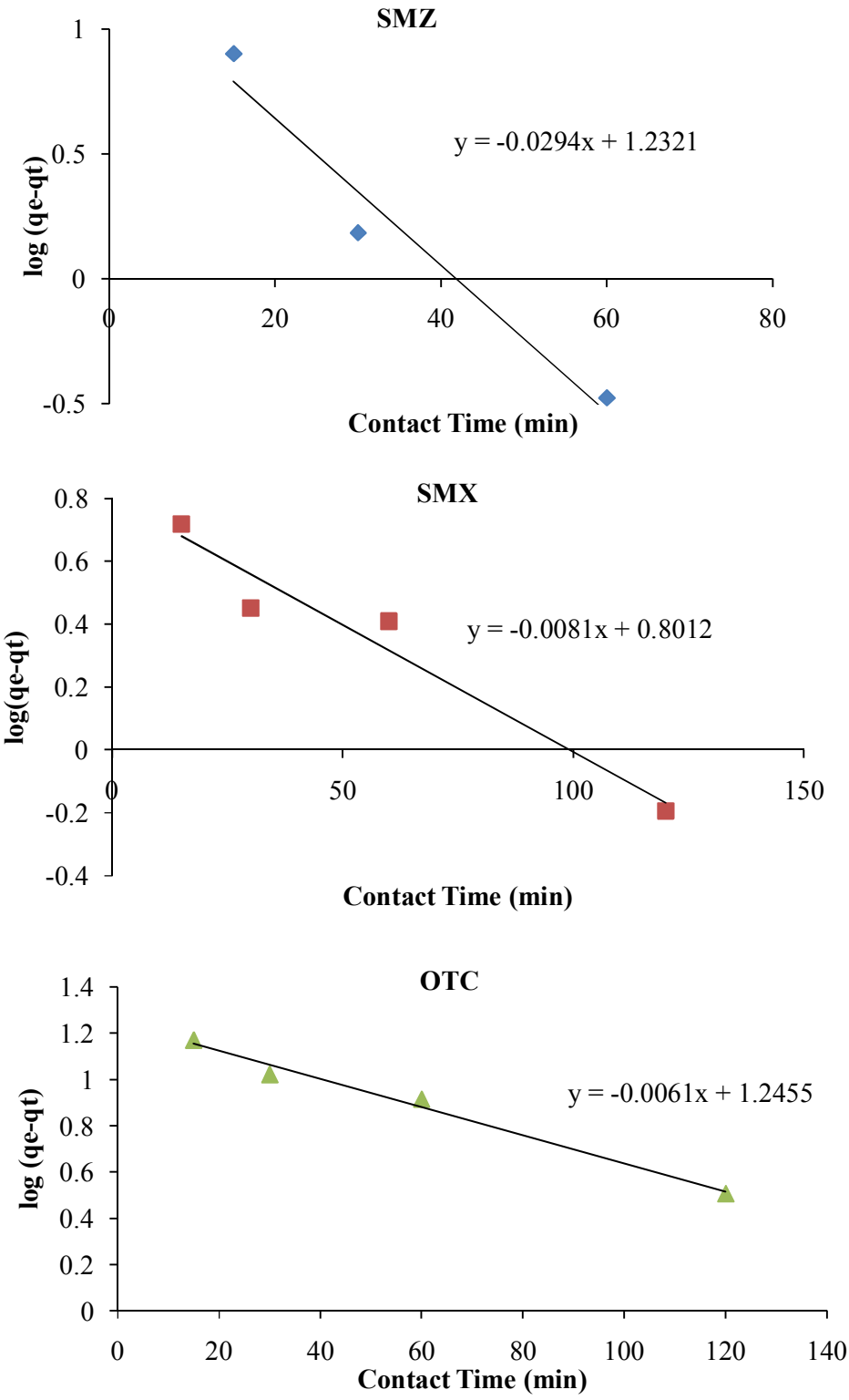

Figure 4.14. Pseudo-first-order plots of antibiotics sorption onto GAC ([antibiotics]$_i$= 0.25 mM; [GAC]=5 g/L; pH$_i$=6.5).

For each antibiotic the predicted values of equilibrium adsorption were calculated according to the pseudo-first-order model (Table 4.7). Besides the comparison of predicted and experimental q_e values, the validity of the model to the experimental data have been analyzed by two statistic parameters, R^2 and SSE.

Table 4.7. Pseudo-first-order model parameters of antibiotics adsorbed on GAC.

	Antibiotics		
	SMZ	**SMX**	**OTC**
q_e *(exp) (mg/g)	13.05	12.01	22.31
q_e *(calc) (mg/g)	17.06	6.33	17.60
k_1 (1/min)	6.8×10^{-2}	1.9×10^{-2}	1.4×10^{-2}
R^2	0.95	0.95	0.99
SSE	181	329	309

As can be seen from Table 4.7, the calculated sorption concentration values do not agree with the experimental sorption capacities although the values of correlation coefficient for the plots were in the range 0.95–0.99. These results suggest that the pseudo-first-order sorption rate expression of Lagergren did not describe the sorption of three antibiotics onto GAC.

In order to clarify the sorption mechanism a series of adsorption kinetics experiments were conducted with different initial concentrations for SMZ onto GAC (Figure 4.15-a). While changing the initial concentration of SMZ solution from 0.06 mM (16.7 g) to 0.8 mM (222.7 g), q_e value increased from 3.06 to 41.03 mg/g. Although removal percentages of antibiotic are similar for all concentrations (Figure 4.15-b) equilibration has been attained in shorter time period for lower antibiotic concentration.

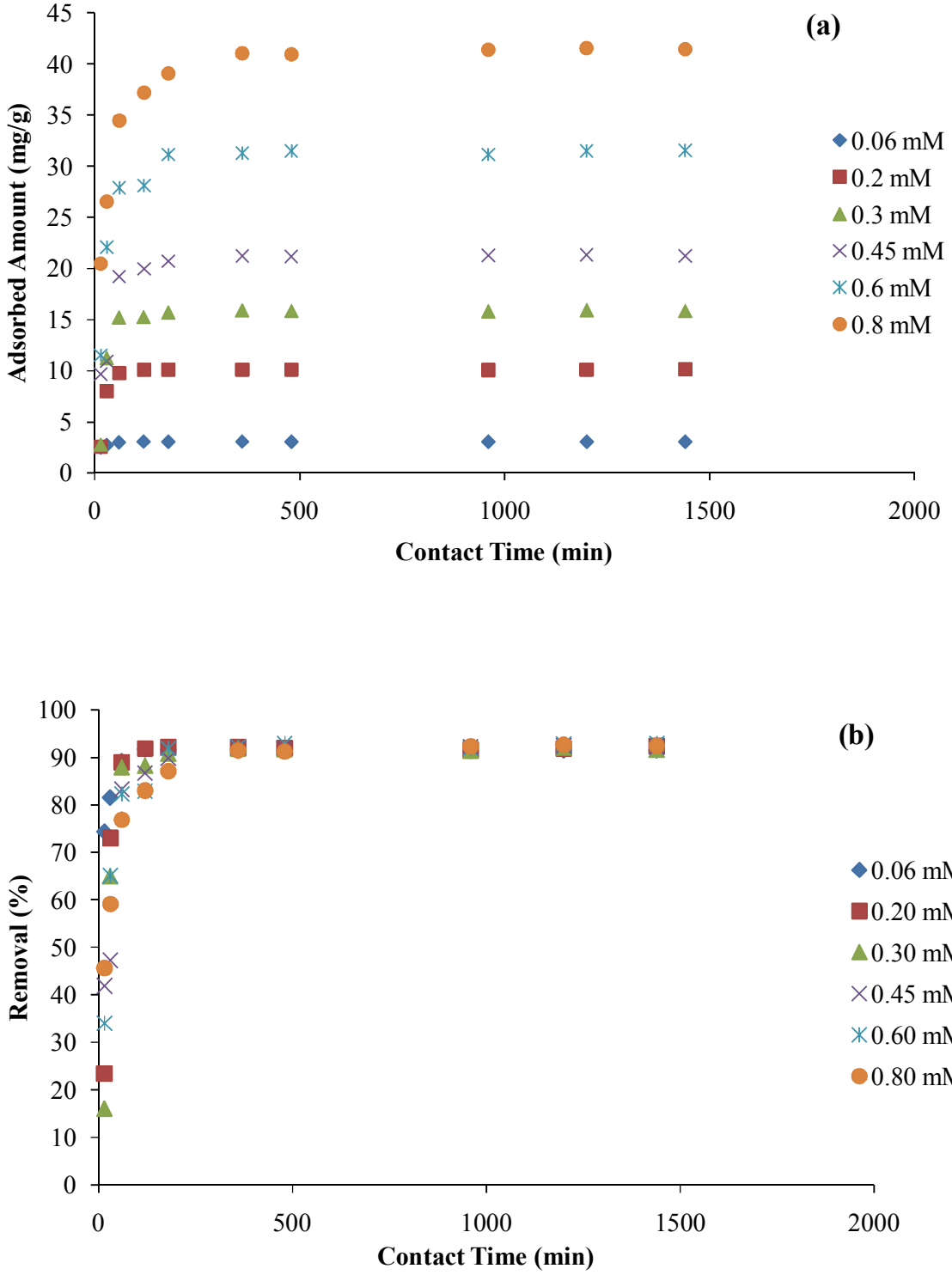

Figure 4.15. Removal efficiency of SMZ onto GAC for different initial concentrations ($[SMZ]_i$= 69.58 mg/L; [GAC]= 5 g/L; pH_i= 6.5).

For each concentration of SMZ pseudo-first-order model was applied to experimental data and the results are presented in Table 4.8.

Table 4.8. Pseudo-first-order model parameters for the sorption of different concentrations of SMZ onto GAC.

C_0 (mM)	q_{exp} (mg/g)	q_{cal} (mg/g)	k_1 (1/min)	R^2	SSE
0.06	2.97	0.96	0.044	1	43
0.20	10.13	18.50	0.066	0.99	710
0.30	15.72	38.85	0.072	0.99	5329
0.45	20.72	28.28	0.047	0.92	556
0.60	31.14	32.73	0.039	0.99	42
0.80	39.07	30.75	0.031	0.99	886

As can be observed from Table 4.8, the predicted sorption capacity at each antibiotic concentration did not agree with the experimental sorption capacity and the pseudo-first-order rate constant exhibited variation with the antibiotic concentration. If the whole process is controlled by a first order mechanism, the values of rate constants (k_1) should be consistent (Al-Degs et al., 2006). However, in this study the value of the pseudo-first-order kinetic constant varied for different initial concentrations.

To find out the potential rate controlling step involved in the adsorption, pseudo-second kinetic model was also applied to the whole data range of each antibiotic unlike to the first-order kinetic model and the obtained results are presented in Figure 4.16.

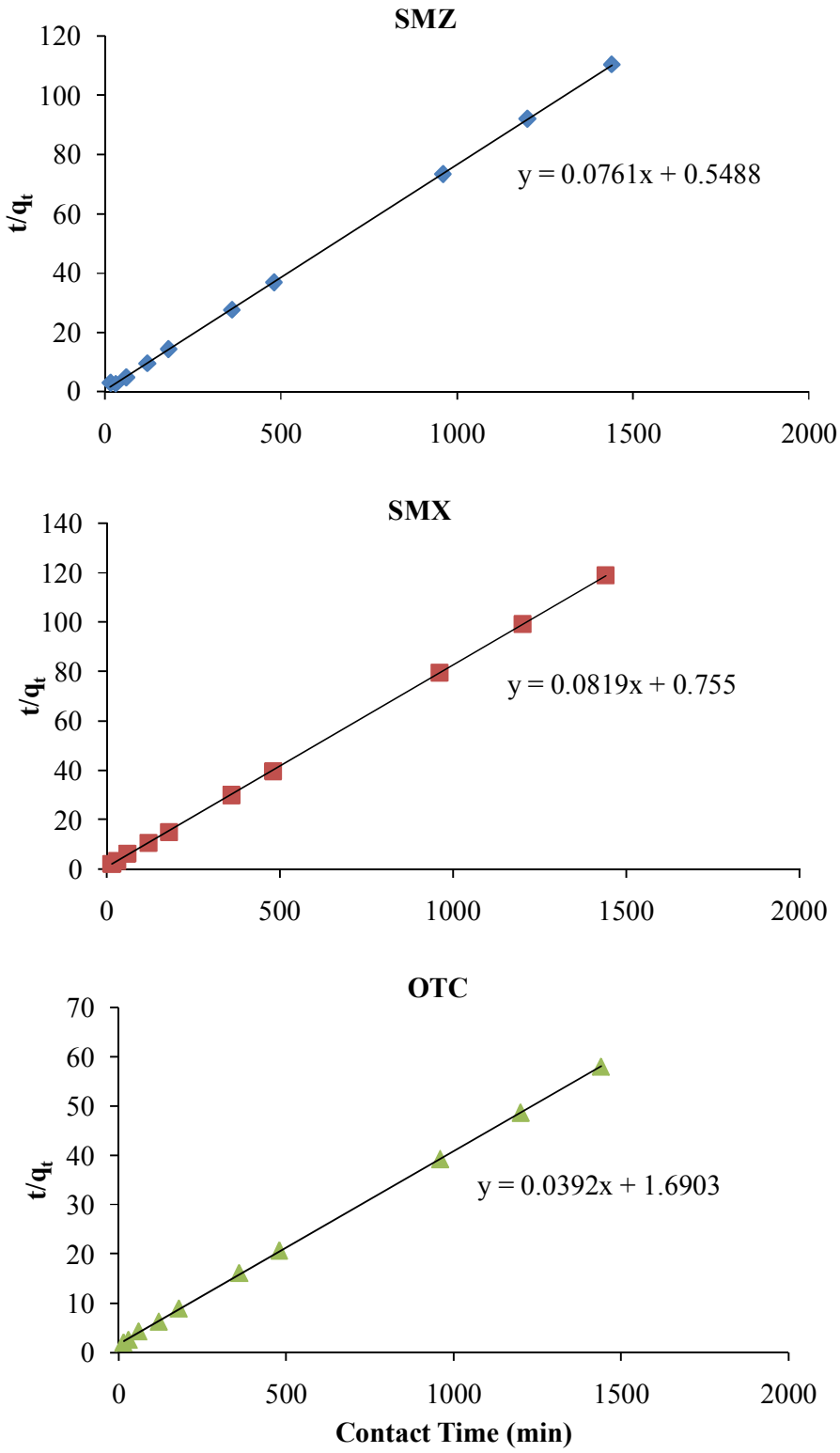

Figure 4.16. Pseudo-second-order plots of antibiotics sorption onto GAC ($[antibiotics]_i$= 0.25 mM; [GAC]=5 g/L; pH_i=6.5).

Table 4.9 presents a comparison between the predicted and calculated adsorption equilibrium values.

Table 4.9. Pseudo-second-order model parameters of antibiotics adsorbed on GAC.

	Antibiotics		
	SMZ	**SMX**	**OTC**
q_e^*(exp) (mg/g)	13.05	12.01	22.31
q_e (calc) (mg/g)	13.14	12.21	25.51
k_2 (g/mg min)	1.05×10^{-2}	8.88×10^{-3}	9.09×10^{-4}
R^2	0.99	0.99	0.99
SSE	16.3	2.1	3.7

Compared to the results achieved by pseudo first order model, higher correlation coefficients and lower SSE values were obtained by the application of pseudo-second-order model to the experimental data (Table 4.9). This model is based on the assumption that the rate limiting step can be chemical sorption (Ho and McKay, 1998) and the adsorption of antibiotics can occur via surface complexation reactions at specific sorption sites. Similarly, the sorption of SMX on powdered activated carbon was described by the second order kinetics (Çalışkan and Göktürk, 2010). OTC adsorption concentration of GAC in this study is 22.313 mg/g, which is comparable to those observed with other adsorbents. It has been reported that the Fe-impregnated mesoporous silicate adsorbs about 17.2-41.7 mg/g of tetracycline (Vu et al., 2010), the hydrous oxide of Fe adsorbs about 17.7-53.3 mg/g of tetracycline (Gu and Karthikeyan, 2005), palygorskite adsorbs about 29.9 mg/g of tetracycline (Chang et al., 2009).

The pseudo-second-order model was also applied to the data obtained by SMZ at various concentrations (Table 4.10). The results show that the process to be highly concentration dependent and the values of the second order rate constants (k_2) decreased from 2.28×10^{-1} to 1.72×10^{-3} g/ mg min as the initial concentration of SMZ increased from 0.06 mM to 0.80 mM. Similar results were reported for several β-lactam antibiotics adsorbed onto activated carbon (Liu and Shen, 2008).

Table 4.10. Pseudo-second-order model parameters for the sorption of different concentrations of SMZ onto GAC.

C_0 (mM)	q_e(mg/g)	q_t(mg/g)	k_2 (g/mg min)	R^2	SSE
0.06	3.06	3.05	0.228	1	0.14
0.20	10.13	10.22	0.0089	0.99	13.59
0.30	15.91	16.15	0.0035	0.99	33.01
0.45	21.23	21.50	0.0037	0.99	25.79
0.60	31.30	31.85	0.0026	0.99	41.46
0.80	41.03	42.02	0.0017	1	7.65

In Figure 4.17, the experimental and predicted q_t values obtained by pseudo-second-order models for the three antibiotics are presented. As can be seen from the figure pseudo-second-order model fits best to all adsorbates.

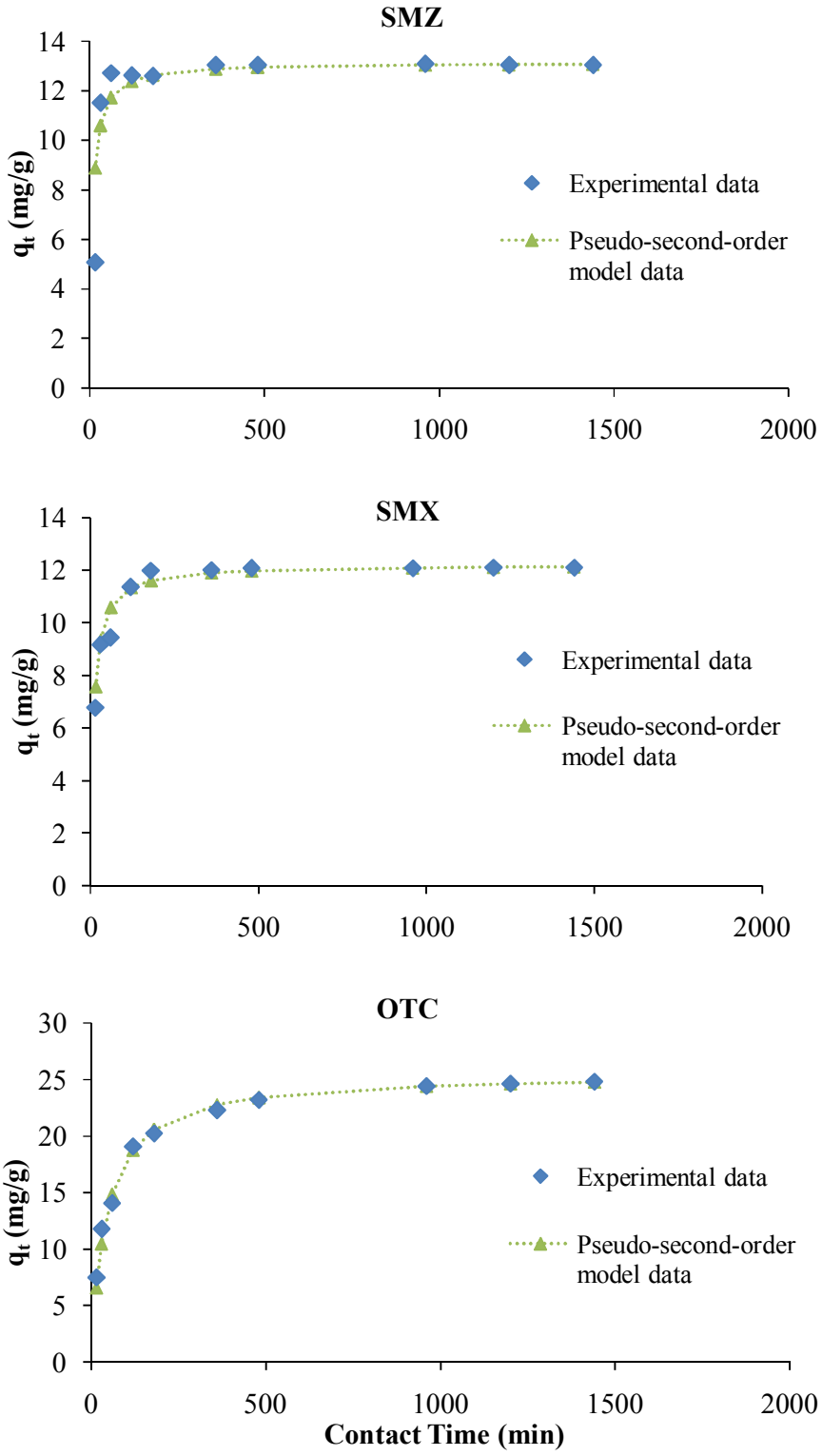

Figure 4.17. Comparison of experimental and estimated sorption kinetics of antibiotics ([antibiotics]$_i$= 0.25 mM; [GAC]=5 g/L; pH$_i$=6.5).

Ho and McKay (Ho and McKay, 2000) suggested that the application of various kinetic models to the experimental data can be more suitable since the heterogeneity of the sorbent surfaces leads to the diversity of sorption phenomena. Considering this fact Elovich model (Eq. 2.6) was also applied to the obtained kinetic data. According to this model, the slope and intercept of the plot of qt vs. ln(t), which is shown in Figure 4.18, were used to calculate the initial adsorption rate constant, a and the extent of surface coverage, b.

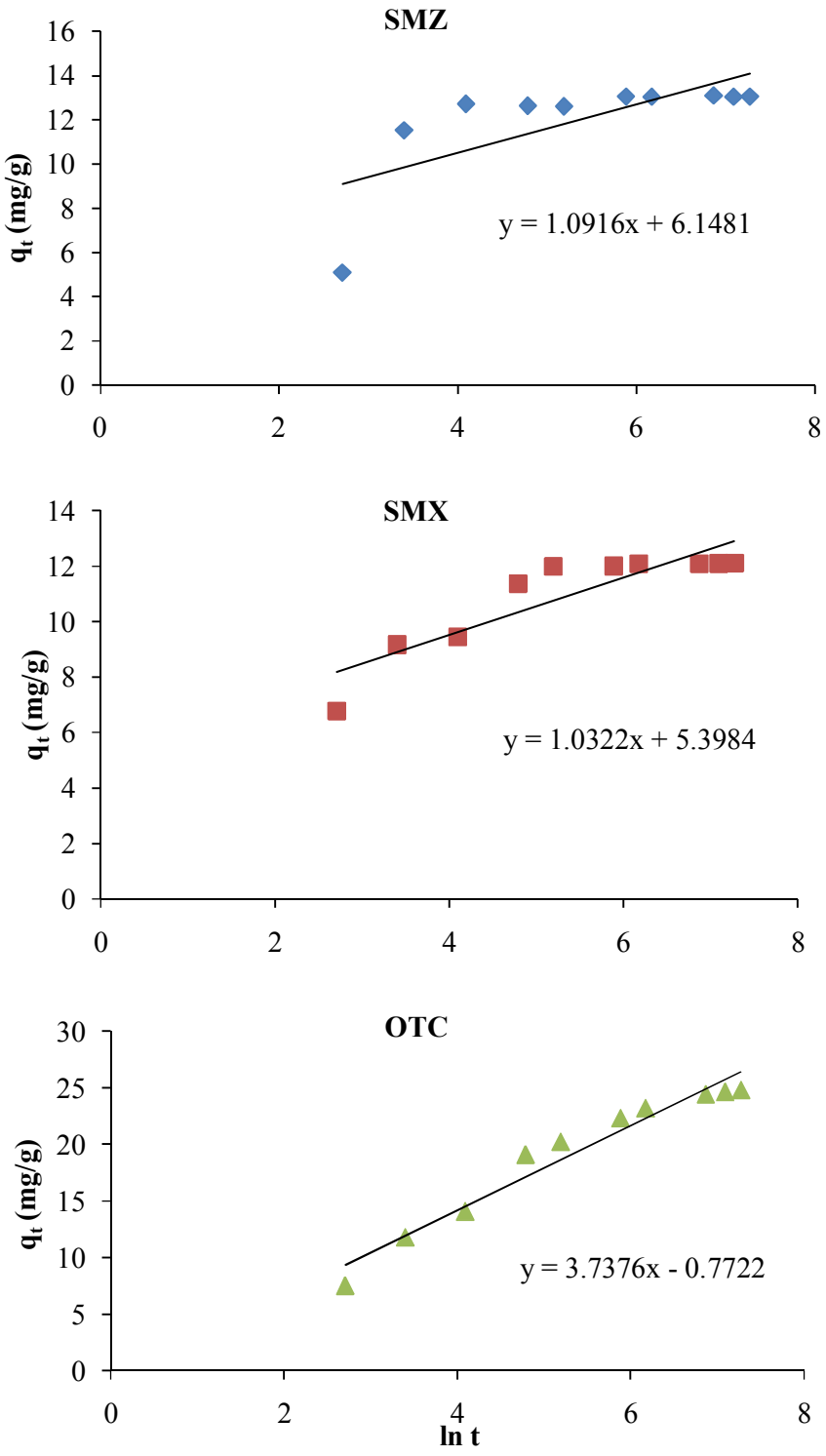

Figure 4.18. Sorption of antibiotics described by Elovich model ($[antibiotics]_i$= 0.25 mM; [GAC]= 5 g/L; pH_i=6.5).

As in the case of pseudo-second-order model Elovich model which suggests that chemisorption mechanism is rate-controlling step in sorption (Juang and Chen 1997; Cheung et al., 2001) was applied to whole range of kinetic data. From the Table 4.11 it can be concluded that this model did not describe the sorption kinetics of SMZ and SMX. However, comparable high correlation coefficient was obtained with this model for OTC adsorption. The value of "b" Elovich model parameter for OTC suggests that adsorption mainly occurs in the interior surface of adsorbent. Since the molecular size of OTC is 8.3 Å in diameter which is smaller than the avarage pore size of GAC (Table 4.2) this result is well expected result.

Table 4.11. Elovich kinetic model parameters of antibiotics adsorbed on GAC.

	Antibiotics		
	SMZ	**SMX**	**OTC**
q_e^*(exp) (mg/g)	13.05	12.01	22.31
a (mg/g min)	304.85	192.80	3.04
b (g/mg)	0.92	0.97	0.27
R^2	0.49	0.79	0.95
SSE	27.92	6.25	15.97

Further examination of kinetic data was performed by intraparticle diffusion model. Depending on the model equation (Eq. 2.9) the plot qt vs. $t^{0.5}$ for all antibiotics is shown in Figure 4.19.

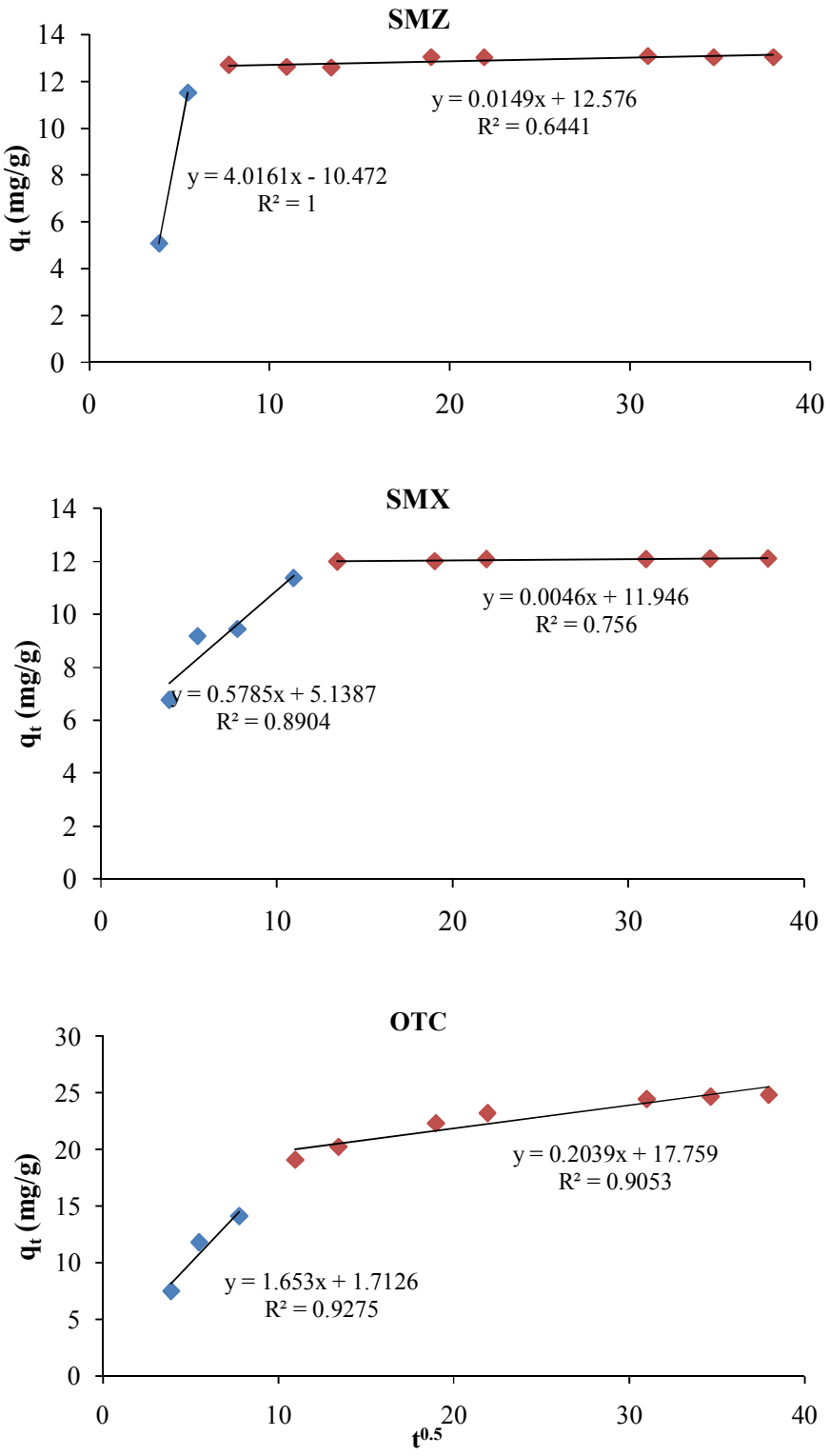

Figure 4.19. Sorption of antibiotics described by intraparticle diffusion model ([antibiotic]$_i$= 0.25 mM; [GAC]=5 g/L; pH$_i$=6.5).

The predicted values of equilibrium adsorption of each antibiotic calculated according to the intraparticle diffusion model are presented in Table 4.12. It is observed from Figure 4.19 that the plots of qt versus $t_{0.5}$ for three antibiotics have an initial curved portion followed by a linear portion. The first curved step represents the diffusion of adsorbate ions from the bulk solution to the external surface and the second step indicates the gradual adsorption stage of intraparticle diffusion where adsorbate molecules diffusion through the porosity of the activated carbon. The correlation coefficient values of two steps for OTC were higher than those of SMZ and SMX. The experimental and calculated adsorption capacities of antibiotics are not consistent and additionally, SSE values are remarkably high. According to these results, intraparticle diffusion model is not appropriate to explain adsorption mechanism of these antibiotics.

Table 4.12. Intraparticle diffusion kinetics of antibiotics adsorbed on GAC.

	Steps	**Antibiotics**		
		SMZ	**SMX**	**OTC**
q_e^*(exp) (mg/g)		13.05	12.01	22.31
k_p (mg $min^{0.5}$/g)	1.	4.02	0.58	1.65
	2.	0.015	0.005	0.204
R^2	1.	1	0.89	0.93
	2.	0.64	0.76	0.90
SSE	1.	60559	320	3485
	2.	1422	1202	2526

4.3. Equilibrium Modeling

Adsorption equilibrium data, known as isotherms, describe how the adsorbate interacts with adsorbent and this data can give a comprehensive understanding of the interaction between adsorbent and adsorbate. Adsorption isotherm experiments of SMZ, SMX, and OTC were conducted at 25 ^{0}C and pH 6.5 in the antibiotic concentration ranged from 0.06 mM to 0.8 mM. Considering the kinetic experiments equilibration time was

selected as 5 h for both SMZ and SMX and as 24 h for OTC. The amount of antibiotic adsorbed per unit mass of adsorbent, q_e (mg/g) was correlated with the liquid phase concentration of antibiotic at equilibrium, C_e (mg/L) (Figure 4.20). As shown from Figure 4.20, the sorption concentration of GAC increased with increasing antibiotic concentration. The initial concentration provides a driving force to overcome all mass transfer resistances.

Langmuir, Freundlich, Temkin, and Redlich-Peterson isotherm models were applied to isotherm data and the isotherm constants were determined according to the Equations 2.11, 2.12, 2.13, and 2.14. The model parameters together with statistical parameters are listed in Table 4.13. The experimental and the predicted data according to Temkin isotherm model are indicated in Figure 4.20.

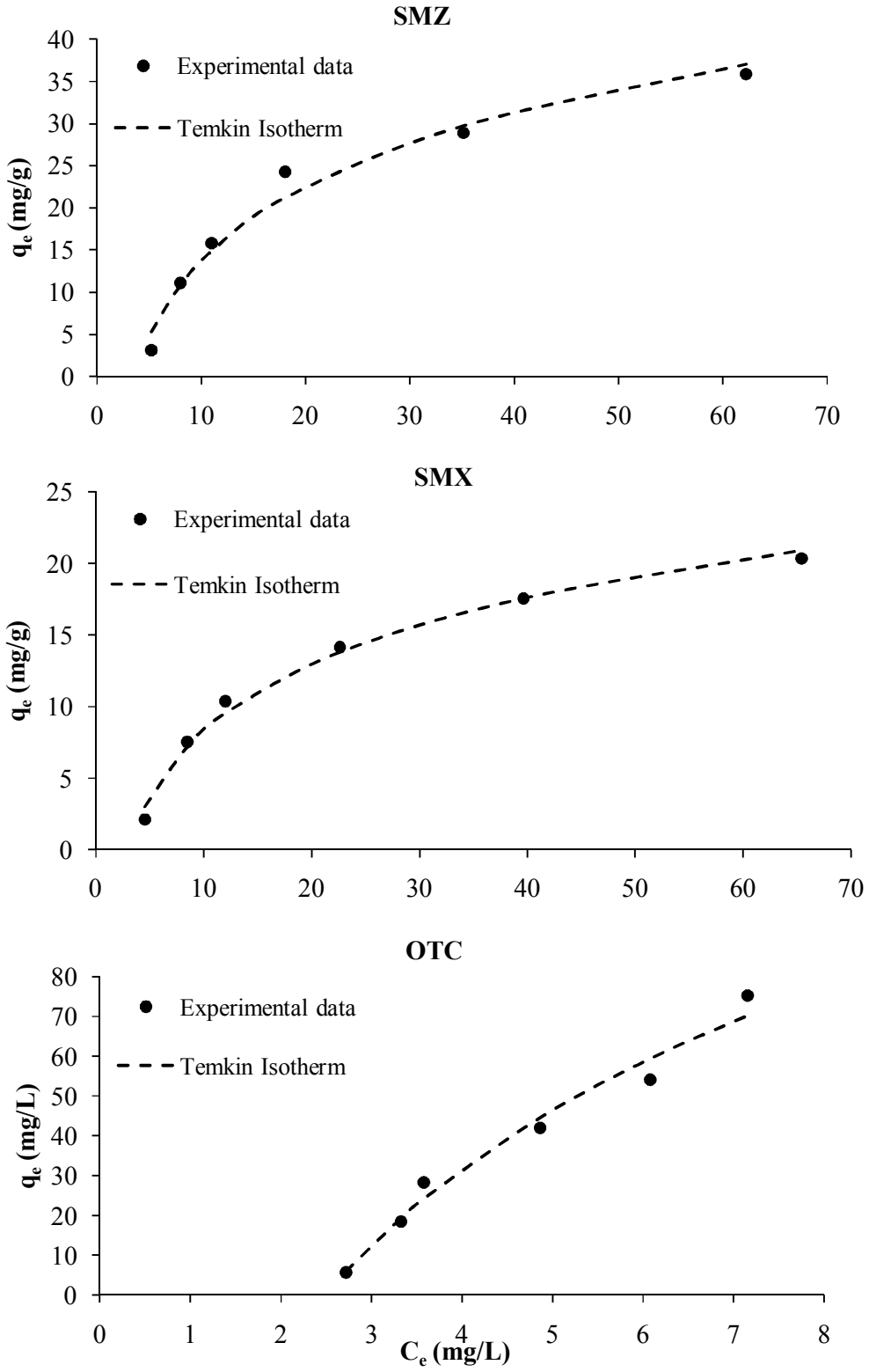

Figure 4.20. Comparison of experimental and estimated sorption isotherms of antibiotics ($[adsorbate]_i$ = 0.06-0.8 mM; [GAC] = 5 g/L; pH_i=6.5).

Table 4.13. Adsorption isotherm parameters.

	Antibiotics		
Isotherm Models	**SMZ**	**SMX**	**OTC**
Freundlich Isotherm			
1/n	0.87	0.76	2.29
K_F (mg/g)(L/mg)^n	1.46	1.11	0.97
R^2	0.79	0.83	0.87
SSE	250.17	60.28	370.54
Langmuir Isotherm			
K_L (L/mg)	0.06	0.05	-0.49
q (mg/g)	2.01	3.82	0.07
R^2	0.81	0.82	0.98
SSE	430.86	178.31	4988.75
Temkin Isotherm			
B_1	12.79	6.71	66.33
K_T (L/mg)	0.06	0.07	0.12
R^2	0.98	0.99	0.97
SSE	17.10	2.20	79.02
Redlich-Peterson isotherm			
K (L/g)	1.88	1.17	0.10
a (L/mg)	0.03	0.04	-0.97
β	1	1	0.01
R^2	0.11	0.33	0.67
SSE	40.88	6.94	140.79

According to the SSE values and correlation coefficients in Table 4.14 the adsorption equilibrium data of SMZ, SMX, and OTC can be satisfactorily described by Temkin isotherm. These results indicates that adsorbent/adsorbate interactions and adsorption are characterized by a uniform distribution of binding energies, up to some maximum binding energy and the heat of adsorption of all the molecules decreases linearly with coverage due to adsorbate–adsorbate interactions (Temkin and Pyzhev, 1940; Kim et al., 2004).

Although in this study Langmuir and Freundlich adsorption isotherms did not well describe the sorption of sulfonamide and tetracycline antibiotics on GAC in some literature studies (Table 4.14) these models were applied successfully to experimental data. As can

be deduced from Table 4.14 Langmuir isotherm was used for the sorption of antibiotics on activated carbon whereas Freundlich isotherm was suitable for the sorption on soil and clay minerals.

Table 4.14. Literature studies about adsorption isotherm models for antibiotics.

Antibiotic	**Adsorbent**	**Isotherm Model**	**Reference**
Amoxicillin	activated carbon	Langmuir and Freundlich	Putra et al., 2009
6-aminopenicillanic acid	activated carbon	Langmuir	Dutta et al., 1997
Triclosan	activated carbon	Langmuir	Behera et al., 2010
Nitroimidazole	activated carbon	Langmuir	Rivera-Utrilla et al., 2009
Sulfamethoxazole and Metronidazole	activated carbon	Langmuir	Çalışkan and Göktürk, 2010
OTC	soil	Langmuir	Figueroa and Mackay, 2005
Sulfachloropyridazine	soil (loam)	Freundlich	Boxall et al., 2002
SMZ	soil	Freundlich	Lertpaitoonpan et al., 2009
Sulfapryridine	soil	Freundlich	Thiele-Bruhn et al., 2004
OTC	soil	Freundlich	Rabolle and Spliid, 2000
OTC	kaolinite, montmorillonite	Langmuir	Figueroa et al., 2004
Triclosan	kaolinite, montmorillonite	Freundlich	Behera et al., 2010
OTC	clay	Freundlich	Kulshrestha et al., 2004
Amoxicillin	bentonite	Langmuir and Freundlich	Putra et al., 2009
Tylosin	manure	Freundlich	Kolz et al., 2005
Tetracycline	marine sediment	Freundlich	Xu and Li, 2010

4.4. pH Effect on Adsorption

The effect of the initial solution pH on adsorption of SMZ and OTC was investigated in the pH range of 2 to 8.5 (Figure 4.21). Equation 4.2 was used to calculate the distribution coefficients of antibiotics.

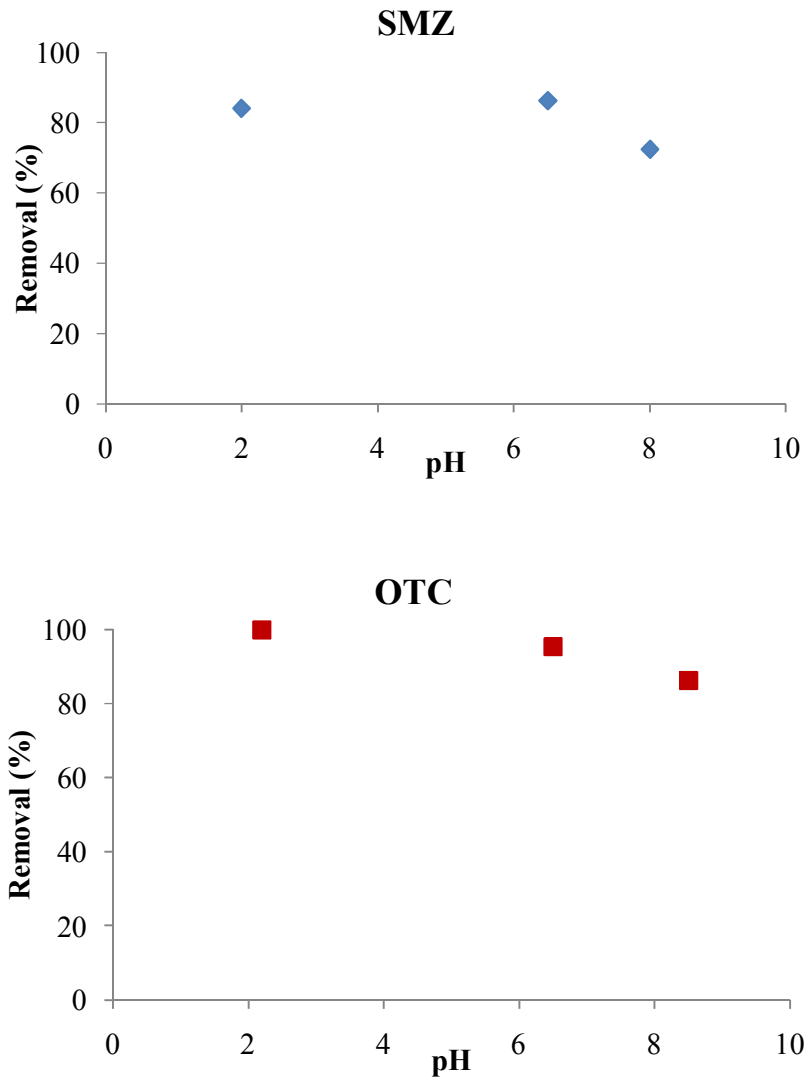

Figure 4.21. Effect of pH on the adsorption of SMZ and OTC ([antibiotics]= 0.25 mM, [GAC] = 5 g/L).

As shown in the Figure 4.21, an increasing in the initial pH of solution resulted in lower adsorption of OTC and SMZ. Almost complete removal of OTC was achieved at

acidic pH and by increasing the pH from 2 to 8 the removal rate decreased to 86.2 %. Maximum SMZ sorption onto GAC was obtained at pH 6.5 and it decreased from 86.25% to 72.45% by increasing the initial pH to 8. The pH_{pzc} of GAC is 6.7 (Figure 4.12) and hence the surface of adsorbent is negatively charged at pH values greater than 6.7. At high pH antibiotics will dissociate to deprotonated anionic form as deduced from pKa values given in Table 3.1. SMZ is negatively charged at pH values above 7.4 and between 2.3 and 7.4 SMZ is in neutral form. Similarly, OTC is found in zwitterionic form in the pH range of 3.6-7.52. Therefore, it can be expected a strong electrostatic attraction in acidic pH values. However, the sorption of these antibiotics is minimum at high pH values probably due to the electrostatic repulsion between antibiotics and GAC. Similarly, Çalışkan and Göktürk (2010) determined a strong pH dependence for the sorption of SMX on powdered activated carbon. On the other hand, Choi et al. (2008) found that the adsorption of sulfonamide antibiotics is closely related with both the hydrophobicity and functional group of antibiotics. While SMZ which has two methyl groups in its structure exhibits higher hydrophobic tendency, oxygen group in SMX decrease its hydrophobicity (Table 3.2),. Accordingly, slightly higher sorption of SMZ was obtained on GAC (Table 4.6). Additionally, it was proposed that the anionic form of antibiotics is much less hydrophobic (Ji et al., 2009). Compared to SMZ higher amount of OTC was removed because OTC is more hydrophobic than SMZ. Similar results were also obtained by Choi et al. (2008) for sulfonamide and tetracycline antibiotics on powdered activated carbon. These results may indicate that the sorption of antibiotics on activated carbon occurs with different mechanisms that act simultaneously.

4.5. Released Ions from Adsorbents

The released ions from the each adsorbent surface to water were determined by experiments carried out by 10 g/L adsorbent at pH 6.5 within 24 h contact time. Experiments were also carried out in the presence of 69.58 mg/L SMZ and 115 mg/L OTC. The concentration of Na^+, K^+, Ca^{2+}, and Mg^{2+} ions released from perlite, pumice, zeolite, and GAC are presented in Figure 4.22.

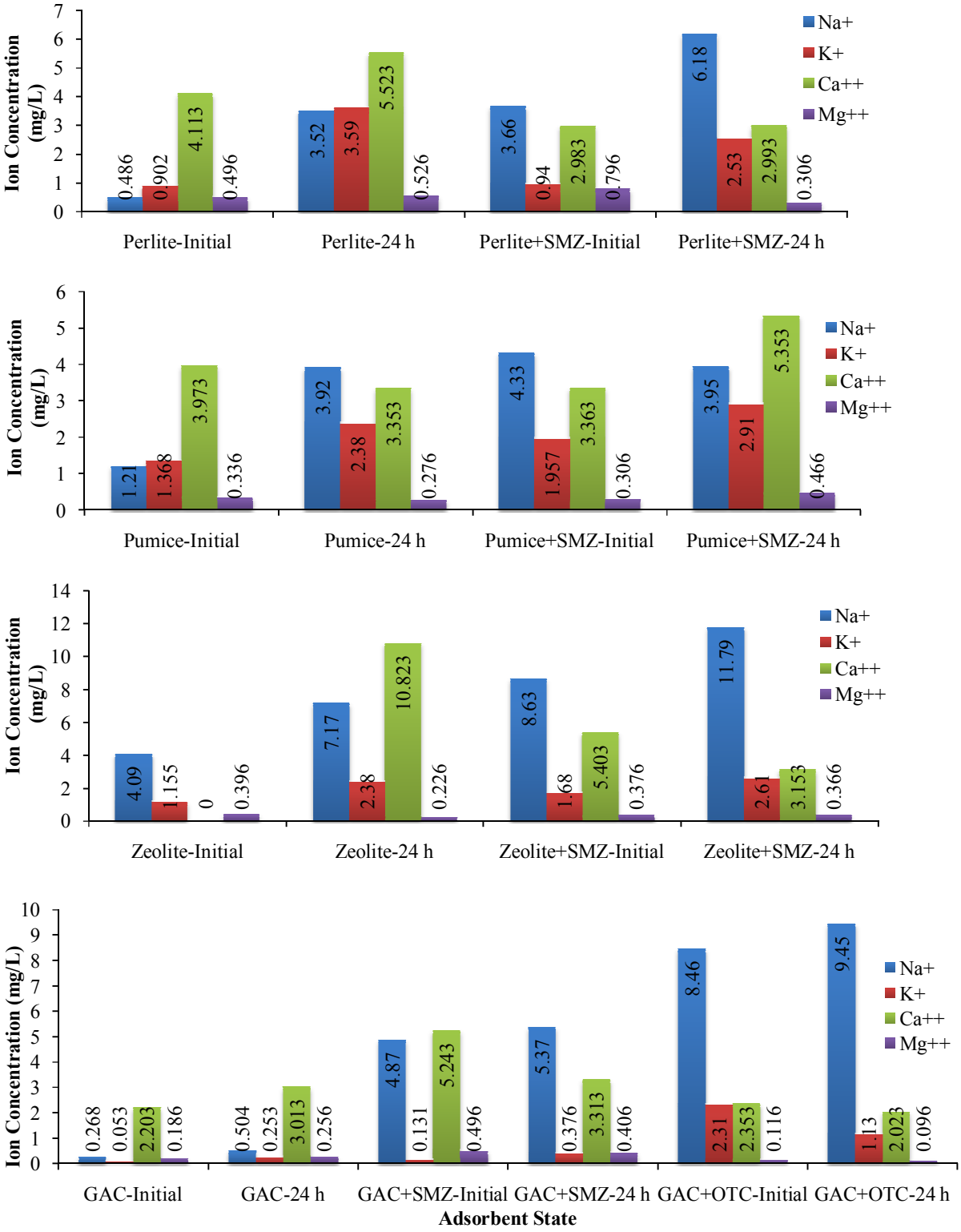

Figure 4.22. Release of cations from adsorbents (pH= 6.5).

As it is shown in Figure 4.22, the release of Ca^{2+} from adsorbents is remarkably high in the absence of antibiotics. Multivalent exchangeable cations can play significant role for the adsorption of sulfonamide and tetracycline group antibiotics which can form soluble complexes with these cations (Gao and Pedersen, 2005; Şalcıoğlu, 2007; Kahle and Stamm, 2007a; Kahle and Stamm, 2007b; Erdinç, 2009). The lower adsorption efficiency of natural minerals can be attributed to this factor. All natural minerals have pore size suitable for the exchange with OTC and SMZ. However, in the presence of SMZ, Ca^{2+} ions released from natural minerals except pumice have lower values. This result can be explained by the formation of complexes with antibiotics on the surface of natural minerals. Similar results were obtained for the sorption of OTC on perlite, sepiolite, and bentonite (Erdinç, 2009). In case of GAC, the sorption of OTC resulted in higher Na+ released into the solution than SMZ due to the smaller molecular size of OTC which is 8.3 Å in diameter compare to that of SMZ (10.50 Å).

5. CONCLUSION

The adsorption of SMZ on three natural minerals along with the adsorption of SMZ, SMX and OTC on GAC were investigated in this study. The following findings emphasize the main results of the study.

- The highest sorption SMZ was achieved with zeolite among the investigated natural minerals probably due to its highest cation exchange capacity. Formation of surface complexes on the zeolite through the cation bridging of calcium with SMZ can be another reason of higher sorption capacity of zeolite.

- Although pumice has 3 times higher surface area and pore volume compared to perlite, the adsorbed concentration of SMZ for pumice and perlite are close to each other indicating that surface area and pore volume are not the major controlling adsorptive factors.

- The lower sorption of SMZ on all natural minerals could be attributed to the formation of soluble complexes of SMZ with multivalent cations released from these minerals into the solution. Since the adsorption equilibrium of sulfonamide antibiotic on the natural minerals was not achieved within 24 h treatment period and the adsorption concentrations of these minerals were nine fold lower than that obtained by GAC they cannot be considered as suitable adsorbents.

- Among the investigated models, pseudo-second-order model is the best to describe the reaction kinetics of all antibiotics. From this result it can be concluded that the rate limiting step of adsorption is a chemical sorption process and the adsorption of antibiotics can occur via surface complexation reactions at specific sorption sites.

- The adsorption isotherm studies revealed that the adsorption equilibrium data of SMZ, SMX, and OTC on GAC can be satisfactorily described by Temkin isotherm

model. It can be concluded that adsorption is characterized by a uniform distribution of binding energies.

- The antibiotic removal percentages of GAC for OTC and SMZ are not highly depended on pH over a wide range. The sorption of SMZ and OTC antibiotics slightly decreased at high pH values because of the anionic antibiotic species increased with increasing pH and the electrostatic repulsion could be responsible for the lower sorption.

REFERENCES

Adams, C., Wang, Y., Loftin, K., Meyer, M., 2002. Removal of antibiotics from surface and distilled water in conventional water treatment processes. Journal of Environmental Engineering, 128, 253–260.

Aksu, Z., Tezer, S., 2000. Equilibrium and kinetic modelling of biosorption of Remazol Black B by Rhizopus arrhizus in a batch system: Effect of temperature. Process Biochemistry, 36, 431–439.

Al-Degs, Y.S., El-Barghouthi, M.I., Issa, A.A., Khraisheh, M.A., Walker, G.M., 2006. Sorption of Zn(II), Pb(II), and Co(II) using natural sorbents: Equilibrium and kinetic studies. Water Research, 40, 2645–2658.

Alexy, R., Kümpel, T., Kümmerer, K., 2004. Assessment of degradation of 18 antibiotics in the closed bottle test. Chemosphere, 57, 505–512.

Andreu, V., Vazquez-Roig, P., Blasco, C., Picó, Y., 2009. Determination of tetracycline residues in soil by pressurized liquid extraction and liquid chromatography tandem mass spectrometry. Analytical and Bioanalytical Chemistry, 394, 1329–1339.

Avisar, D., Primor, O., Gozlan, I., Mamane, H., 2010. Sorption of sulfonamides and tetracyclines to montmorillonite clay. Water Air Soil Pollution, 209, 439–450.

Balcıoğlu, I.A., Ötker, M., 2003. Treatment of pharmaceutical wastewater containing antibiotics by O_3 and O_3/H_2O_2 processes. Chemosphere, 50, 85–95.

Batt, A.L., Snow, D.D., Aga, D.S., 2006. Occurrence of sulfonamide antimicrobials in private water wells in Washington County, Idaho, USA. Chemosphere, 64, 1963–1971.

Batt, A.L, Kim, S., Aga, D.S., 2007. Comparison of the occurrence of antibiotics in four full-scale wastewater treatment plants with varying designs and operations. Chemosphere, 68, 428–435.

Behera, S.K., Oh, S.Y., Park, H.S., 2010. Sorption of triclosan onto activated carbon, kaolinite and montmorillonite: Effects of pH, ionic strength, and humic acid. Journal of Hazardous Materials, 179, 684–691.

Ben, W., Qiang, Z., Pan, X., Chen, M., 2009. Removal of veterinary antibiotics from sequencing batch reactor (SBR) pretreated swine wastewater by Fenton's reagent. Water Research, 43, 4392–4402.

Boxall, A. B. A., Blackwell, P., Cavallo, R., Kay, P., Tolls, J., 2002. The sorption and transport of a sulphonamide antibiotic in soil systems. Toxicology Letters, 131, 19–28.

Boxall, A.B.A., Kolpin, D.W., Halling-Sørensen, B., Tolls, J., 2003. Are veterinary medicines causing environmental risks? Environmental Science and Technology, 37, 286A–294A.

Brown, K.D., Kulis, J., Thomson, B., Chapman, T.H., Mawhinney, D.B., 2006. Occurrence of antibiotics in hospital, residential, and dairy effluent, municipal wastewater, and the Rio Grande in New Mexico. Science of the Total Environment, 366, 772–783.

Burkhardt, M., Stamm, C., 2007. Depth Distribution of Sulfonamide Antibiotics in Pore Water of an Undisturbed Loamy Grassland Soil. Journal of Environmental Quality, 36, 588–596.

Cabello, F.C., 2006. Heavy use of prophylactic antibiotics in aquaculture: a growing problem for human and animal health and for the Environment. Environmental Microbiology, 8, 1137–1144.

Campagnolo, E. R., Johnson, K. R., Karpati, A., Rubin, C. S., Kolpin, D. W., Meyer, M. T., Esteban, J. E., Currier, R. W., Smith, K., Thu, K. M., McGeehin, M., 2002.

Antimicrobial residues in animal waste and water resources proximal to large-scale swine and poultry feeding operations. Science of the Total Environment, 299, 89–95.

Campbell, K. L., 1999. Sulphonamides: Updates on use in veterinary medicine. Veterinary Dermatology, 10, 205–215.

Cengiz., M., Balcioglu, I.A., Oruc, H.H., Cengiz, T.G., 2010. Evaluation of the interaction between soil and antibiotics. Journal of Environmental Science and Health Part B, 45, 183–189.

Chakir, A., Bessiere, J., El.Kacemi, K., Marouf, B., 2002. A comparative study of the removal of trivalent chromium from aqueous solutions by bentonite and expanded perlite. Journal of Hazardous Materials, 95, 29–46.

Chang, P.H., Li, Z., Yu, T.L., Munkhbayer, S., Kuo, T.H., Hung, Y.C., Jean, J.S., Lin, K.H., 2009. Sorptive removal of tetracycline from water by palygorskite. Journal of Hazardous Materials, 165, 148–155.

Chefetz, B., Mualem, T., Ben-Ari, J., 2008. Sorption and mobility of pharmaceutical compounds in soil irrigated with reclaimed wastewater. Chemosphere, 73, 1335–1343.

Chen, G., Liu, S., Chen, S., Qi, Z., 2001. FTIR spectra, thermal properties, and dispersibility of a polystyrene/montmorillonite nanocomposite. Macromolecular Chemistry and Physics, 202, 1189–1193.

Cheung, C.W., Porter, J.F., McKay, G., 2001. Sorption kinetic analysis for the removal of cadmium ions from effluents using bone char. Water Research, 35, 605–612.

Chiou, M.S., Li, H.Y., 2002. Equilibrium and kinetic modelling of adsorption of reactive dye on crosslinked chitosan beads. Journal of Hazardous Materials B, 93, 233–248.

Choi, K. -J., Kim, S. -G. and Kim, S. -H., 2008. Removal of tetracycline and sulfonamide classes of antibiotic compound by powdered activated carbon. Environmental Technology, 29, 333–342.

Christian, T., Schneider R. J., Färber H. A., Skutlarek D., Meyer M. T., Goldbach H. E., 2003. Determination of antibiotic residues in manure, soil, and surface waters. Acta Hydrochimica et Hydrobiologica, 31, 36–44.

Cirini, G., Peindy, H.N., Gimbert, F., Robert, C., 2007. Removal of C.I. Basic Green 4 (Malachite Green) from aqueous solutions by adsorption using cyclodextrin-based adsorbent: Kinetic and equilibrium studies. Separation and Purification Technology, 53, 97–110.

Compant, S., Duffy, B., Nowak, J., Clement, C., Barka, E.A., 2005. Use of Plant Growth Promoting Bacteria for Biocontrol of Plant Diseases: Principles, Mechanisms of Action, and Future Prospects. Applied and Environmental Microbiology, 71, 4951–4959.

Costanzo, S. D., Murby, J., Bates, J., 2005. Ecosystem response to antibiotics entering the aquatic environment. Marine Pollution Bulletin, 51, 218–223.

Council recommendation of 15 November 2001 on the prudent use of antimicrobial agents in human medicine. Official Journal of the European Communities L34, 2002, 45, 13–6.

Çalışkan, E., Göktürk, S., 2010. Adsorption characteristics of sulfamethoxazole and metronidazole on activated carbon. Separation Science and Technology, 45, 244–255.

Davis, J.G., Truman, C.C., Kim, S.C., Ascough II, J.C., Carlson, K., 2006. Antibiotic transport via runoff and soil loss. Journal of Environmental Quality, 35, 2250–2260.

Demirbas, E., Kobya, M., Senturk, E., Ozkan, T., 2004. Adsorption kinetics for the removal of chromium (VI) from aqueous solutions on the activated carbons prepared from agricultural wastes. Water S.A., 30, 533–540.

Diaz-Cruz, M.S., Lopez de Alda, M.J., Barceló, D., 2003. Environmental behavior and analysis of veterinary and human drugs in soils, sediments and sludge. Trends in Analytical Chemistry, 22, 340–351.

Dodd, M. C., Buffle M. O., von Gunten, U., 2006. Oxidation of antibacterial molecules by aqueous ozone: moiety-specific reaction kinetics and application ozone-based wastewater treatment. Environmental Science and Technology, 40, 1969–1977.

Dodd, M.C., Kohler, H.P.E., Gunten, U.V., 2009. Oxidation of antibacterial compounds by ozone and hydroxyl radical: elimination of biological activity during aqueous ozonation processes. Environmental Science and Technology, 43, 2498–2504.

Doğan, M., Alkan, M., 2003. Removal of methyl violet from aqueous solution by perlite. Journal of Colloid and Interface Science, 267, 32–41.

Dutta, M., Baruah, R., Dutta, N.N., 1997. Adsorption of 6-aminopenicillanic acid on activated carbon. Separation and Purification Technology, 12, 99–108.

Erdinç, A., 2009. Sorption and destruction of veterinary antibiotics on natural materials. M.S. Thesis. Boğaziçi University.

FEDESA European Federation of Animal Health, 2001. Antibiotic Use in Farm Animals does not threaten Human Health. FEDESA/ FEFANA Press release. 13 July. Brussels, Belgium.

European Commission Regulation 1831/2003/EC on additives for use in animal nutrition, replacing Directive 70/524/ EEC on additives in feeding-stuffs, 2003.

Fajardo, A., Martinez, J.L., 2008. Antibiotics as signals that trigger specific bacterial responses. Current Opinion in Microbiology, 11, 161–167.

Figueroa, R.A., Leonard, A., Mackay, A.A., 2004. Modeling tetracycline antibiotic sorption to clays. Environmental Science and Technology, 38, 476–483.

Figueroa, R.A., MacKay, A.A., 2005. Sorption of oxytetracycline to iron oxides and iron oxide-rich soils. Environmental Science and Technology, 39, 6664–6671.

Garcia-Galan, M.,J., Garrido, T., Fraile, J., Ginebreda, A., Diaz-Cruz, M.S., Barcelo, D., 2010. Simultaneous occurrence of nitrates and sulfonamide antibiotics in two ground water bodies of Catalonia (Spain). Journal of Hydrology, 383, 93–101.

Gartiser, S., Urich, E.,Alexy, R., Kümmerer, K., 2007. Ultimate biodegradation and elimination of antibiotics in inherent tests. Chemosphere, 67, 604–613.

Gao, J., Pedersen, J.A., 2005. Adsorption of sulfonamide antimicrobial agents to clay minerals. Environmental Science and Technology, 39, 9509–9516.

Glassmeyer, S.T., Furlong, E.T., Kolpin, D.W., Cahill, J.D., Zaugg, S.D., Werner, S.L., Meyer, M.T., Kryak, D.D., 2005. Transport of chemical and microbial compounds from known wastewater discharges: Potential for use as indicators of human fecal contamination. Environmental Science and Technology, 39, 5157–5169.

Goel, J., Kadirvelu, K., Rajagopal, C., Garg, V.K., 2005. Removal of lead(II) by adsorption using treated granular activated carbon: Batch and column studies. Journal of Hazardous Materials, 125, 211–220.

Göbel, A., McArdell, C. S., Suter, M. J. F., 2004. Trace determination of macrolide and sulfonamide antimicrobials, a human sulfonamide metabolite, and trimethoprim in wastewater using liquid chromatography coupled to electrospray tandem mass spectrometry. Analytical Chemistry, 76, 4756–4764.

Göbel, A., McArdell, C. S., Joss, A., Siegrist, H., Giger, W., 2007. Fate of sulfonamides, macrolides, and trimethoprim in different wastewater treatment technologies. Science of the Total Environment, 372, 361–371.

Gu, C., and Karthikeyan, K. G., 2005. Interaction of tetracycline with aluminum and iron hydrous oxides. Environmental Science and Technology, 39, 2660–2667.

Hawkey, P.M., 2008. The growing burden of antimicrobial resistance. Journal of Antimicrobial Chemotherapy, 62, (Suppl. 1), i1–i9.

Haller, M. Y., Muller, S. R., McArdell, C. S., Alder, A. C., Suter, M. J. F., 2002. Quantification of veterinary antibiotics (sulfonamides and trimethoprim) in animal manure by liquid chromatography mass spectrometry. Journal of Chromatography A., 952, 111–120.

Halling-Sørensen, B., Nielsen, S. N., Lanzky, P. F., Ingerslev, F., Lutzhoft, H. C. H., Jorgensen, S. E., 1998. Occurrence, fate and effects of pharmaceutical substances in the environment-A review. Chemosphere, 36, 357–394.

Halling-Sørensen, B., 2001. Inhibition of aerobic growth and nitrification of bacteria in sewage sludge by antibacterial agents. Archives of Environmental Contamination and Toxicology, 40, 451–460.

Halling-Sørensen, B., Sengelov, G., Ingerslev, L., Bensen, B., 2003. Reduced antimicrobial potencies of oxytetracycline, tylosin, sulfadiazine, streptomycin, ciprofloxacin, and olaquindox due to environmental processes. Archives of Environmental Contamination and Toxicology, 44, 7–16.

Hamscher, G., Sczesny, S., Hoper, H., Nau, H., 2002. Determination of persistent tetracycline residues in soil fertilized with liquid manure by high-performance liquid chromatography with electrospray ionization tandem mass spectrometry. Analytical Chemistry, 74, 1509–1518.

Hamscher, G., Pawelzick, H. T., Höper, H., Nau, H., 2005. Different behaviour of tetracyclines and sulfonamides in sandy soils after repeated fertilization with liquid manure. Environmental Toxicology and Chemistry, 24, 861–868.

Heuer, H., Smalla, K., 2007. Manure and sulfadiazine synergistically increased bacterial antibiotic resistance in soil over at least two months. Environmental Microbiology, 9, 657–666.

Hirsch, R., Ternes, T., Haberer, K., Kratz, K. L., 1999. Occurrence of antibiotics in the aquatic environment. Science of the Total Environment, 225, 109–118.

Ho, Y.S., McKay, G., 1998. Sorption of dye from aqueous solution by peat. Chemical Engineering Journal, 70, 11.5–124.

Ho Y.S., McKay, G., 1999. Pseudo-second order model for sorption processes. Process Biochemistry, 34, 451–465.

Ho, Y.S., McKay, G., 2000. The kinetics of sorption of divalent metal ions onto sphagnum moss peat. Water Research, 34, 735–742.

Ho, Y.S., McKay, G., 2004. Sorption of copper(II) from aqueous solution by peat. Water, Air, and Soil Pollution, 158, 77–97.

Hu, X., Zhou, Q., Luo, Y., 2010. Occurrence and source analysis of typical veterinary antibiotics in manure, soil, vegetables and groundwater from organic vegetable bases, northern China. Environmental Pollution, 158, 2992-2998.

Jacobsen, A.M., Halling-Sørensen, B., Ingerslev, F., Honoré Hansen, S., 2004. Simultaneous extraction of tetracycline, macrolide and sulfonamide antibiotics from agricultural soils using pressurised liquid extraction, followed by solid-phase xtraction and liquid chromatography–tandem mass spectrometry. Journal of Chromatography A, 1038, 157–170.

Ji, L., Chen, W., Zheng, S., Xu, Z., Zhu, D., 2009. Adsorption of sulfonamide antibiotics to multiwalled carbon nanotubes. Langmuir, 25, 11608–11613.

Jorgensen, S.E., Halling-Sørensen, B., 2000. Drugs in the environment. Chemosphere, 40, 691–699.

Juang, R.S., Chen, M.L., 1997. Application of the Elovich equation to the kinetics of metal sorption with solvent-impregnated resins. Industrial and Engineering Chemistry Research, 36, 813–820.

Kahle, M., Stamm., C., 2007a. Time and pH-dependent sorption of the veterinary Antimicrobial sulfathiazole to clay minerals and ferrihydrite. Chemosphere, 68, 1224–1231.

Kahle, M., Stamm., C., 2007b. Sorption of the Veterinary Antimicrobial Sulfathiazole to Organic Materials of Different Origin. Environmental Science and Technology, 41, 132–138.

Karabay, O., Hosoglu, S., 2008. Increased antimicrobial consumption following reimbursement reform in Turkey. Journal Antimicrobial Chemotherapy, 61, 1169–1171.

Karci, A., 2008. Investigation of tetracycline, sulfonamide and fluoroquinolone antimicrobial compounds in manure and agricultural soils in north Marmara region, M.Sc Thesis, Bogazici University.

Karci, A., Akmehmet-Balcioglu, I., 2009. Investigation of the tetracycline, sulfonamide, and fluoroquinolone antimicrobial compounds in animal manure and agricultural soils in Turkey. Science of the Total Environment, 407, 4652–4664.

Karthikeyan, K.G., Meyer, M.T., 2006. Occurrence of antibiotics in wastewater treatment facilities in Wisconsin, USA. Science of the Total Environment, 361, 196– 207.

Kemper N., 2008. Veterinary antibiotics in the aquatic and terrestrial environment. Ecological Indicators, 8, 1–13.

Khraisheh, M.A.M., Al-Degs, Y.S., Allen, S.J. Ahmad, M.N., 2002. Elucidation of controlling steps of reactive dye adsorption on activated carbon. Industrial and Engineering Chemistry Research, 41, 1651–1657.

Kim, Y., Kim, C., Choi, I., Rengraj, S., Yi, J., 2004. Arsenic removal using mesoporous alumina prepared via a templating method. Environmental Science and Technology, 38, 924–931.

Kim, S., Jensen , J. N., Aga, D. S., Weber, A. S., 2007. Tetracycline as a selector for resistant bacteria in activated sludge. Chemosphere, 66, 1643–1651.

Kim, S.H., Shon, H.K., Ngo, H.N., 2010. Adsorption characteristics of antibiotics trimethoprim on powdered and granular activated carbon. Journal of Industrial and Engineering Chemistry, 16, 344–349.

Kolpin, D.W., Furlong, E.T., Meyer, M.T., Thurman, E.M., Zaugg, S.D., Barber, L.B., Buxton, H.T., 2002. Pharmaceuticals, hormones, and other organic wastewater contaminants in U.S. streams, 1999– 2000: a national reconnaissance. Environ Science and Technology, 36, 1202–1211.

Kolz, A. C., Ong, S. K., Moorman, T. B., 2005. Sorption of tylosin onto swine manure. Chemosphere, 60, 284–289.

Kulshrestha, P., Giese Jr., R.F., Aga, D.S., 2004. Investigating the molecular interactions of oxytetracycline in clay and organic matter. Insights on factors affecting its mobility in soil. Environmental Science and Technology, 38, 4097–4105.

Kumar, K., Gupta, S.C., Chander , Y., Singh, A.K., 2005a. Antibiotic use in agriculture and their impact on the terrestrial environment. Advances in Agronomy, 87.

Kumar, K., Gupta, S.C., Baidoo, S.K., Chander, Y., Rosen, C.J, 2005b. Antibiotic uptake by plants from soil fertilized with animal manure. Journal of Environmental Quality, 34, 2082–2085.

Kumar, A., Kumar, S., Kumar, S., Gupta, D.V., 2007. Adsorption of phenol and 4 nitrophenol on granular activated carbon in basal salt medium: Equilibrium and kinetics. Journal of Hazardous Materials, 147, 155–166.

Kümmerer, K., 2004. Resistance in the environment. Journal of Antimicrobial Chemotherapy, 54, 311–320.

Kümmerer, K., 2008. Pharmaceuticals in the environment. Sources, fate, effects and risk, 3rd edn. Springer, Berlin.

Kümmerer, K., 2009. Antibiotics in the aquatic environment – A review – Part I. Chemosphere, 75, 417–434.

Langmuir, I., 1918. The adsorption of gases on plane surfaces of glass, mica, and platinum. Journal of the American Chemical Society, 40, 1361–1403.

Lertpaitoonpan, W., Ong, S.K., Moorman, T.B., 2009. Effect of organic carbon and pH on soil sorption of sulfamethazine. Chemosphere, 76, 558–564.

Li, K., Yediler, A., Yang, M., Schulte-Hostede, S., Wong, M., H., 2008. Ozonation of oxytetracycline and toxicological assessment of its oxidation by-products. Chemosphere, 72, 473–478.

Lin, A., Y., -C., Lin, C., -F., Chiou, J., -M., Hong, P.K., A., 2009. O3 and O3/H2O2 treatment of sulfonamide and macrolide antibiotics in wastewater. Journal of Hazardous Materials, 171, 452–458.

Lin, A. Y. C., Tsai, Y. T., 2009. Occurrence of pharmaceuticals in Taiwan's surface waters: Impact of waste streams from hospitals and pharmaceutical production facilities. Science of the Total Environment, 407, 3793–3802.

Lindberg, R. H., Jarnheimer, P. A., Olsen, B., Johansson, M., Tysklind, M., 2004. Determination of antibiotic substances in hospital sewage water using solid phase extraction and liquid chromatography/mass spectrometry and group analogue internal standards. Chemosphere, 57, 1479–1488.

Lindsey, M. E., Meyer, M., Thurman, E. M., 2001. Analysis of trace levels of sulfonamide tetracycline antimicrobials in groundwater and surface water using solid-phase extraction and liquid chromatography/mass spectrometry. Analytical Chemistry, 73, 4640–4646.

Liu, P., Zhang, L., 2007. Adsorption of dyes from aqueous solutions or suspensions with clay nano-adsorbents. Separation and Purification Technology, 58, 32–39.

Liu, Y., Shen, L., 2008. From langmuir kinetics to first- and second-order rate equations for adsorption. Langmuir, 24, 11625–11630.

Liu, F., Ying, G., Tao, R., Zhao, J., Yang, J., Zhao, L., 2009. Effects of six selected antibiotics on plant growth and soil microbial and enzymatic activities. Environmental Pollution, 157, 1636–1642.

Loke, M.L., Tjornelund, J., Halling-Sørensen, B., 2002. Determination of the distribution coefficient (log K_d) of oxytetracycline, tylosin A, olaquindox and metronidazole in manure. Chemosphere, 48, 351–361.

Lorenc-Grabowska, E., Gryglewicz, G., 2005. Adsorption of lignite-derived humic acids on coal-based mesoporous activated carbons. Journal of Colloid and Interface Science, 284, 416–423.

Low M. J. D., 1960. Kinetics of chemisorption of gases on solids. Chemical Reviews, 60, 267–312.

Madejova, J., 2003. FTIR techniques in clay mineral studies. Vibrational Spectroscopy, 31, 1–10.

Managaki, S., Murata, A., Takada, H., Tuyen, B., Chiem, N., 2007. Distribution of macrolides, sulfonamides and trimethoprim in tropical waters: ubiquitous occurrence of veterinary antibiotics in the Mekong delta. Environmental Science and Technology, 41, 8004–8010.

Mangun, C.L., Benak, K.R., Economy, J., Foster, K.L., 2001. Surface chemistry, pore sizes and adsorption properties of activated carbon fibers and precursors treated with ammonia. Carbon, 39, 1809–1820.

Mascolo, G., Balest, G., Cassano, D., Laera, G., Lopez, A., Pollice, A., Sallerno, C., 2009. Biodegradability of pharmaceutical industrial wastewater and formation of recalcitrant organic compounds during aerobic biological treatment. Bioresource Technology, 101, 2585–2591.

McArdell, C.S., Molnar, E., Suter, M.J.F., Giger, W., 2003. Occurrence and fate of macrolide antibiotics in wastewater treatment plants and in the Glatt Valley Watershed, Switzerland. Environmental Science and Technology, 37, 5479–5486.

McKay, G., Otterburn, M.S., Sweeney, A.G, 1980. The removal of color from effluent using various adsorbents III silica: rate processes. Water Research, 14, 15–20.

McKay, G., Ho, Y.S., 1999a. The sorption of lead (II) on peat. Water Research, 33, 578–584.

McKay, G., Ho, Y.S., 1999b. Pseudo-second order model for sorption processes. Process Biochemistry, 34, 451– 465.

Mellon, M., Benbrook, C., Benbrook, K.L., 2001. Estimates of antimicrobial abuse in livestock. Union of Concerned Scientists. Food and Environment Program.

Miao, X-S., Bishay, F., Chen, M., Metcalfe, C.D., 2004. Occurrence of antibiotics in the final effluents of wastewater treatment plants in Canada. Environmental Science and Technology, 38, 3533–3541.

Navalon, S., Alvaro, M., Garcia, H., 2008. Reaction of chlorine dioxide with emergent water pollutants: Product study of the reaction of three ß-lactam antibiotics with ClO_2. Water Research, 42, 1935–1942.

Nikolaou, A., Meric, S., Fatta, D., 2007. Occurrence patterns of pharmaceuticals in water and wastewater environments. Analytical and Bioanalytical Chemistry, 387, 1225–1234.

Panuccio, M.R., Sorgona, A., Rizzo, M., Cacco, G., 2009. Cadmium adsorption on vermiculite, zeolite and pumice: Batch experimental studies. Journal of Environmental Management, 90, 364–374.

Pei, R., Kim, S.C., Carlson, K.H., Pruden, A., 2006. Effect of River Landscape on the sediment concentrations of antibiotics and corresponding antibiotic resistance genes (ARG). Water Research, 40, 2427–2435.

Pena, A., Paulo, M., Silva, L.J.G., Seifrtová, M., Lino, C.M., Solich, P., 2010. Tetracycline antibiotics in hospital and municipal wastewaters: a pilot study in Portugal. Analytical and Bioanalytical Chemistry, 396, 2929–2936.

Pharmaceutical Industry Special Expert Commission Report, 2001.

Pharmaceutical Industry Special Expert Commission Report, 2006.

Pils, J.R.V., Laird, D.A., 2007. Sorption of tetracycline and chlortetracycline on K- and Ca-saturated soil clays, humic substances, and clay-humic complexes. Environmental Science and Technology, 41, 1928–1933.

Polubesova, T., Zadaka, D., Groisman, L., Nir, S., 2006. Water remediation by micelle clay system: case study for tetracycline and sulfonamide antibiotics. Water Research, 40, 2369–2374.

Prado, N., Ochoa, J., Amrane, A., 2009. Biodegradation and biosorption of tetracycline and tylosin antibiotics in activated sludge system. Process Biochemistry, 44, 1302–1306.

Putra, E.K., Pranowo, R., Sunarso, J., Indraswati, N., Ismadji, S., 2009. Performance of activated carbon and bentonite for adsorption of amoxicillin from wastewater: Mechanisms, isotherms and kinetics. Water Research, 43, 2419–2430.

Qiang, Z., Macauley, J. J., Mormile, M. R., Surampalli, R., Adams, C. D., 2006. Treatment of antibiotics and antibiotic resistant bacteria in swine wastewater with free chlorine. Journal of Agricultural and Food Chemistry, 54, 8144–8154.

Rabolle, M., Spliid, N.,H., 2000. Sorption and mobility of metronidazole, olaquindox, oxytetracycline and tylosin in soil. Chemosphere, 40, 715–722.

Redlich, O., Peterson, D.L., 1959. A useful adsorption isotherm. Journal of Physical Chemistry, 63, 1024.

Rivera-Utrilla, J., Bautista-Toledo, I., Ferro-Garcia, M.A., Moreno-Castilla, C., 2001. Activated carbon surface modifications by adsorption of bacteria and their effect on aqueous lead adsorption. Journal of Chemical Technology and Biotechnology, 76, 1209–1215.

Rivera-Utrilla, J., Prados-Joya, G., Sánchez-Polo, M., Ferro-García, M.A., Bautista-Toledo, I., 2009. Removal of nitroimidazole antibiotics from aqueous solution by adsorption/bioadsorption on activated carbon. Journal of Hazardous Materials, 170, 298–305.

Sarmah, A. K., Meyer, M. T., Boxall, A. B. A., 2006. A global perspective on the use, sales, exposure pathways, occurrence, fate and effects of veterinary antibiotics (VAs) in the environment. Chemosphere, 65, 725–759.

Senthilkumaar, S., Varadarajan, P.R., Porkodi, K., Subbhuraam, C.V., 2005. Adsorption of methylene blue onto jute fiber carbon: kinetics and equilibrium studies. Journal of Colloid Interface Science, 284, 78–82.

Serpen, A., Atac, B., Gokmen, V., 2007. Adsorption of Maillard reaction products from aqueous solutions and sugar syrups using adsorbent resin. Journal of Food Engineering, 82, 342–350.

Smith, D.L., Harris, A.D., Johnson, J.A., Silbergeld, E.K., Morris Jr., J.G., 2002. Animal antibiotic use has an early but important impact on the emergence of Antibiotic resistance in human commensal bacteria. The Proceedings of the National Academy of Sciences, U.S.A. 99, 6434–6439.

Snyder, A., Kim, D., Cho, J., Kim, S., Vanderford, J., 2007. Occurrence and removal of pharmaceuticals and endocrine disruptors in South Korean surface, drinking, and waste waters. Water Research, 41, 1013–1021.

Stichele, R.H.V., Elseviers, M. M., Ferech, M., Blot, S., Goossens, H., 2006. Hospital consumption of antibiotics in 15 European countries: results of the ESAC Retrospective Data Collection (1997–2002). Journal of Antimicrobial Chemotherapy, 58, 159–167.

Sun, Q., Yang, L., 2003. The adsorption of basic dyes from aqueous solution on modified peat-resin particle. Water Research, 37, 1535–1544.

Şalcıoğlu, A.Ş., 2007. Sorption of tetracycline antibiotics on natural and modified zeolite. M.S. Thesis. Boğaziçi University.

Temkin, M.I., Pyzhev, V., 1940. Kinetic of ammonia synthesis on promoted iron catalyst. Acta Physiochimica URSS, 12, 327–356.

Teng, H., Hsieh, C., 1999. Activation energy for oxygen chemisorption on carbon at low temperatures. Industrial and Engineering Chemistry Research, 38, 292–297.

Thiele-Bruhn, S., Seibicke, T., Schulten, H.-R., Leinweber, P., 2004. Sorption of sulfonamide pharmaceutical antibiotics on whole soils and particle-size fractions. Journal of Environmental Quality, 33, 1331–1342.

Thiele-Bruhn, S., Beck, I.-C., 2005. Effects of sulfonamide and tetracycline antibiotics on soil microbial activity and microbial biomass. Chemosphere, 59, 457–465.

Tolls, J., 2001. Sorption of veterinary pharmaceuticals in soils: a review. Environmental Science and Technology, 35, 3397–3406.

Tseng, R.L., Wu, F.C., Juang, R.S., 2003. Liquid-phase adsorption of dyes and phenols using pinewood-based activated carbons, Carbon, 41, 487–495.

Tuncer, H.I., 2007. To banned usage of hormones, antibiotics, anticoccidials and drugs in compound animal feed (a rewiev). Lalahan Hayvancilik Araştırma Entitüsü Dergisi, 47, 29–37.

USEPA (United States Environmental Protection Agency), 2000. National management measures to control non-point pollution from agriculture. Office of Water, Non-point Source Control Branch, Draft report.

Uslu, M.O., Balcioglu, I.A., 2008. Ozonation of animal wastes containing oxytetracycline. Ozone: Science and Engineering, 30, 290–299.

Uslu, M., Balcıoğlu, I., 2009. Comparison of the ozonation and Fenton process performances for the treatment of antibiotic containing manure. Science of the Total Environment, 407, 3450–3458.

Vasudevan, D., Bruland, G.L., Torrance, B.S., Upchurch, V.G., MacKay, A.A., 2009. pH dependent ciprofloxacin sorption to soils: Interaction mechanisms and soil factors influencing sorption. Geoderma, 151, 68–76.

Vu, B.K., Shin, E.W., Snisarenko, O., Jeong, W.S., Lee, H.S., 2010. Removal of the antibiotic tetracycline by Fe-impregnated SBA-15. Korean Journal of Chemical Engineering, 27, 116–120.

Wang, S., Li, H., 2007. Kinetic modeling and mechanism of dye adsorption on unburned carbon. Dyes and Pigments, 72, 308–314.

Wang, C.J., Li., Z., Jiang, W.T., Jean, J.S., Liu, C.C., 2010. Cation exchange interaction between antibiotic ciprofloxacin and montmorillonite. Journal of Hazardous Materials, 183, 309–314.

Watkinson, A.J., Murby, E.J., Costanzo, S.D., 2007. Removal of antibiotics in conventional and advanced wastewater treatment: Implications for environmental discharge and wastewater recycling. Water Research, 41, 4164–4176.

Watkinson, A. J., Murby, E. J., Kolpin, D. W., Costanzo, S. D., 2009. The occurrence of antibiotics in an urban watershed: From wastewater to drinking water. Science of the Total Environment, 407, 2711–2723.

Weber, W.J., Morris, J.C., 1963. Kinetics of adsorption on carbon from solution. Journal of the Sanitary Engineering Division, 89, 31–59.

Wise, R., 2002. Antimicrobial resistance: priorities for action. Journal of Antimicrobial Chemotherapy, 49, 585–586.

Wong, Y.C., Szeto, Y.S., Cheung, W.H., McKay, G.,2008. Sorption kinetics for the removal of dyes from effluents onto chitosan. Journal of Applied Polymer Science, 109, 2232–2242.

Xu, W., Zhang, G., Zou, S., Li, X., Liu, Y., 2007. Determination of selected antibiotics in the Victoria Harbour and the Pearl River, South China using high-performance liquid chromatography– electrospray ionization tandem mass spectrometry. Environmental Pollution, 145, 672–679.

Xu, X.R., Li, X.Y., 2010. Sorption and desorption of antibiotic tetracycline on marine sediments. Chemosphere, 78, 430–436.

Yalap, K.S., Balcioglu, I.A., 2009. Effects of inorganic anions and humic acid on the photocatalytic and ozone oxidation of oxytetracycline in aqueous solution. Journal of Advance Oxidation Technology, 12, 134–143.

Yang, S., Cha, J., Carlson, K., 2005. Simultaneous extraction and analysis of 11 tetracycline and sulfonamide antibiotics in influent and effluent domestic wastewater by solid-phase extraction and liquid chromatography-electrospray ionization tandem mass spectrometry. Journal of Chromatography A, 1097, 40–53.

Ye, Z., Weinberg, H.S., 2007. Trace analysis of trimethoprim and sulfonamide, macrolide, quinolone, and tetracycline antibiotics in chlorinated drinking water using liquid chromatography electrospray tandem mass spectrometry. Analytical Chemistry, 79, 1135–1144.

Yu, L., Fink, G., Wintgens, T., Melin, T., Ternes, T., 2009. Sorption behavior of potential organic wastewater indicators with soils. Water Research, 43, 951–960.

Yukselen, Y., Kaya, A., 2008. Suitability of the methylene blue test for surface area, cation exchange capacity and swell potential determination of clayey soils. Engineering Geology, 102, 38–45.

Zhang, W., Xu, Z., Pan, B., Lu, L., Zhang, Q., Zhang, Q., Du, W., Pan, B., Zhang, Q., 2007. Assessment on the removal of dimethyl phthalate from aqueous phase using a hydrophilic hypercrosslinked polymer resin NDA-702. Journal of Colloid and Interface Science, 311, 382–390.

Zhang, D., Pan, B., Zhang, H., Ning, P., Xing, B., 2010. Contribution of different sulfamethoxazole species to their overall adsorption on functionalized carbon nanotubes. Environmental Science and Technology, 44, 3806–3811.

APPENDIX A

Calibration Curves of Antibiotics

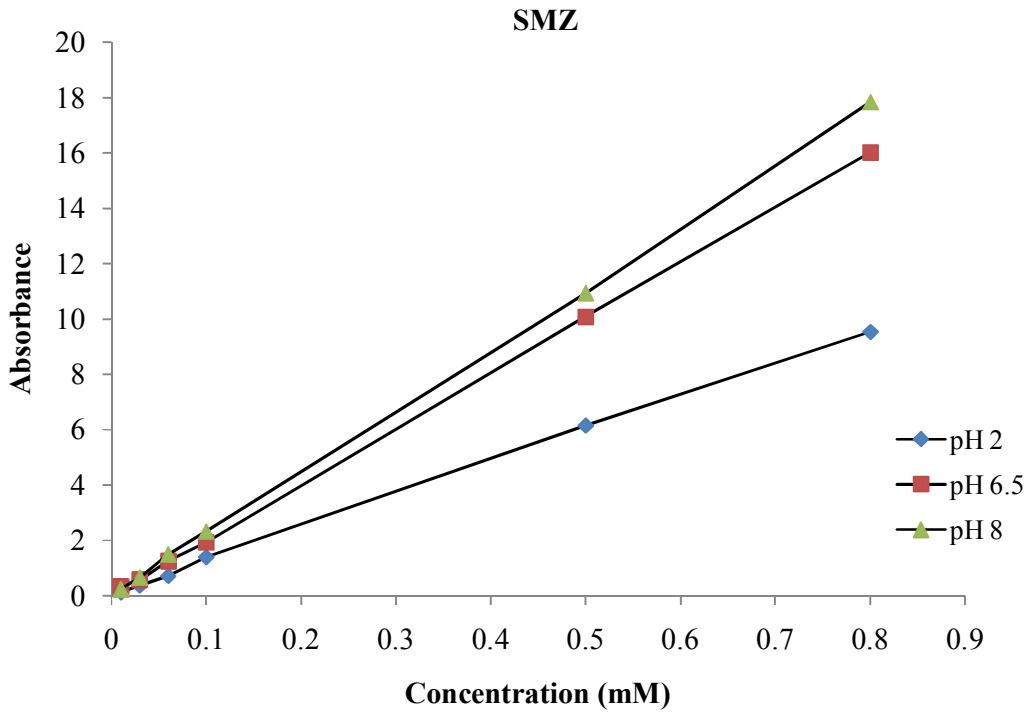

Figure A. 1. Calibration curves of SMZ at different pH values.

Table A.1. Maximum absorption peak and extinction coefficient of SMZ at different pH values.

pH	λ (nm)	ε (R^2)
2	243.5	12.042 (0.999)
6.5	262.5	20.045 (0.999)
8	259.5	22.203 (0.999)

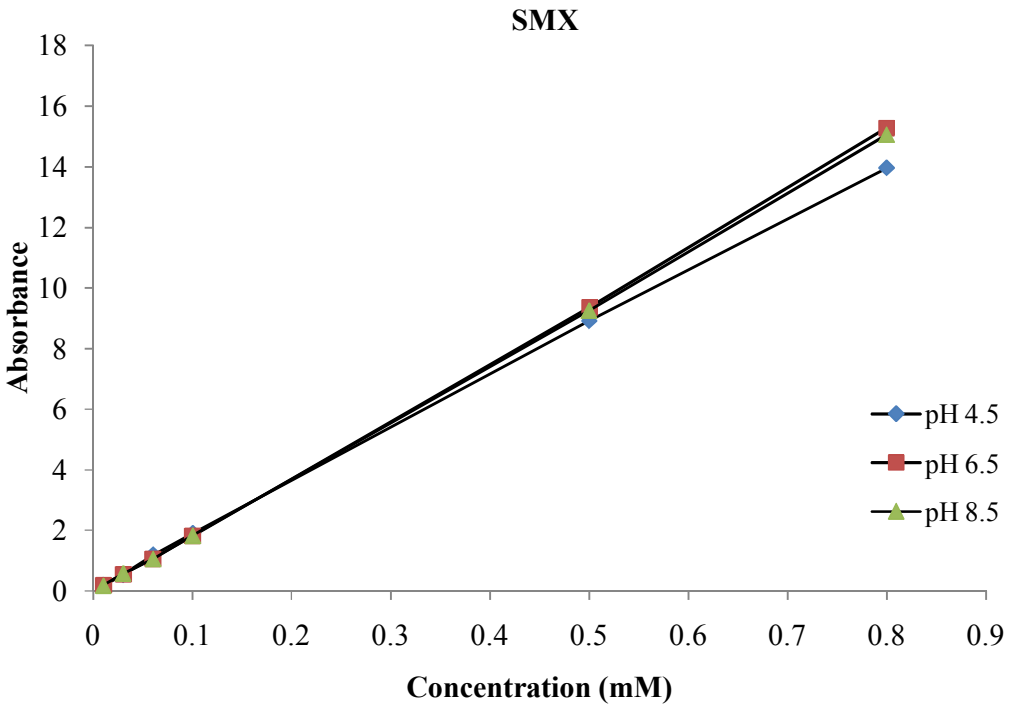

Figure A.2. Calibration curves of SMX at different pH values.

Table A.2. Maximum absorption peak and extinction coefficient of SMX at different pH values.

pH	λ (nm)	ε (R^2)
4.5	265.5	17.586 (0.999)
6.5	258	18.978 (0.999)
8.5	257	18.725 (0.999)

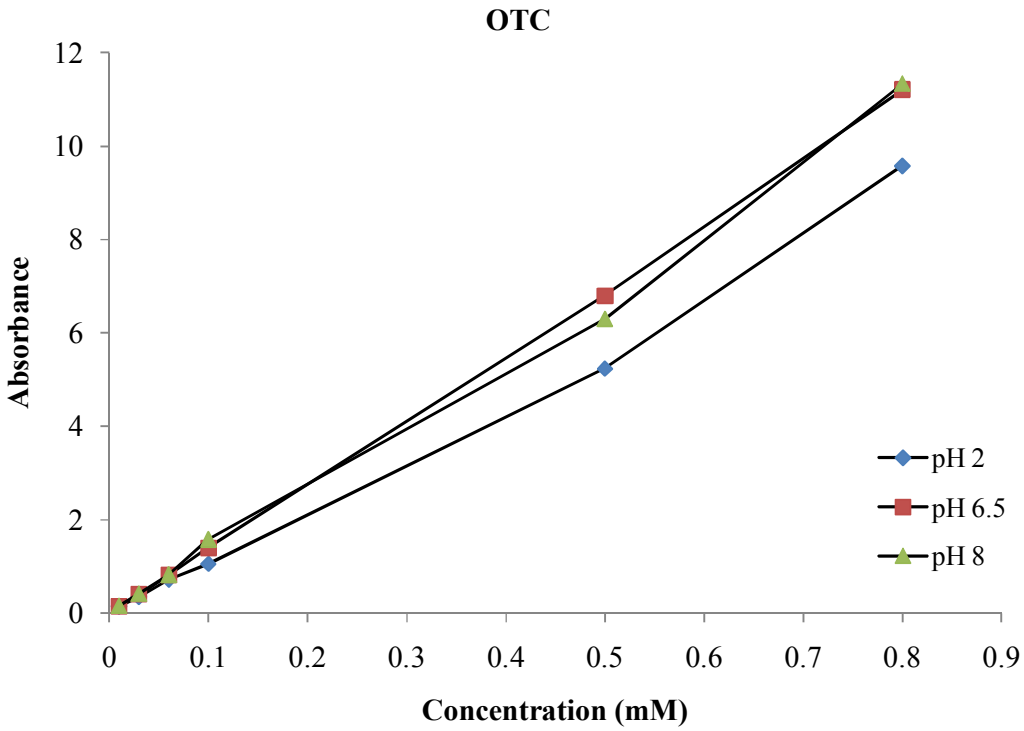

Figure A.3. Calibration curves of OTC at different pH values.

Table A.3. Maximum absorption peak and extinction coefficient of OTC at different pH values.

pH	λ (nm)	ε (R^2)
2	355.5	11.574 (0.994)
6.5	358	13.896 (0.999)
8.5	372	13.756 (0.995)

APPENDIX B

Interlayer Spacings and Peak Intensities of Adsorbents

Table B.1. Interlayer spacings and peak intensities of raw perlite.

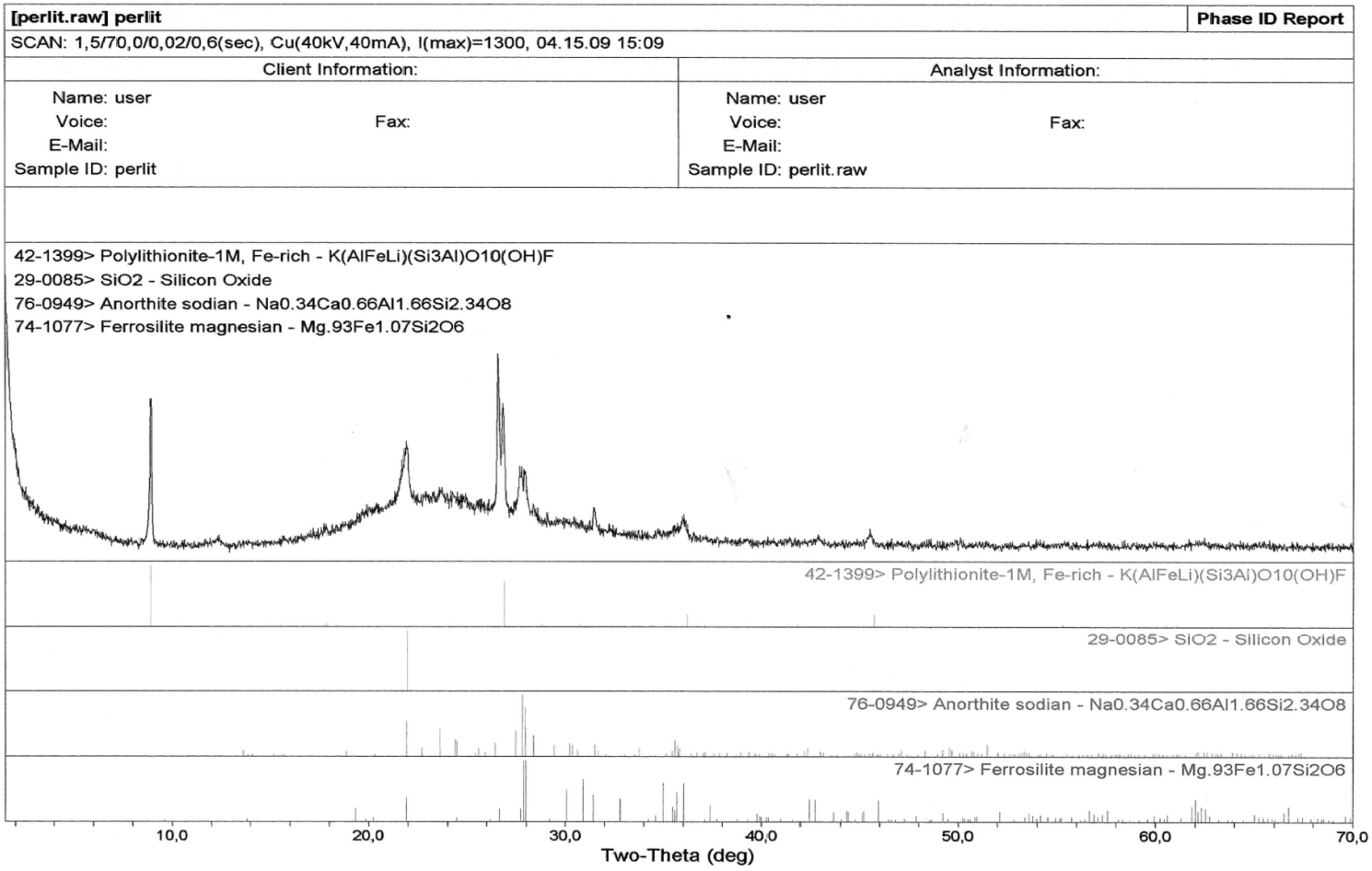

Materials Data, Inc.

[BOUN-080507|user]<C:\Documents and Settings\user\Desktop> Perþembe, Nis 16, 2009 02:47p (MDI/JADE6)

Table B.1. Continued.

[perlit.raw] perlit — **Peak ID Report**

SCAN: 1,5/70,0/0,02/0,6(sec), Cu(40kV,40mA), I(max)=1300, 04.15.09 15:09

PEAK: 19-pts/Parabolic Filter, Threshold=3,0, Cutoff=0,0%, BG=3/1,0, Peak-Top=Summit

NOTE: Intensity = Counts, 2T(0)=0,0(deg), Wavelength to Compute d-Spacing = 1,54056Å (Cu/K-alpha1)

#	2-Theta	d(Å)	Height	Height%	Phase ID	d(Å)	I%	(h k l)	2-Theta	Delta
1	8,918	9,9076	628	94,6	Polylithionite-1M, Fe-rich - K(AlFeLi)(Si3Al)O1...	9,9000	100,0	(0 0 1)	8,925	0,007
2	17,835	4,9692	40	6,0	Polylithionite-1M, Fe-rich - K(AlFeLi)(Si3Al)O1...	4,9550	3,0	(0 0 2)	17,886	0,051
3	21,995	4,0378	227	34,2	SiO2 - Silicon Oxide	4,0400	100,0		21,983	-0,012
4	26,600	3,3483	664	100,0	Ferrosilite magnesian - Mg.93Fe1.07Si2O6	3,3372	18,3	(1 2 1)	26,690	0,090
5	26,843	3,3186	454	68,4	Polylithionite-1M, Fe-rich - K(AlFeLi)(Si3Al)O1...	3,3090	73,0	(0 0 3)	26,922	0,079
6	27,780	3,2087	202	30,4	Ferrosilite magnesian - Mg.93Fe1.07Si2O6	3,2127	18,8	(4 1 1)	27,745	-0,035
7	27,961	3,1884	191	28,8	Anorthite sodian - Na0.34Ca0.66Al1.66Si2.34O8	3,1855	78,9	(0 0 2)	27,986	0,025
8	31,465	2,8408	97	14,6	Ferrosilite magnesian - Mg.93Fe1.07Si2O6	2,8429	41,4	(5 1 1)	31,442	-0,023
9	35,566	2,5221	49	7,4	Anorthite sodian - Na0.34Ca0.66Al1.66Si2.34O8	2,5200	23,8	(-3-1 2)	35,597	0,031
10	36,058	2,4888	98	14,8	Ferrosilite magnesian - Mg.93Fe1.07Si2O6	2,4885	61,9	(2 3 1)	36,063	0,004
11	42,878	2,1074	38	5,7	Ferrosilite magnesian - Mg.93Fe1.07Si2O6	2,1123	33,6	(3 2 2)	42,773	-0,105
12	45,518	1,9911	61	9,2	Anorthite sodian - Na0.34Ca0.66Al1.66Si2.34O8	1,9920	1,8	(-1 3 3)	45,497	-0,021
13	48,511	1,8751	32	4,8	Ferrosilite magnesian - Mg.93Fe1.07Si2O6	1,8728	0,7	(4 4 1)	48,573	0,062
14	58,443	1,5778	31	4,7	Anorthite sodian - Na0.34Ca0.66Al1.66Si2.34O8	1,5779	0,7	(-5-1 1)	58,442	-0,001

Line Shifts of Individual Phases:

PDF#42-1399 - Polylithionite-1M, Fe-rich <2T(0) = 0,0, d/d(0) = 1,0>

PDF#29-0085 - Silicon Oxide <2T(0) = 0,0, d/d(0) = 1,0>

PDF#76-0949 - Anorthite sodian <2T(0) = 0,0, d/d(0) = 1,0>

PDF#74-1077 - Ferrosilite magnesian <2T(0) = 0,0, d/d(0) = 1,0>

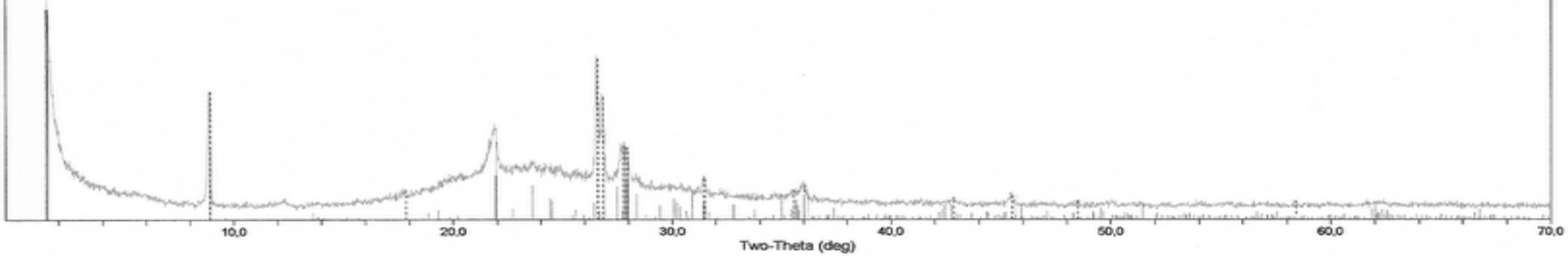

Table B.2. Interlayer spacings and peak intensities of raw pumice.

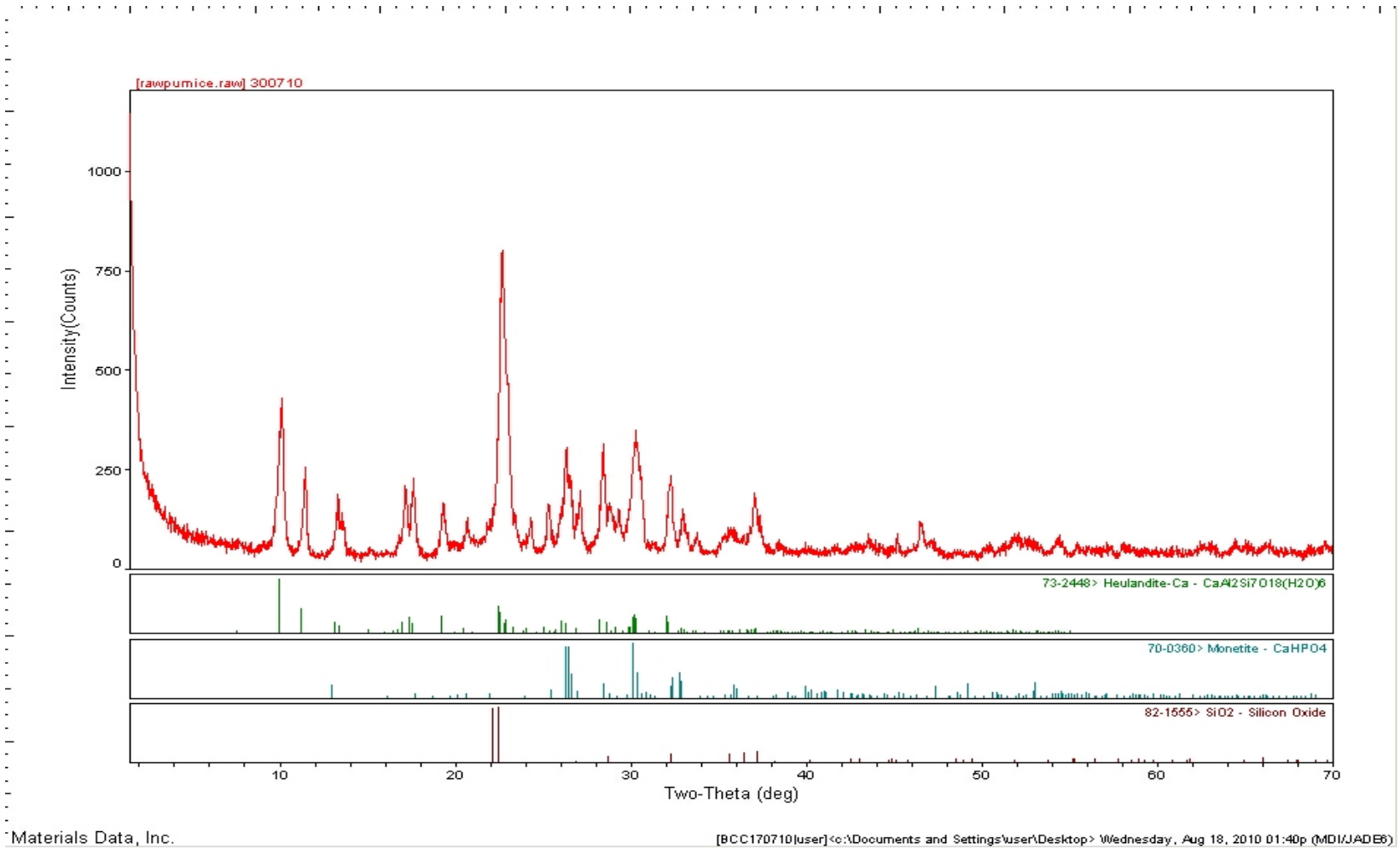

Table B.2. Continued.

Peak ID Extended Report (36 Peaks, Max P/N = 12,9)									
[rawpumice.raw] 300710									
PEAK: 21-pts/Parabolic Filter, Threshold=3,0, Cutoff=0,0%, BG=3/1,0, Peak-Top=Summit									
2-Theta	d(Å)	Height	Height%	Phase ID	d(Å)	I%	(h k l)	2-Theta	Delta
10,178	86,835	426	53,2						
11,500	76,886	253	31,6	C8H12CdN6Ni!0.5(CH3)2CH(CH2)2OH	77,959	53,8	(0 0 1)	11,341	-0,159
13,344	66,296	184	23,0	Heulandite-Ca	66,524	11,9	(0 0 1)	13,298	-0,046
13,682	64,669	115	14,4	C8H12CdN6Ni!0.5(CH3)2CH(CH2)2OH	63,938	29,0	(2 1 0)	13,839	0,157
17,201	51,509	206	25,7	Heulandite-Ca	51,218	27,6	(1 1 1)	17,299	0,098
17,660	50,179	224	28,0	Monetite	49,897	5,4	(0-1 1)	17,761	0,101
19,322	45,900	164	20,5	C8H12CdN6Ni!0.5(CH3)2CH(CH2)2OH	45,521	16,7	(3 1 0)	19,484	0,162
20,719	42,835	125	15,6	Monetite	42,804	5,4	(1 0 1)	20,734	0,015
21,982	40,402	122	15,2	Monetite	40,284	4,7	(-1 1 1)	22,047	0,065
22,739	39,073	801	100,0	C8H12CdN6Ni!0.5(CH3)2CH(CH2)2OH	39,171	100,0	(3 1 1)	22,681	-0,058
23,038	38,574	463	57,8	Heulandite-Ca	38,396	10,1	(2 2 1)	23,146	0,108
24,324	36,562	126	15,7	Heulandite-Ca	36,266	1,7	(4 2 0)	24,526	0,201
25,361	35,090	159	19,9	Heulandite-Ca	35,219	3,4	(-1 1 2)	25,267	-0,094
26,378	33,759	302	37,7	Monetite	33,784	92,1	(0 0 2)	26,359	-0,019
26,599	33,485	232	29,0	Quartz	33,442	100,0	(1 0 1)	26,633	0,034
27,140	32,829	194	24,2	Monetite	32,932	10,0	(0 2 0)	27,053	-0,087
28,460	31,336	312	39,0	Monetite	31,274	23,7	(-1-1 2)	28,517	0,057
28,861	30,910	162	20,2	Monetite	30,930	5,1	(0-2 1)	28,841	-0,019
29,356	30,400	148	18,5	Heulandite-Ca	30,358	3,8	(-5 1 2)	29,397	0,041
30,340	29,435	346	43,2	Monetite	29,359	45,4	(-1-2 1)	30,421	0,081
32,301	27,692	230	28,7	Monetite	27,655	19,0	(1 0 2)	32,346	0,045
33,021	27,105	147	18,4	Heulandite-Ca	27,072	1,3	(-4 4 2)	33,062	0,041
33,835	26,471	73	9,1	Monetite	26,320	0,5	(1-1 2)	34,035	0,200
35,297	25,407	78	9,7	Heulandite-Ca	25,355	4,2	(6 2 0)	35,372	0,075
35,763	25,087	101	12,6	Monetite	25,058	3,2	(2 1 1)	35,805	0,042
37,100	24,213	189	23,6	Heulandite-Ca	24,267	7,6	(4 4 1)	37,014	-0,086
45,251	20,022	61	7,6	Heulandite-Ca	20,038	0,1	(-7 3 3)	45,215	-0,037
46,519	19,506	113	14,1	Heulandite-Ca	19,482	1,9	(4 8 0)	46,580	0,061
50,565	18,036	58	7,2	Heulandite-Ca	18,048	0,5	(-6 6 3)	50,530	-0,036
54,260	16,892	74	9,2	Monetite	16,892	4,6	(3 0 2)	54,260	0,000
54,599	16,795	67	8,4	Heulandite-Ca	16,801	0,6	(7 5 1)	54,577	-0,023
55,465	16,553	63	7,9	Monetite	16,540	6,1	(-3-2 3)	55,513	0,048
58,125	15,857	65	8,1	Monetite	15,855	1,8	(2-3 2)	58,134	0,009
64,427	14,450	72	9,0	Monetite	14,465	1,8	(-3-2 4)	64,349	-0,078

Table B.3. Interlayer spacings and peak intensities of raw zeolite.

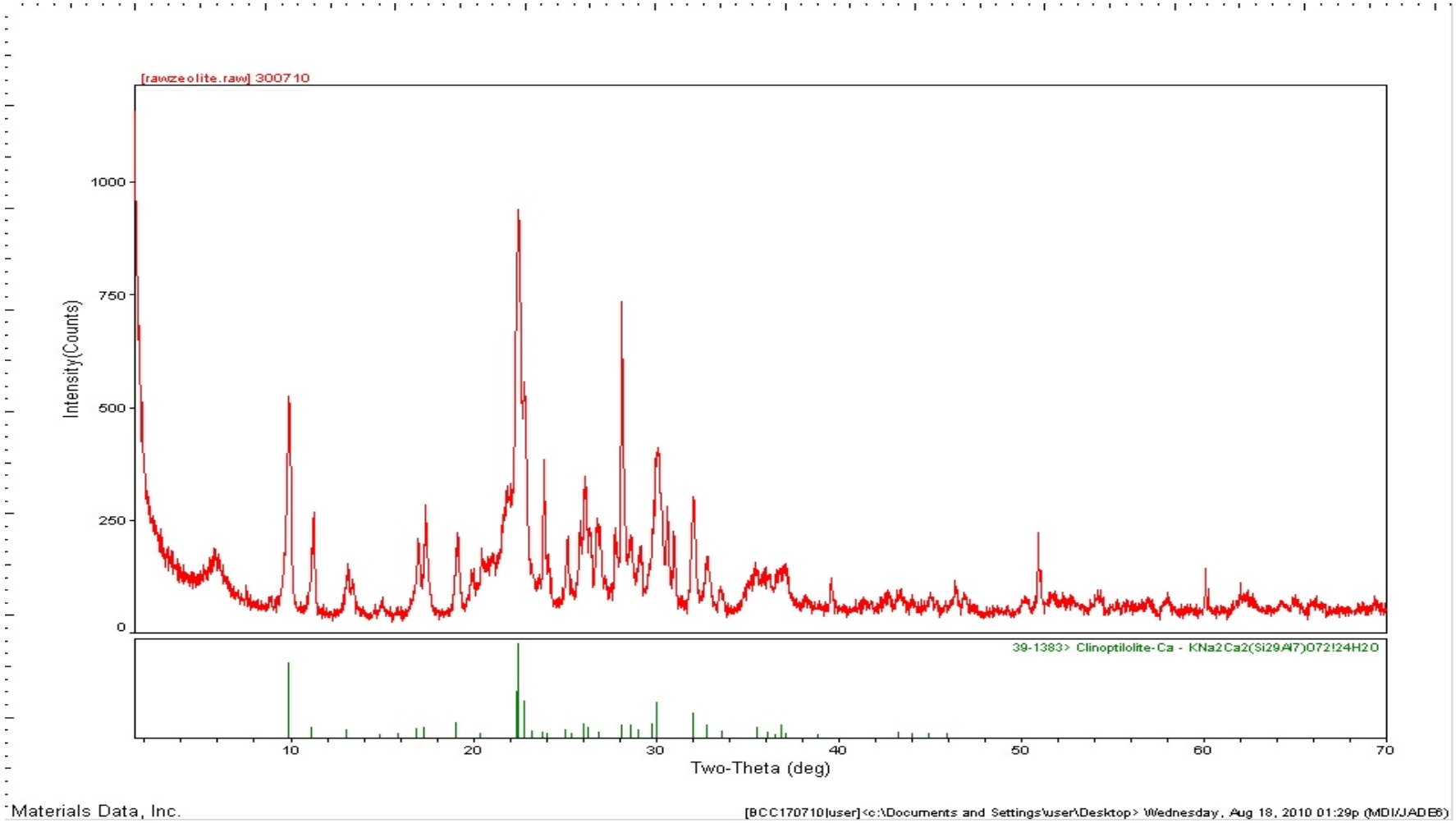

Table B.3. Continued.

Peak ID Extended Report (48 Peaks, Max P/N = 13,1)									
[rawzeolite.raw] 300710									
PEAK: 21-pts/Parabolic Filter, Threshold=3,0, Cutoff=0,0%, BG=3/1,0, Peak-Top=Summit									
2-Theta	d(Å)	Height	Height%	Phase ID	d(Å)	I%	(h k l)	2-Theta	Delta
5,956	148,256	182	19,4						
9,961	88,724	524	55,8	Clinoptilolite-Ca	89,500	79,4	(0 2 0)	9,875	-0,087
11,318	78,116	265	28,2	Clinoptilolite-Ca	79,300	10,3	(2 0 0)	11,148	-0,170
13,158	67,228	150	16,0	Clinoptilolite-Ca	67,800	7,1	(2 0-1)	13,047	-0,112
13,459	65,732	117	12,5						
15,076	58,716	77	8,2	Clinoptilolite-Ca	59,400	2,4	(2 2 0)	14,902	-0,175
17,023	52,045	207	22,0	Clinoptilolite-Ca	52,400	7,9	(3 1-1)	16,906	-0,116
17,439	50,810	280	29,8	Clinoptilolite-Ca	51,200	9,5	(1 1 1)	17,305	-0,134
19,182	46,231	220	23,4	Clinoptilolite-Ca	46,500	15,1	(1 3-1)	19,070	-0,112
19,937	44,498	138	14,7						
20,538	43,210	184	19,6	Clinoptilolite-Ca	43,500	4,0	(4 0-1)	20,399	-0,139
21,920	40,515	323	34,4						
22,500	39,483	939	100,0	Clinoptilolite-Ca	39,550	100,0	(4 0 0)	22,462	-0,038
22,840	38,903	554	59,0	Clinoptilolite-Ca	39,050	38,1	(2 4 0)	22,753	-0,087
23,904	37,194	381	40,6	Clinoptilolite-Ca	37,070	4,0	(0 4 1)	23,986	0,081
24,156	36,812	154	16,4						
25,213	35,292	211	22,5	Clinoptilolite-Ca	35,130	3,2	(1 1-2)	25,332	0,119
25,899	34,373	246	26,2	Clinoptilolite-Ca	34,240	14,3	(2 2-2)	26,002	0,102
26,160	34,036	345	36,7	Clinoptilolite-Ca	33,920	9,5	(4 0-2)	26,251	0,091
26,437	33,686	230	24,5						
26,858	33,168	253	26,9	Clinoptilolite-Ca	33,160	4,8	(0 0 2)	26,864	0,006
27,802	32,062	231	24,6						
28,161	31,661	734	78,2	Clinoptilolite-Ca	31,700	12,7	(4 2-2)	28,126	-0,035
28,640	31,143	215	22,9	Clinoptilolite-Ca	31,200	11,9	(4 4-1)	28,586	-0,053
29,198	30,561	190	20,2	Clinoptilolite-Ca	30,740	7,1	(1 3-2)	29,024	-0,174
30,160	29,607	410	43,7	Clinoptilolite-Ca	29,710	37,3	(1 5 1)	30,053	-0,107
30,661	29,134	278	29,6						
31,020	28,806	223	23,7						
32,098	27,862	301	32,1	Clinoptilolite-Ca	27,950	25,4	(5 3 0)	31,995	-0,104
32,860	27,234	168	17,9	Clinoptilolite-Ca	27,300	12,7	(2 6-1)	32,778	-0,082
33,659	26,605	91	9,7	Clinoptilolite-Ca	26,670	6,3	(2 0 2)	33,575	-0,085
35,221	25,460	124	13,2						
35,499	25,267	149	15,9	Clinoptilolite-Ca	25,270	9,5	(6 2 0)	35,495	-0,004
36,781	24,415	139	14,8	Clinoptilolite-Ca	24,370	12,7	(2 6 1)	36,852	0,071
37,141	24,187	151	16,1	Clinoptilolite-Ca	24,220	4,0	(4 4 1)	37,088	-0,053
39,658	22,708	120	12,8						
42,836	21,094	87	9,3						
43,438	20,815	96	10,2	Clinoptilolite-Ca	20,890	4,8	(3 7-2)	43,275	-0,164
45,060	20,103	86	9,2	Clinoptilolite-Ca	20,160	3,2	(6 4-3)	44,926	-0,135

APPENDIX C

Surface Area Data of Adsorbents

Table C.1. Surface area data of raw perlite.

Quantachrome NovaWin2 - Data Acquisition and Reduction
for NOVA instruments
©1994-2007, Quantachrome Instruments
version 9.0

Quantachrome INSTRUMENTS
Optimizing particle performance

Analysis				Report			
Operator:	serife	**Date:**	2009/03/20	**Operator:**		**Date:**	3/25/2009
Sample ID:	perlite	**Filename:**		C:\QCdata\Physisorb\perlite20mart.qps			
Sample Desc:		**Comment:**					
Sample weight:	0.3554 g	**Sample Volume:**	0.3554 cc			**Sample Density:**	1 g/cc
Outgas Time:	2.5 hrs	**OutgasTemp:**	200.0 C				
Analysis gas:	Nitrogen	**Bath Temp:**	77.3 K				
Press. Tolerance:	0.100/0.100 (ads/des)	**Equil time:**	60/60 sec (ads/des)			**Equil timeout:**	240/240 sec (ads/des)
Analysis Time:	257.5 min	**End of run:**	2009/03/20 16:07:25			**Instrument:**	Nova Station A
Cell ID:	1						

Area-Volume Summary

Data Reduction Parameters Data

Adsorbate	Nitrogen	Temperature	77.350K		
	Molec. Wt.: 28.013 g	**Cross Section:**	16.200 Å²	**Liquid Density:**	0.808 g/cc

Surface Area Data

MultiPoint BET	1.178e+01 m²/g
Langmuir surface area	2.017e+01 m²/g
t-method external surface area	1.178e+01 m²/g
DR method micropore area	1.279e+01 m²/g
NLDFT cumulative surface area	4.747e+00 m²/g

Pore Volume Data

DR method micropore volume	4.545e-03 cc/g
HK method cumulative pore volume	3.029e-03 cc/g
SF method cumulative pore volume	3.155e-03 cc/g
NLDFT method cumulative pore volume	5.002e-03 cc/g

Pore Size Data

DR method micropore Half pore width	2.048e+01 Å
DA method pore Radius (Mode)	1.120e+01 Å
HK method pore Radius (Mode)	1.838e+00 Å
SF method pore Radius (Mode)	2.261e+00 Å
NLDFT pore Radius (Mode)	1.210e+01 Å

Table C.2. Surface area data of raw pumice.

Quantachrome NovaWin2 - Data Acquisition and Reduction for NOVA instruments
©1994-2007, Quantachrome Instruments version 9.0

Analysis Report

Operator: derya Date:2010/09/13 Operator: Date:9/13/2010
Sample ID: Pumice Filename: C:\QCdata\Physisorb\Pumice.qps
Sample Desc: Comment:
Sample weight: 0.4793 g Sample Volume: 0.4793 cc Sample Density:1 g/cc
Outgas Time: 2.5 hrs OutgasTemp: 200.0 C
Analysis gas: Nitrogen Bath Temp: 77.3 K
Press. Tolerance:0.100/0.100 (ads/des) Equil time: 60/60 sec (ads/des)
Equil timeout: 240/240 sec (ads/des)
Analysis Time: 102.8 min End of run: 2010/09/13 14:12:47
Instrument: Nova Station A
Cell ID: 66
Adsorbate Nitrogen Temperature 77.350K
Molec. Wt.: 28.013 g Cross Section: 16.200 Å² Liquid Density: 0.808 g/cc

Surface Area Data

MultiPoint BET	3.273e+01 m²/g
Langmuir surface area	4.789e+01 m²/g
t-method external surface area	3.273e+01 m²/g
DR method micropore area	4.246e+01 m²/g
NLDFT cumulative surface area	2.210e+01 m²/g

Pore Volume Data

DR method micropore volume	1.509e-02 cc/g
HK method cumulative pore volume	1.323e-02 cc/g
SF method cumulative pore volume	1.355e-02 cc/g
NLDFT method cumulative pore volume	1.506e-02 cc/g

Pore Size Data

DR method micropore Half pore width	1.365e+01 Å
DA method pore Radius (Mode)	8.700e+00 Å
HK method pore Radius (Mode)	1.838e+00 Å
SF method pore Radius (Mode)	2.261e+00 Å
NLDFT pore Radius (Mode)	6.443e+00 Å

Table C.3. Surface area data of raw zeolite.

Quantachrome NovaWin2 - Data Acquisition and Reduction for NOVA instruments
©1994-2007, Quantachrome Instruments version 9.0

Analysis Report

Operator: derya Date:2010/09/07 Operator: Date:9/7/2010
Sample ID: Zeol Filename: C:\QCdata\Physisorb\DErya ZEOLITE7.9.2010.qps
Sample Desc: Comment:
Sample weight: 0.4224 g Sample Volume: 0.4224 cc Sample Density:1 g/cc
Outgas Time: 2.5 hrs OutgasTemp: 200.0 C
Analysis gas: Nitrogen Bath Temp: 77.3 K
Press. Tolerance: 0.100/0.100 (ads/des) Equil time: 60/60 sec (ads/des)
Equil timeout: 240/240 sec (ads/des)
Analysis Time: 44.3 min End of run: 2010/09/07 13:38:49
Instrument: Nova Station B
Cell ID: 67
Adsorbate Nitrogen Temperature 77.350K
Molec. Wt.: 28.013 g Cross Section: 16.200 Å² Liquid Density: 0.808 g/cc

Surface Area Data

MultiPoint BET	2.025e+01 m²/g
Langmuir surface area	3.037e+01 m²/g
t-method external surface area	2.025e+01 m²/g
DR method micropore area	2.674e+01 m²/g
NLDFT cumulative surface area	1.276e+01 m²/g

Pore Volume Data

DR method micropore volume	9.503e-03 cc/g
HK method cumulative pore volume	7.747e-03 cc/g
SF method cumulative pore volume	7.983e-03 cc/g
NLDFT method cumulative pore volume	9.266e-03 cc/g

Pore Size Data

DR method micropore Half pore width	1.680e+01 Å
DA method pore Radius (Mode)	9.500e+00 Å
HK method pore Radius (Mode)	1.838e+00 Å
SF method pore Radius (Mode)	2.261e+00 Å
NLDFT pore Radius (Mode)	1.324e+01 Å

Table C.4. Surface area data of raw GAC.

Quantachrome NovaWin2 - Data Acquisition and Reduction for NOVA instruments
©1994-2007, Quantachrome Instruments version 9.0

Analysis Report

Operator:derya Date:2010/09/07 Operator: Date:9/7/2010
Sample ID: GAC-1 Filename: C:\QCdata\Physisorb\GAC-1.qps
Sample Desc: Comment:
Sample weight: 0.2864 g Sample Volume: 0.2864 cc Sample Density:1 g/cc
Outgas Time: 2.5 hrs OutgasTemp: 200.0 C
Analysis gas: Nitrogen Bath Temp: 77.3 K
Press. Tolerance:0.100/0.100 (ads/des) Equil time: 60/60 sec (ads/des)
Equil timeout: 240/240 sec (ads/des)
Analysis Time: 137.8 min End of run: 2010/09/07 16:25:50
Instrument: Nova Station A
Cell ID: 66
Adsorbate Nitrogen Temperature 77.350K
Molec. Wt.: 28.013 g Cross Section: 16.200 Å² Liquid Density: 0.808 g/cc

Surface Area Data

MultiPoint BET	9.303e+02 m²/g
Langmuir surface area	1.335e+03 m²/g
t-method external surface area	7.237e+02 m²/g
t-method micropore surface area	2.066e+02 m²/g
DR method micropore area	1.267e+03 m²/g
NLDFT cumulative surface area	7.355e+02 m²/g

Pore Volume Data

t-method micropore volume	1.110e-01 cc/g
DR method micropore volume	4.503e-01 cc/g
HK method cumulative pore volume	4.141e-01 cc/g
SF method cumulative pore volume	4.202e-01 cc/g
NLDFT method cumulative pore volume	4.226e-01 cc/g

Pore Size Data

DR method micropore Half pore width	1.196e+01 Å
DA method pore Radius (Mode)	7.900e+00 Å
HK method pore Radius (Mode)	1.838e+00 Å
SF method pore Radius (Mode)	2.261e+00 Å
NLDFT pore Radius (Mode)	5.888e+00 Å